The Thesis Committee for Moonsoo Shin
Certifies that this is the approved version of the following thesis:

ARCHITECTURE OF COARSE GRAINED (CONGLOMERATIC) DEEP WATER LOBES AT THE BASE OF A SANDSTONE DOMINATED FAN, JURASSIC LOS MOLLES FORMATION, NEUQUEN BASIN, ARGENTINA

APPROVED BY
SUPERVISING COMMITTEE:

Supervisor: _____
Ron Steel

Co-Supervisor: _____
Cornel Olariu

_____
David Mohrig

ARCHITECTURE OF COARSE GRAINED (CONGLOMERATIC) DEEP WATER LOBES AT THE BASE OF A SANDSTONE DOMINATED FAN, JURASSIC LOS MOLLES FORMATION, NEUQUEN BASIN, ARGENTINA

by

Moonsoo Shin, B.S.Geo.Sci.

Thesis

Presented to the Faculty of the Graduate School of

The University of Texas at Austin

in Partial Fulfillment

of the Requirements

for the Degree of

Master of Science in Geological Sciences

The University of Texas at Austin

May 2015

Dedication

Dedicated to all beloved members of the Shin family.

Acknowledgements

I would like to thank my co-supervisors, Drs. Ron Steel and Cornel Olariu for allowing me to have spent two extra years at UT and to learn about the outstanding deepwater deposits in Argentina. I still remind myself how lucky I am to have a top-notch intellectual opportunity under exceptionally knowledgeable and intimate two supervisors whom I have met since my undergraduate studies. Especially, I owe a great debt of gratitude to Dr. Cornel Olariu. I am able to graduate successfully because of his constant helps and advices in regard of researches, classes, and all other miscellaneous tasks. Thank you to Cornel again for guiding me through challenges I had with fieldworks and thesis. Thank you to Ron for always giving me simple yet best answers to difficult questions and checking my progress constantly for last two years. Dr. David Mohrig has been supportive of my research, especially lifting huge burdens from being assigned to a TA two semesters in a row with light loads of works.

I appreciate Statoil and Jackson School of Geosciences for providing me essential funds to advance my journey in graduate studies. Also, appreciation goes to Familia Angelino for living accommodations, and Cordero, Bagly, and Belisle Estancia owners for the access to field areas in Argentina.

I thank Woongmo Koo for the special brotherhood and academic advices, Eugen Tudor for all good talks and helps back in the field in Alumine, Argentina, Yang Peng for being an awesome officemate with your pleasing smiles, Rattanaporn Fongngern for all your positive energies, and all other friends in Dr. Steel's Dynamic Stratigraphy Group.

Lastly, I would like to show the utmost appreciation to my family for the unconditional support and love. My father has always been a great mentor giving me wise solutions and motivations when making sensible decisions and judgements. Thanks,

Dad! The super supportive nature of my mom makes me completely oblivious to living life of study abroad. Even more sincere thanks to her for the immeasurable love and care. Also, I have an amazing sister, Dana, who always shows deep interests in my progress as a graduate student and life away from home. Thank you so much.

Abstract

ARCHITECTURE OF COARSE GRAINED (CONGLOMERATIC) DEEP WATER LOBES AT THE BASE OF A SANDSTONE DOMINATED FAN, JURASSIC LOS MOLLES FORMATION, NEUQUEN BASIN, ARGENTINA

Moonsoo Shin, MS Geo Sci

The University of Texas at Austin, 2015

Supervisors: Ron Steel and Cornel Olariu

The complex structural and stratigraphic framework of the Neuquén Basin developed by Triassic-Jurassic extensional processes formed a deep basin and accumulated coarse-grained gravity flow deposits on slope and basin floor. The Los Molles Formation exposes the succession of gravity flow deposits from conglomerates to mudstones over a 9 km outcrop belt in southern Neuquén Basin. The Los Molles Fm. is over 1,000 meters thick and its basal part is ~200 meters thick consisting of two fan units capped by 0.5-3 m of conglomerate beds. The initial deepwater fan units start with unusual pebble- and cobble-rich conglomerate beds at their base. To characterize the conglomerate lobes and their link with the correlative and overlaying basin-floor lobe complexes, satellite images, DEM (Digital Elevation Model), photomosaics (a few km), and 19 measured sections (30-190m thick) have been collected and interpreted. In all

units measured, each lobe contains, from bottom to top, very coarse, poorly sorted, and erosional-based conglomerates (1-3m) overlain by amalgamated, normal graded turbidite sandstone beds (20-30m), and silty mudstone beds (up to 15m). Each of these three facies associations forms a succession (about 30-40 m thick) of lobe complexes with an overall fining upward trend. The conglomerate thickness and lateral extent decreases upwards as the third (uppermost) conglomerate layer demonstrates rather discontinuous, lenticular bodies. In contrast, the sandstone beds increase upward in thickness with finer grain size and better sorting. The conglomerate beds are interpreted as debris flow deposits based on their structureless and poorly sorted texture. However, some conglomerates are at times erosional at the base, poorly sorted throughout, but others are capped by normal grading for up to a third of their thickness. Normal grading suggests debris flow transforming into turbidity flow vertically. Flute marks associated with sandstone and conglomerate beds indicate paleoflow toward the east, in contrast to younger sandy fans that shows progradation dominantly north-northeastwards. The modern Var River system in southern France has a similar morphology with pebbles and cobbles transported to deepwater via steep gradient slope. As in the Var system, coarse sediments in the Los Molles Fm. bypass the shelf and steep slope to build the initial base of the fan. In summary, the earliest Los Molles conglomeratic fans were linked with high relief of the basin margin. Later, this margin relief decreased, and sandstone dominated fans.

Table of Contents

List of Tables

List of Figures

1. INTRODUCTION

The present study on deepwater depositional systems in the lower Los Molles Formation (Lower Jurassic) in Neuquén Basin primarily focuses on coarse turbiditic fan system architecture and causes local accumulations of few meters-thick conglomerates into areas of initial deeper bathymetry (local depocenters). “Initial” represents the first surface morphology formed at an original slope to basin-floor along which sand or coarser sediments were transported and deposited on the basin floor. At the basin floor, outcrop models traditionally display unchannelized, sheet-like, distal lobes prograde and build the upward-thickening and –coarsening stacking patterns within a fan (Mutti and Normark, 1987, 1991). Previous studies in regard of submarine fans and related turbidite systems have improved understanding architectural elements and depositional environments present at a variety of lobe scales (Mutti and Ricci Lucchi, 1972; Mutti, 1977; Shanmugam and Moiola, 1988; Prelat et al., 2009; Mulder and Etienne, 2010). The study in the Los Molles Formation highlights the architecture of coarse grained fan deposits with focus on the two main drivers for deposition of conglomeratic units in lobe deposits: turbidity current and debris flow. The variable (along depositional dip and strike) depositional rates of sediments and their affiliated changes in grain sorting and size heavily influence succession of distinctive stratigraphic lithofacies throughout the system (Mutti, 1977; Mutti and Normark, 1987). Thus, from a scale of a lobe to a fan, recognizing architecture elements in turbidites such as thickening-coarsening-upward or thinning-fining-upward trend for varying bed thickness and grain size in addition to facies association, bed geometry, and continuity can illustrate evolution of lobes (Hodgson et al., 2006; Prelat et al., 2009; Kane and Ponten, 2012; Prelat and Hodgson, 2013). Deep water conglomerates and associated high density turbidites have been

previously described in outcrops of channelized slope reflecting canyon deposits and channel-levee complex, where channelized or slumped conglomerates truncate successions of interbedded turbiditic sandstones indicating channel-fill or overbank system based on a vertical sequence of fining-upward facies association (Johnson and Walker, 1979; Hickson and Lowe, 2002; Kane et al., 2007). However, conglomerates at distal fans have not been studied well in terms of relationship to bounding sandstones or mudstones, except a tectonically comparable submarine basin of the Var River located in the Maritime Alps of the southeastern France (Stanley, 1980), which is later discussed as an analogue for the Los Molles Formation.

For this study, coarse grained lobes and conglomerates deposited in distal fan area are described, a series of facies association (sedimentary structure, depositional process and environment, bed thickness and continuity, grain size) and architectural elements (stacking pattern) are analyzed in divisions of different scale of elements: lobe, lobe complex, and fan (size ascending from lobe). The interpretation of distal lobe deposits and changes in fan architecture suggests substantial degree of external controls such as sea-level change and tectonic activity that generated forward-stacking of coarse sediments in a narrow and confined depocenter. With integrated lobe facies from centimeter bed-scale to fan systems in kilometer-scale, vertical and lateral bed variability was described in a 4.5 kilometers long outcrop correlation of 200 m thick turbidites of the Los Molles Formation succession in the La Jardinera area (Fig. 1). Applying interpreted facies data and architecture of the outcrop-based lobe models led to a better understanding of coarse grained distal lobe deposition in the basin floor setting.

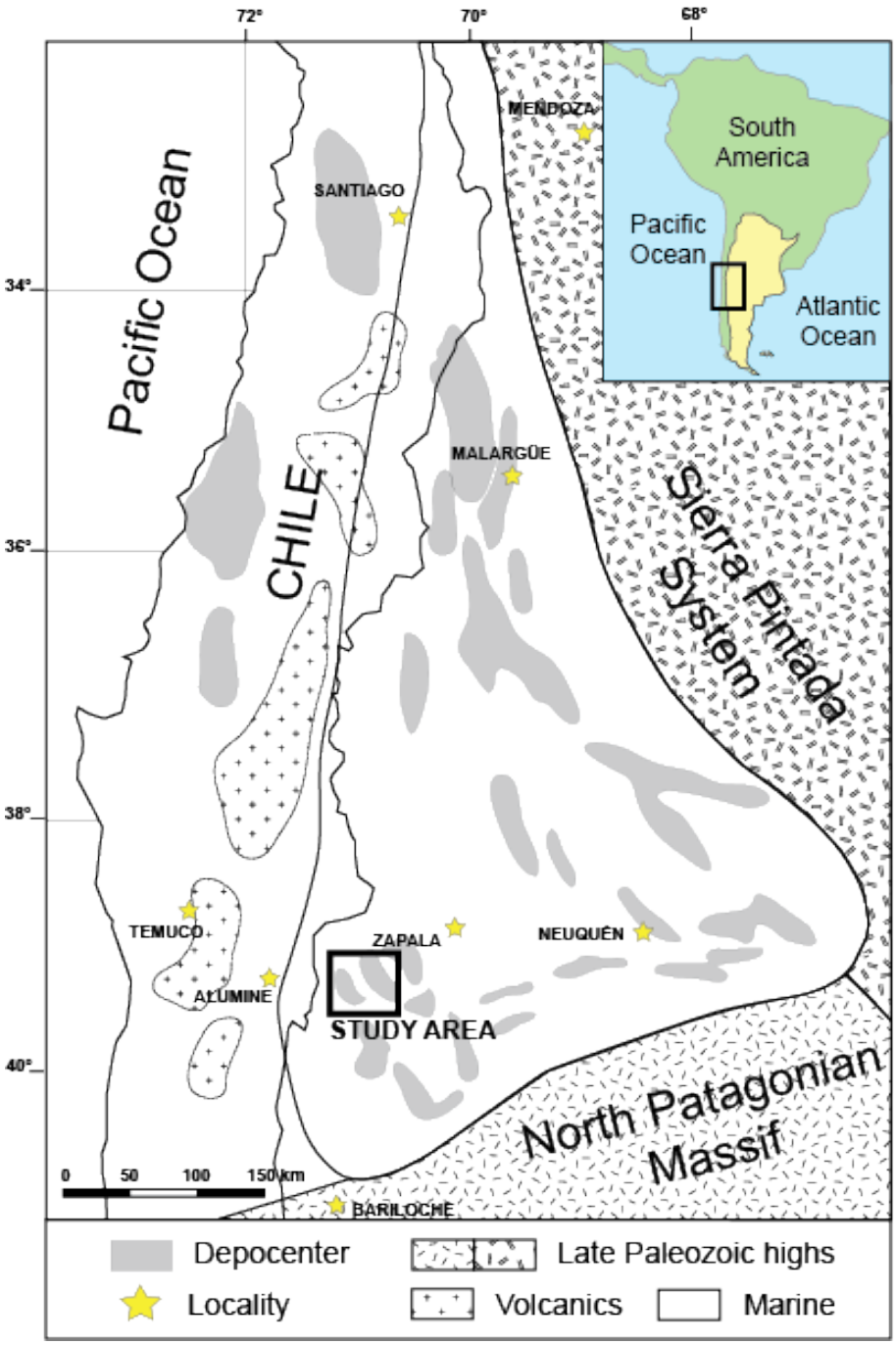

Figure 1. Regional map of the Neuquén Basin and the study area with rift depocenter distribution and adjacent highs (Sierra Pintada Massif to NE and North Patagonian Massif to S-SE). The area of study is located at SE of Alumine, approximately 39.36°S/70.7°W (Modified after Franzese et al., 2006; Tudor, 2014).

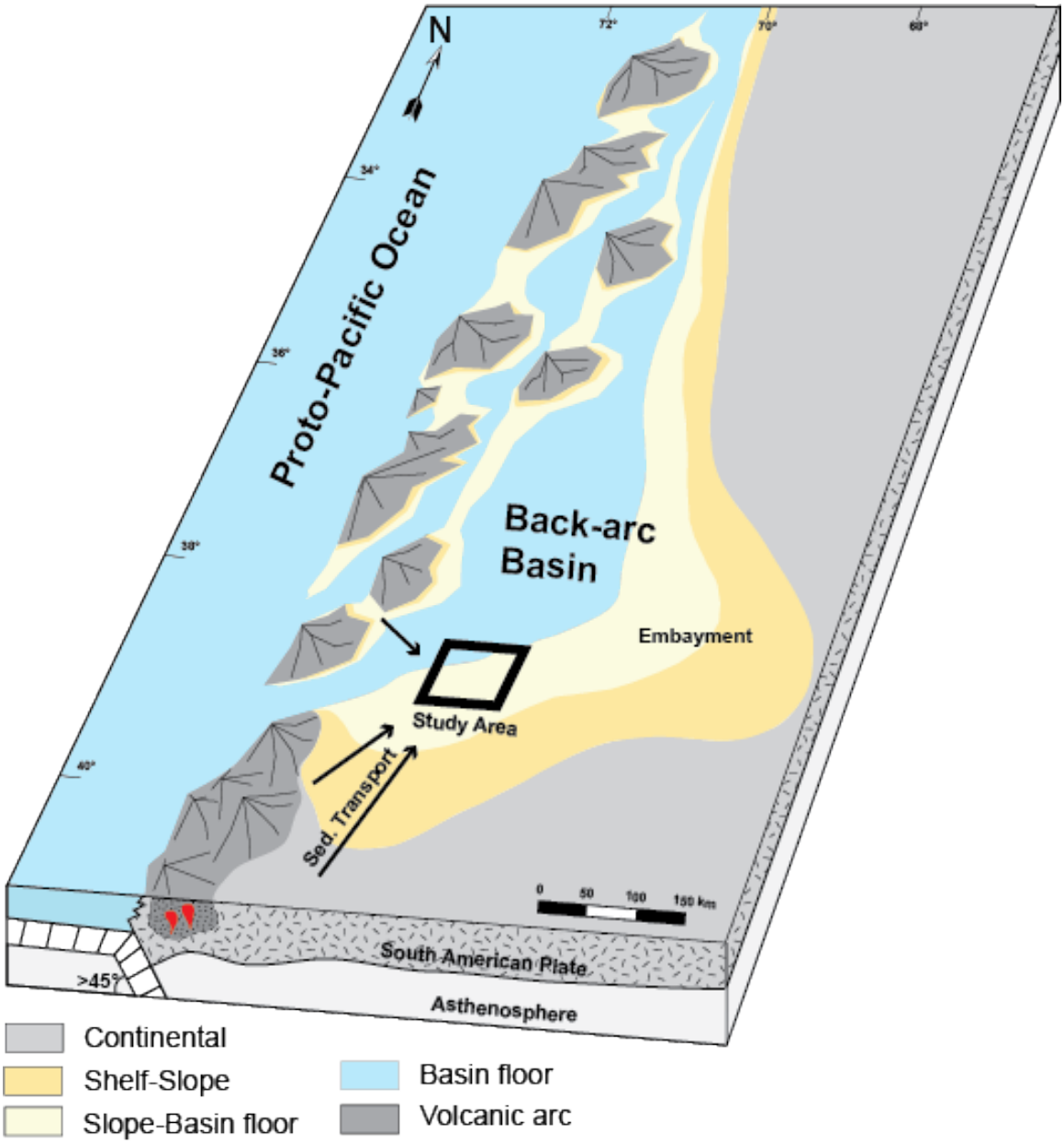

Figure 2: Paleogeography of the study area during the Late Triassic-Early Jurassic period; Retroarc foreland basin developing from inversion of previously formed backarc basin (Modified after Howell et al., 2005).

2. GEOLOGIC SETTING

As a part of the Mesozoic back-arc basin along the southwestern South America between 36° and 40° S, the Neuquén Basin (Fig. 1) records multiple tectonic movements during the periods between the Early Triassic and the Early Jurassic (Ramos, 1988; Legarreta and Uliana, 1991; Vergani et al., 1995). The Neuquén Basin is infilled by both marine and non-marine deposits with siliciclastics, carbonates, evaporates, and even pyroclastics deposits over more than 160,000 km2 (Fig. 2) , while the Andean Cordillera bound the westward margin of the basin and the Neuquén Embayment begins to grow toward the east (Paim et al., 2008). During its 220 Ma Neuquén Basin history and subsidence, over 7000 m of an Upper Triassic-Cenozoic stratigraphy was associated with the significant fault development leading to unconformities and structural inversions (Vergani et al, 1995). The fault-controlled subsidence in the southwest near the study area separated the main basin depocenter in the north by inversion-induced, inter-basin highs (Fig. 3; Burgess et al., 2000). Based on Grimaldi and Dorobek (2011), the east-west oriented faulting zone called as the Huincul Arch divided the Neuquén Basin into the northern and southern sub-basins, and the southern depocenter becomes a target area for this study. The Early to Middle Jurassic Los Molles Formation in the study consists of the first major marine deposits above syn-rift continental units (Fig. 4). The Los Molles Formation is over 1000 m thick, but this study focuses on the lower 200 meters that include two fans and one interfan, underlain by tens of meters thick basin floor mud at base.

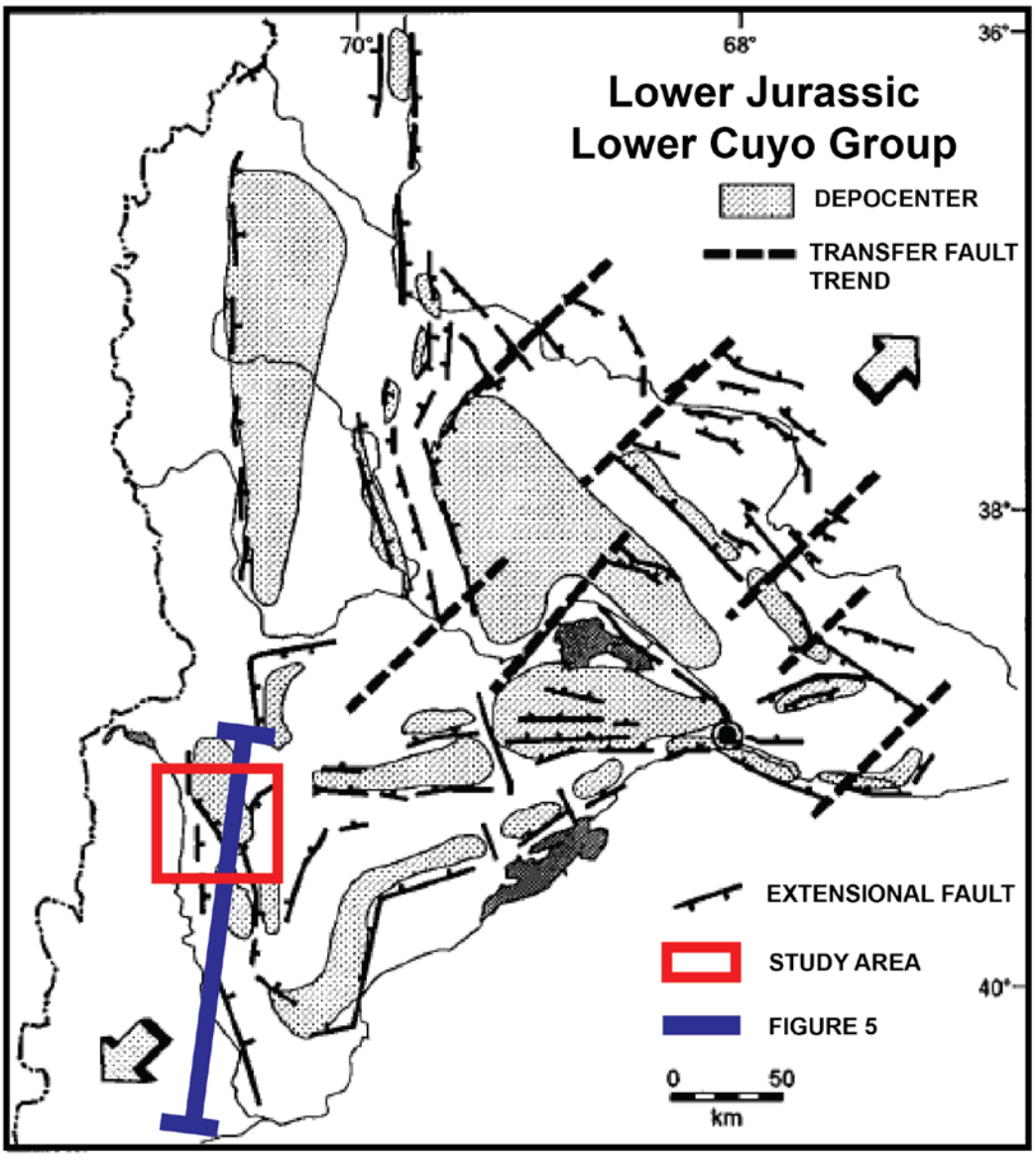

Figure 3: Figure 3. Structural map of the Neuquén Basin during the Aalenian (Modified after Vergani et al., 1995). Note that the blue line indicates the approximate location of Figure 5.

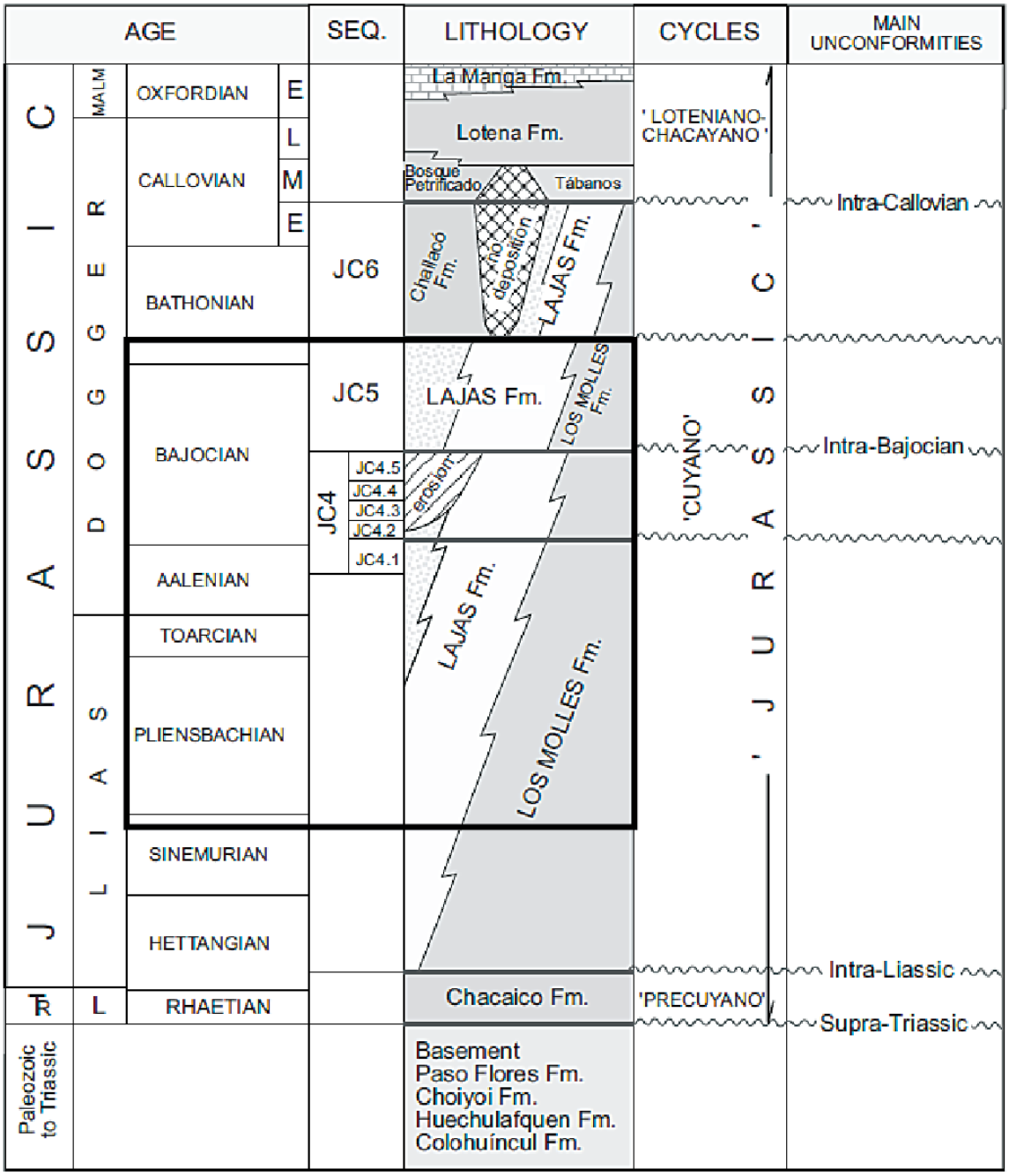

Figure 4: Figure 4. Stratigraphic column of the Neuquén Basin. Note of the black rectangle indicating age controls of lobe deposits found in the La Jardinera region (Martinez et al., 2008)

In terms of sediment source, a western island arc system supplied volcanic materials, and both cratonic Sierra Pintada System at the northeast and North Patagonian Massif at the south shed mature clastic sediments into the basin (Figs. 1, 2) (Burgess et al., 2000). The mixed provenance signatures and diverse fossil faunas found in the Neuquén Basin imply the source of sediment from both island arc and cratonic areas, and suggest that the basin was connected with the proto-Pacific Ocean through gaps (straits) in the arc system (Burgess et al., 2000). The inter-basin passageways around the volcanic arc were enlarged by the back-arc subsidence that led to the expansion of the marine realm and deepening of the basin (Spalletti et al., 2000; Macdonald et al., 2003). Multiple reactivations through different phases of Mesozoic extension and inversion, extensional faults formed in Triassic – Early Jurassic rift basins show the northwest trends and the north-south structural trends (Fig. 3) that imply the maximum deformational stress oriented toward the southwest (Vergani et al., 1995). As a result of steep subduction and negative roll-back velocity, the Jurassic rifting in the Triassic – Early Jurassic period involved northeast-oriented transfer faults after following the pattern of fault offsets, different scales of extensional tracts, variable structural styles, and northeast-trending structural boundaries or sidewalls (Vergani et al., 1995; Ramos, 1999). The structural northeastern trends also controlled the initial dispersion of siliciclastic deposits in the Neuquén Basin. Regional unconformities and subsequent lowstand wedges of the postrift stage seem to be controlled and/or intensified by episodes of tectonic inversion along the preexistent faults (Spalletti and Veiga, 2007).

The distinctive paleoenvironments in the lower Cuyo Group, including the Los Molles Formation (Fig. 2), span from lacustrine, non-marine to marine environments with coarsening-upward trend since the succession incorporates assemblages of various invertebrate faunas (Zumberge, 1993). Ammonoids of the Puchenquia malarguensis,

Pseudotoites singularis Assemblage Zones and an ammonoid fauna assigned to the Emileia giebeli submicrostoma Assemblage Subzone found approximately 30 km NE of the study area may correspond to the local ammonite assemblage of La Jardinera (Westermann and Riccardi, 1979; Zavala, 1996). The calibrated biozonation and stratigraphic sequence analysis using fossil records suggest the approximate age for the ammonite-bearing Los Molles Formation in the central-western Neuquén Basin as late Aalenian (174 Ma) to early Bajocian (168 Ma) (Martinez et al., 2008). Relative changes of sea level in Cuyo Group were initiated by retrogradation and transgression during Pliensbachian (190.8 Ma) to Toarcian (174 Ma) period (~15 Ma), followed by rapid clastic progradation between Aalenian (174 Ma) and Bathonian (166 Ma) time, and terminated by a relative sea-level fall and subsequent basin desiccation during the middle Callovian (163-166 Ma) (Legarreta and Uliana, 1996). The Los Molles Formation consists of shale, turbidites, and lenticular sandstone, and began to deposit in structurally low elongated depocenters when the basin involved several episodes of fault-controlled subsidence and northeast-oriented extensional faults in the Pliensbachian-Toarcian period (Figs. 1, 3; Vergani, 1995). Tectonically well-constrained setting such as the La Jardinera region provides an ideal environment to understand basin floor and coeval shallow-water-equivalent deposits for their facies distribution and geometry interpretation at lobe-scale.

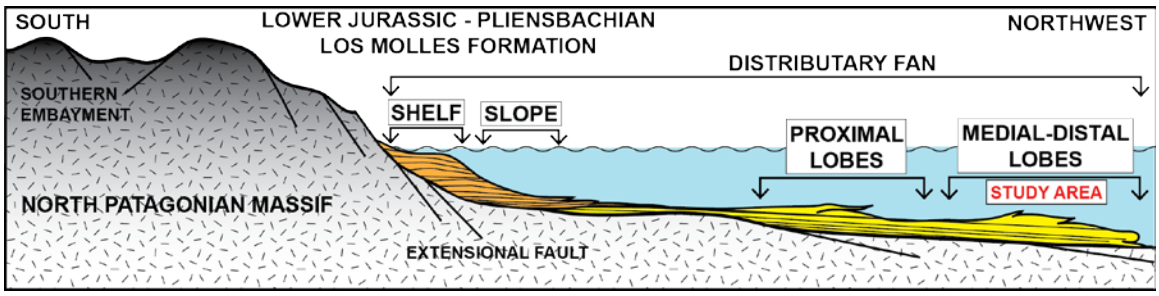

Figure 5: Cross-section of the reconstructed paleogeography of the study area in the lower Jurassic periods (Pleinsbachian-Aalenian).

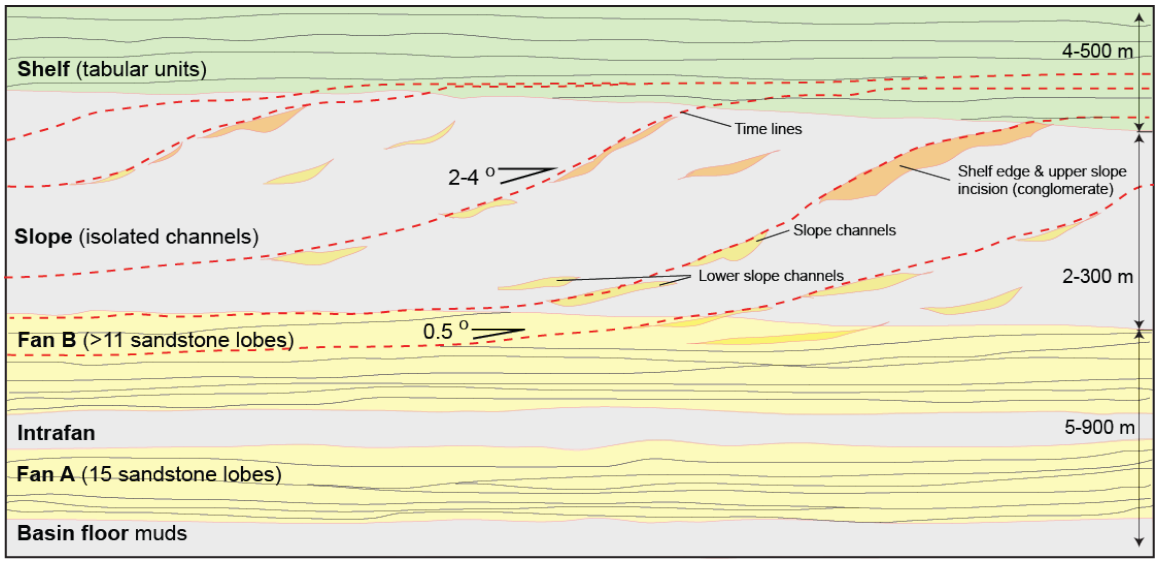

Figure 6: Regional-scale, source-to-sink clinoform sketch model in La Jardinera area which compile observations from Vann (2013) and Tudor (2014). This study focus on the lower deposits of “Fan A”.

3. METHODOLOGY

The studied basin floor deposits in the Los Molles Formation display the base of a source-to-sink depositional environment exposed in outcrops extending in a belt of over 20 km that cut a slice through entire basin margin stratigraphy from shelf to basin floor (Figs. 5, 6). Oriented slightly oblique and down-dip to the basal clinoform of the La Jardinera region, the outcrop dataset exhibits submarine lobe deposits along approximately 3.5 km in the N-S dip orientation and 3.3 km in the W-E strike orientation (Fig. 7, 8). To perform an outcrop-based study for facies variability and architecture, high-resolution satellite imagery (0.5 m) and Digital Elevation Model (1 m) have been used to build a basis for the analysis of different stratigraphic facies models. Using both Global Mapper and Google Earth defined base surfaces for three different units and indicated how each unit varies in relative vertical thickness and lateral extent.

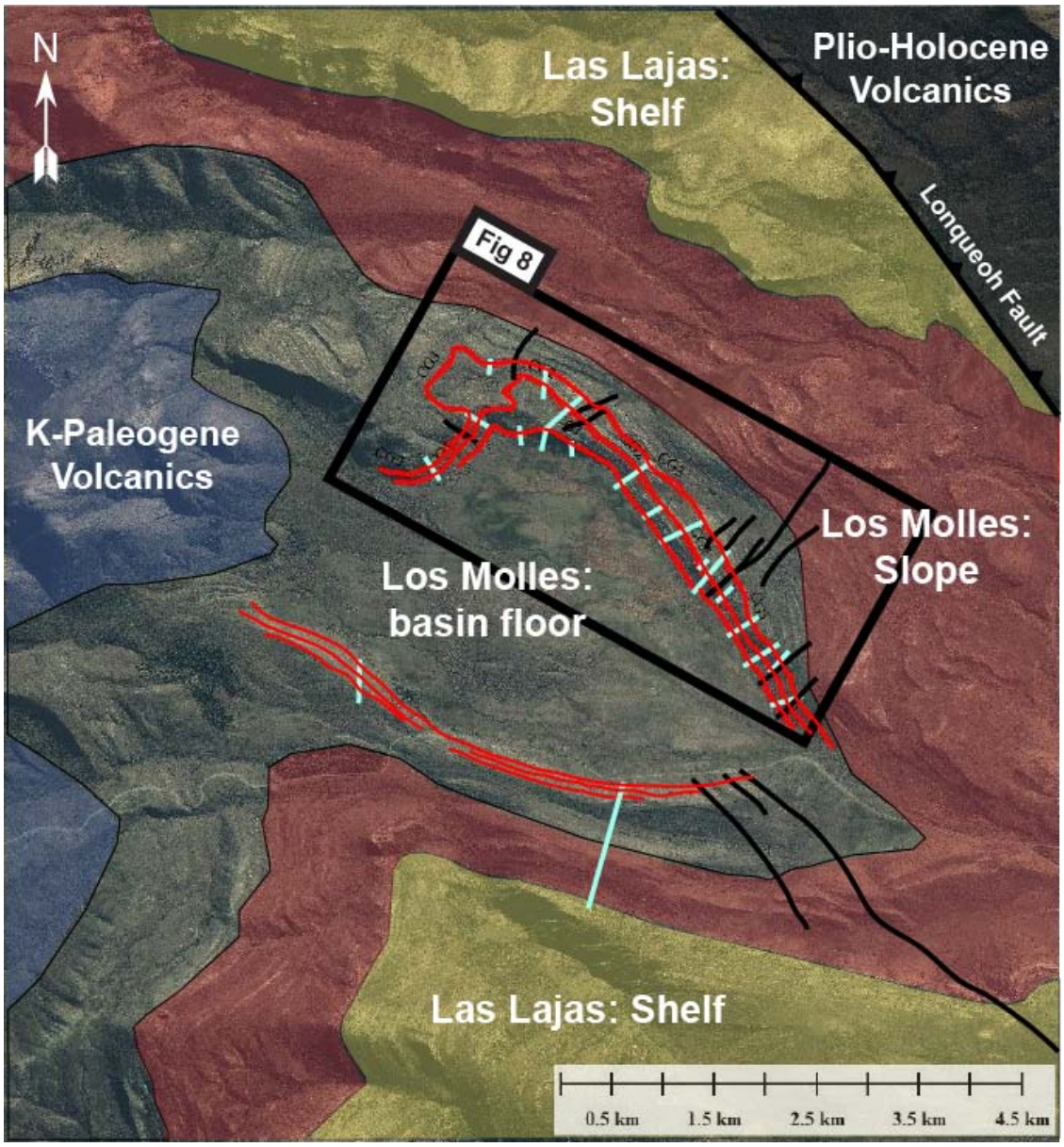

Figure 7: Local stratigraphy and depositional system in La Jardinera area (Modified after Paim et al., 2008; Morabito et al., 2012; Vann, 2013; Tudor, 2014)

For a transect laterally extending ~5km with the NW-SE trending orientation and vertically over 100 meters thick in the Los Molles Formation, the total of 19 graphic logs (total ~2,395 m thick) of the sedimentary successions were collected (Figs. 7,8) to understand the facies variability of both dip and strike outcrops. Two measured sections across the center dome (~2.4 km away from the main transect) toward the SW, which follows the whole outcrop belt and are closer to the relative coeval slope and shelf, allowed observing how facies vary away from the source in a dip direction. Correlation of 17 measured sections in the main outcrop belt demonstrates the stratigraphic relationship of multiple lobes and assigns unit for each thick conglomerate bed in addition to packages of sandstone beds associated mudstone beds (lobe) (Conglomerate = CU) based on unit thickness, bedding transition, facies, facies association, and succession trend. Heavily vegetated intervals are counted as mudstone units that conserve soil on surface, in the ravines where the entire stratigraphy is exposed the mudstone correspond laterally to vegetated areas. The correlation has its datum at the top of the third conglomerate unit, which overlies one of the thickest mudstone units. High resolution (Gigapan) photomosaics were collected for hundreds of meters- to kilometer-scale outcrops and used to build bedding diagrams (bed and bed set correlations) and locate the measured sections (Fig. 8). Almost equidistant measured section ensured more accurate observations of changing facies in terms of grain size, bed thickness, geometry, and type of depositional processes. Within each unit, the detailed observation of different lithofacies allowed the interpretation of depositional environment and various architectural elements in the field. Each measured section has the information on bed thickness, bed top and bottom surfaces transition, grain size, sedimentary texture, bedding orientation, and paleocurrent orientation.

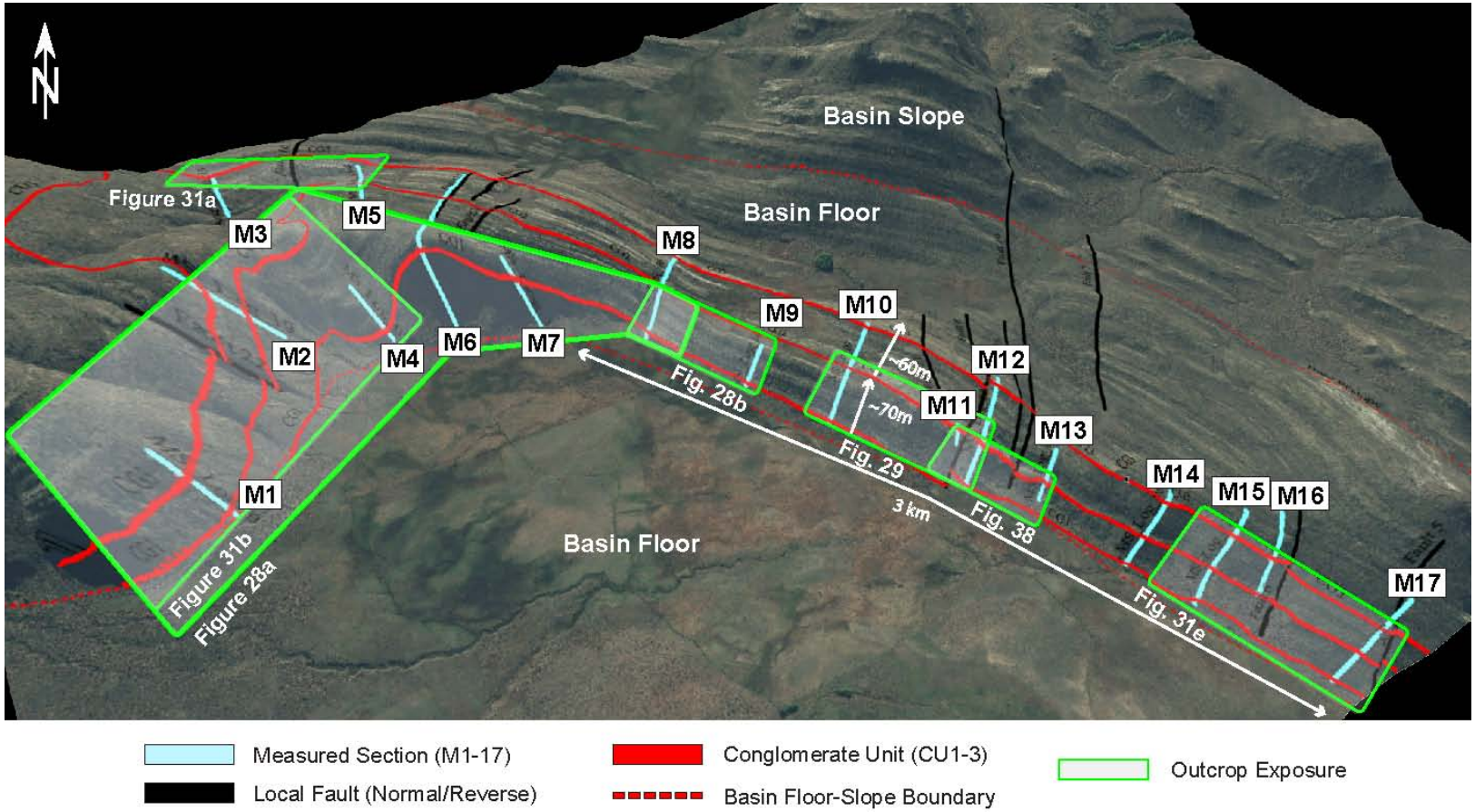

Figure 8: A 3D map of the studied outcrop with measured sections and photopanel locations. Each cyan-colored line represents location and thickness of measured sections. Red horizontal lines show three conglomerate units. The lowermost dotted line reflects the base of outcrop. Black lines are local normal and reverse faults that produce meter-scale small offsets.

Ripples and flute marks preserved at the bottom of conglomerate and structureless sandstone beds were used for flow indicators and indicate the general paleocurrents in W-E direction. When logging at the field, a GPS device was used to collect the exact location of the base and the top of each measured section. A 1.6 m Jacob's staff labeled with 10 cm increments made the measuring process efficient with a magnifying Abney level (clinometer). The level fixed at the top 1.5 m measured the degree of dipping beds as seen looking downward and perpendicular to strike direction.

In order to describe lobe systems, modified terms have been used from Prelat et al. (2009). The longest and parallel to a lobe axis, lobe length can be divided into 'proximal', 'medial', 'distal', and 'fringe' from a lobe apex (lobe mouth) to the opposite end. Lobe width, perpendicular to a lobe axis, is determined by the longest transect across the paleoflow direction and separated to 'axis', 'off-axis', and 'fringe' (Fig. 9). The outcrop-based hierarchy of architectural elements of lobes is defined by relationship between bed geometry (lateral/vertical variability) and facies of thick- to thin-bedded sandstones and bounding mudstones. The hierarchical divisions of lobe deposits begin with: a bed (a single event deposition of turbidite sandstone capped by mudstone; <1-2 m thick), a lobe (two or more sandstone units interfingering with mudstone; few meters thick), a lobe complex, (multiple lobe succession; >10 m thick), and a fan (a succession of multiple lobe complexes; tens to few hundreds of m thick) (Figs. 10 and 11).

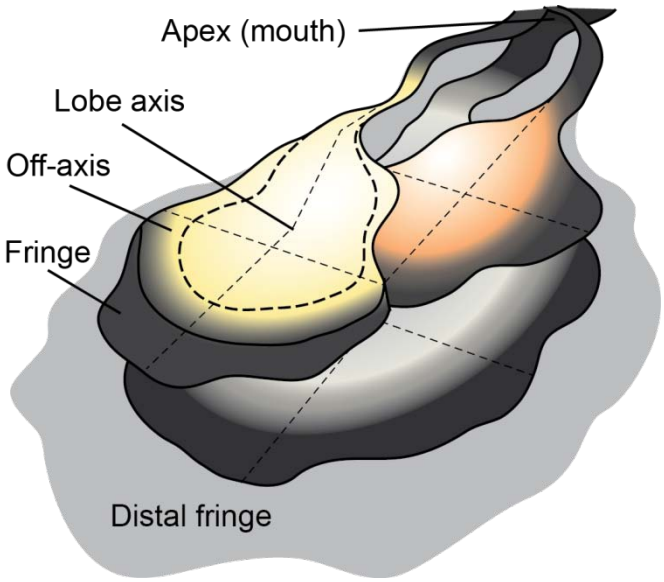

Figure 9: A representative basin floor lobe showing variable parts along the length and width. No scale.

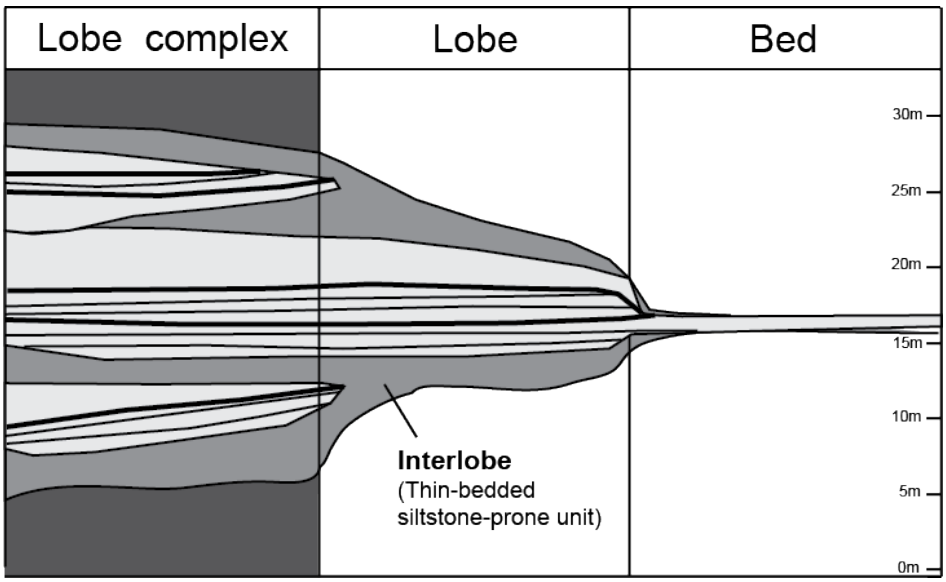

Figure 10: Hierarchical scheme representing three scales of elements used to define a deepwater fan: bed, lobe, and lobe complex. Lobes separated vertically by heterolithics (thin bedded, sand-prone siltstone-mudstone and silty mudstone; interlobe), and thick intervals of mudstones separated lobe complexes (Modified after Prelat et al., 2009).

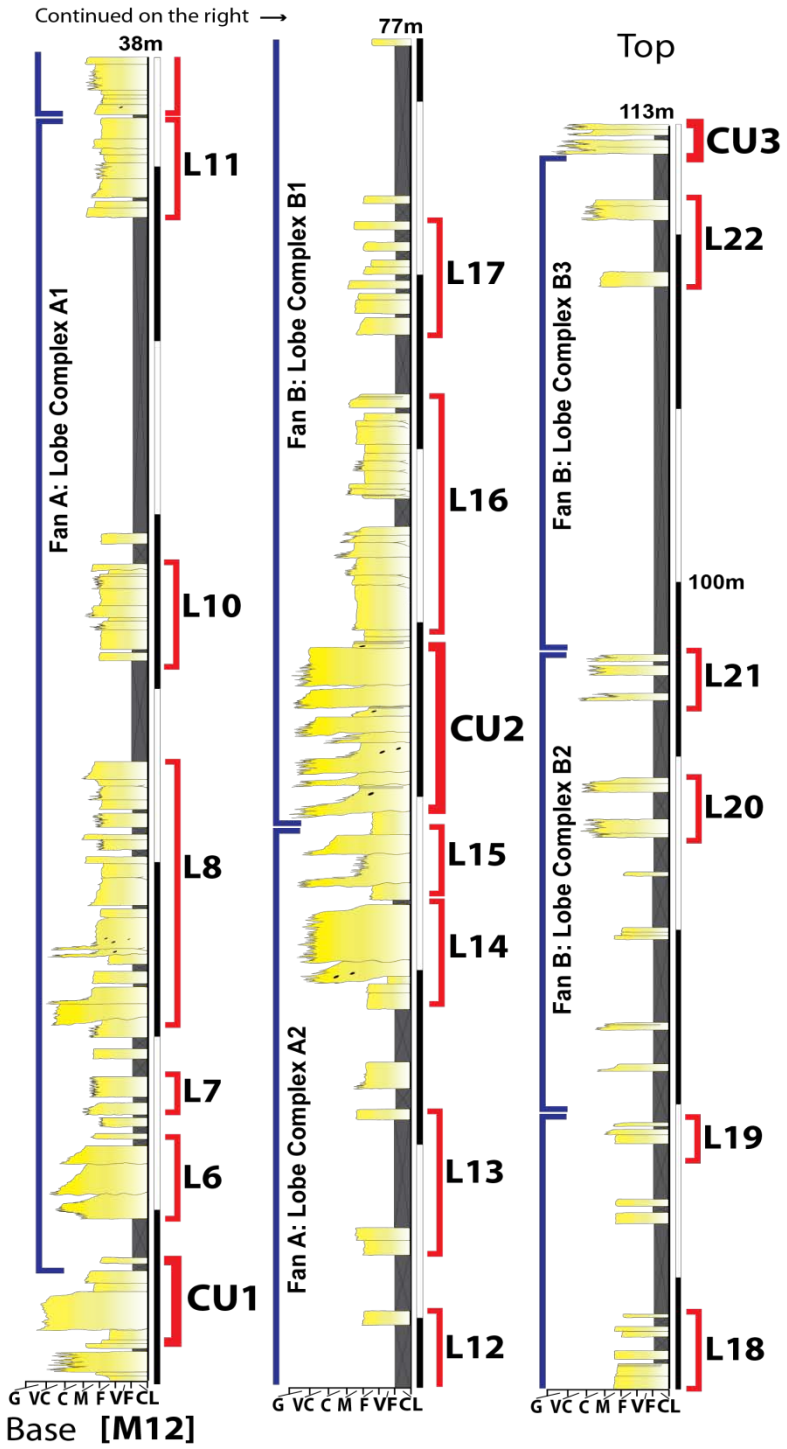

Figure 11: A representative measured log profile (M12) located close to the center of outcrop correlation. Note that M12 clearly shows all three conglomerate dominated units (CU1-3) and 17 sandstone dominated lobes.

4. RESULTS

This study focus on a 200 meters thick and over 4 kilometers extensive deep water fan outcrops which contains coarse grained, conglomerate units. Detail facies description and interpretation is based on multiple vertical measured sections (Figs. 8, 11). Bedding geometry and architecture of the conglomerate lobes are based on high resolution photomosaics (Fig. 8). Three dimensional variability is combining All measured sections, photomosaic mapping, and a high resolution DEM are combined to delineate spatial variability of extensive conglomerates and lobes.

In addition to mudstone, which is presumably covered by vegetation in outcrop, the coarse- to medium-grained sandstone is the most common lithology in the Los Molles Formation in terms of frequency and volume of succession and is the facies building the deep water lobes. The sandstone is the most common lithology of the lobes, and the beds are highly amalgamated and structureless, but exhibits grading at times just before the transition to laminated or interbedded facies. The vertical and lateral facies changes were also observed as tens of centimeters to a few meters thick, sharp-based sandstone beds or bedsets show significant changes in facies and sedimentary textures in a single bed. The very coarse grained (conglomerate) event-type bed is usually thick and undulating as it becomes vertically transitional from pebble to very coarse-grained sandstone to planar- or ripple-laminated fine-grained sandstone. For this study, seven distinct facies and five facies associations were separated and discussed below.

4.1 LITHOFACIES

4.1.1 Facies 1a (F1a): Clast-supported conglomerate

Description: Clast-supported, poorly sorted, 10 cm- to 2 m-thick conglomerate beds contain highly disorganized pebbles, cobbles (Figs. 12a-b, 12d-e). Mud clasts are common at the base with size of mud clasts in range of 1 to 20 cm. While mud clasts are preserved randomly within bed, ones bigger than ~10 cm often are found at the base. Normal-grading is observed at the middle to upper half of some beds with very coarse to medium sands (Fig. 12a). Well- to sub-rounded, very poorly sorted, extrabasinal clasts are comprised of metamorphic or volcanic clasts sourced from the North Patagonian Massif present south of the study area. The clast size ranges between upper-medium (< 0.5 mm) and cobble (~5-7 cm). Bed base is sharp to erosive, when cut into the underlying mudstones or thinly bedded sandstones. Protruding basal contacts occasionally show flute casts and sediment loading. Beds are locally discontinuous (significant thickness changes) and undulating with few local scours (Figs. 12b, 12d-e). However, despite the lenticular geometries, the three major conglomeratic units (CU1-CU3) have an outstanding lateral continuity in a regional scope, larger than the outcrop exposure (>4.5 km).

Interpretation: Clast-supported conglomerates are interpreted as cohesive debris flows or hyperconcentrated density flow (friction-dominated), creating particle interactions with very high sediment concentrations (>25 volume %) (Mulder and Alexander, 2001). Random clast-supported grain dispersion and flute casts at basal contacts, the lower two-thirds of unit might reflect some turbulent flow. In contrast, the matrix-supported, upper one-thirds indicates weak turbulent flow followed by laminar flow as cohesive or hybrid-type debris flow (Haughton et al., 2009). Thus, disorganized sedimentary structure and weak internal transition from clast- to matrix-supported regime

suggest both non-cohesive and cohesive flows during deposition of the coarse grain beds of F1a. In many beds, fairly undulating and discontinuous bed boundaries indicate a deposition that occurred instantaneously by a fast and frictionless flow that was probably erosional and bypass on slope, and depositional at basin floor. Such cohesive flows allow gravels and very coarse sands from shelf to be transported on the slope and basin-floor (Mulder and Alexander, 2001). A laminar flow within debris flows, as observed toward the base of some beds, can be initiated by turbulence suppression and can transport large clasts further down to distal lobe areas (Mulder and Alexander, 2001).

Facies 1b (F1b): Matrix-supported conglomerate

Description: Silty to muddy matrix-supported, structureless, poorly sorted, ungraded conglomerates contain pebbles and cobbles less than 15% of the total volume (Figs. 12c-d). Clasts have no signs of imbrication or any sedimentary pattern, however more angularity (sub-angular to sub-rounded) than clast-supported conglomerates. Mud rip-up clasts are present, but are less common than gravels. Bed contact is sharp, yet occasionally erosive while bounded by thin- or thick-bedded sandstones. F1a is observed significantly less than clast-supported conglomerate (F1b); however its occurrence increases closer to the sediment source (to the south).

Interpretation: Matrix-supported conglomerates are interpreted as in condition of non-cohesive debris flow deposits of which the muddy matrix within a flow causes non- or less cohesive current downdip (Haughton et al., 2009). Based on the muddy matrix, F1b can be classified as muddy ‘debrites’ formed by a very high-energy, laminar flow (Talling et al., 2004; Jackson et al., 2009). Randomly deposited clasts and mud rip-ups reflect an abrupt collapse, freezing and deposition of a previously high turbulent flow.

The freezing of the flow occurs with *en masse* settling of sediments (Lowe, 1982; Talling et al., 2012). Deposition can occur at slope, proximal fan, distributary channel axis, and as far as medial-distal fan where conglomerates become gradually thinning laterally.

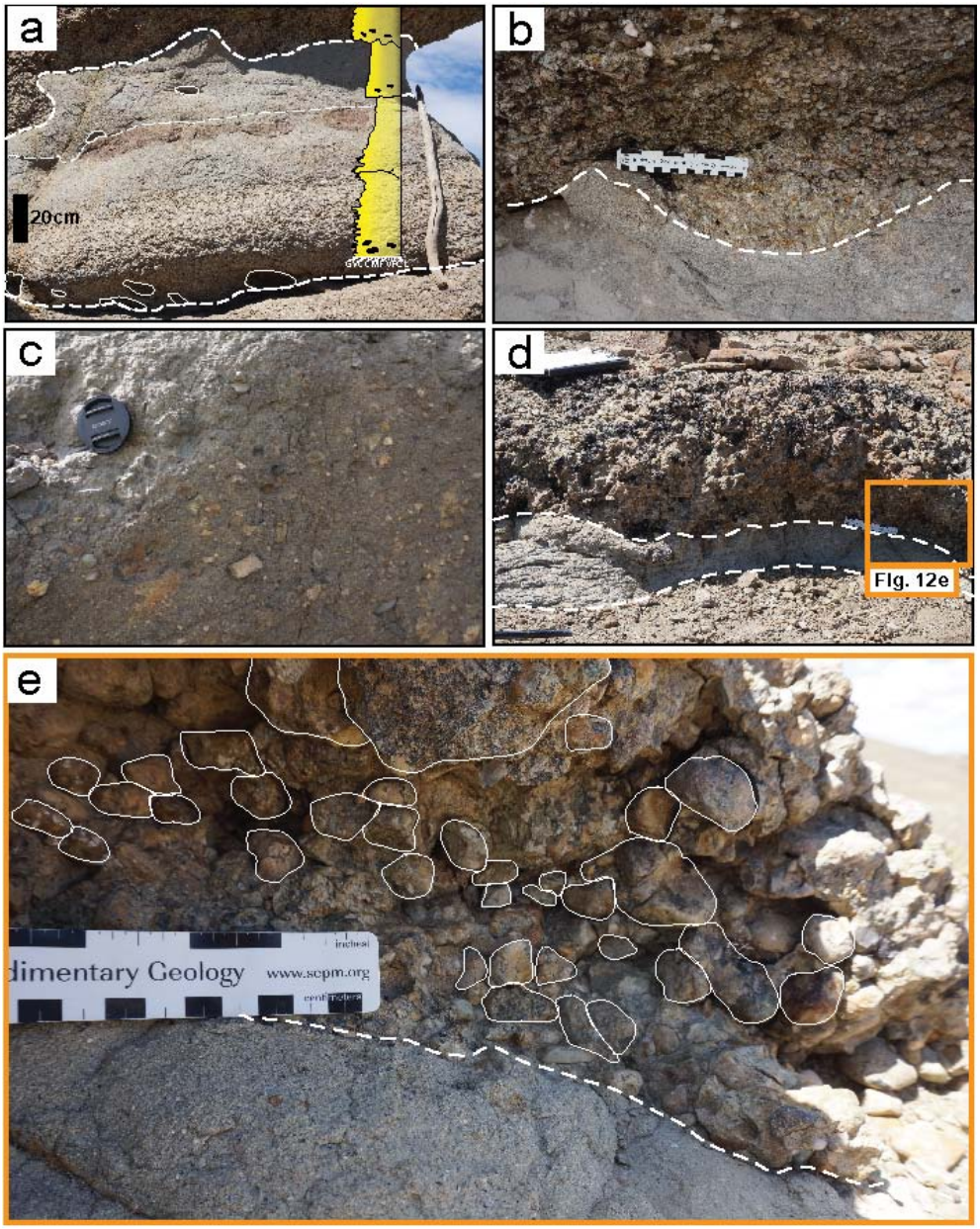

Figure 12: Clast-supported and matrix-supported conglomerate. (a) A thick, normal-graded, very coarse- to medium-grained sandstone bed that contains small pebbles and mud rip-up clasts (10-20 cm) at the base. A few mud rip-ups floating within the bed; Wood stick = 1 m. (b) Erosive basal contact above a very coarse to medium-grained poorly sorted sandstone, implying a high-energy, cohesive debris flow that erodes an underlying sandstone bed. (c) Sub-angular, matrix-supported conglomerates. (d) A thin-bedded, weakly laminated, coarse grained sandstone bed truncated by clast-supported conglomerate with erosive bed contacts. (e) Large clasts deposited very closely, almost touching each other, in the clast-supported conglomerate.

4.1.2 Facies 2 (F2): Amalgamated sandstone

Description: Structureless, very coarse- to fine-grained sandstone beds have a thickness range of 0.1-1 m. Multiple beds stack and amalgamate forming up to 3 m thick sandstone beds (units) (Fig. 12a). The amalgamated surface is represented, and commonly can be recognized), by transitional or abrupt change in grain size and sorting and occasional scour-lag clasts. Well to moderate clast sorting varies vertically, but generally improves toward upper half with weak normal grading and faint laminations. Occasionally erosive, sharp-based beds directly overlie other amalgamated sandstones or silty mudstones. Well-rounded mud rip-up clasts (1-15 cm; Fig. 12a) are observed at the base. Several tool marks and flute casts were found in this facies at the base of the beds and indicate paleocurrent direction to W-E (Figure 14a). The number of collected flow indicators is 9 in total.

Interpretation: The sharp bed contacts overlying the heterolithic sand/mudstones or silty mudstones imply an abrupt change of the flow energy and in depositional environment. The occasional incorporation of the mudclasts and outsized clasts at the base of the beds suggest the flows were highly energetic and erosional updip of the observed area. As the high density turbidity current weakens and dilutes downdip direction, degree of amalgamation and sandstone thickness significantly decreases. Abrupt particle fallout onto beds caused by rapid deceleration or suspension rate suppresses development of tractional structures or grain sorting at the base and leads to the formation of structureless deposits (Lowe, 1988; Kneller and Branney, 1995). Also, overriding turbulent flow, sequential collapse of laminar sheared layers with high bed aggradation rates (experimentally >0.44 mm/s) are able to generate structureless and ungraded beds (Sumner et al., 2008). Therefore, changing velocity of turbidity flows and

aggradation rates can explain the poor sorting and occasional normal-grading observed in the beds. Gravel to very coarse grains and mud rip-ups at the base of the beds reflect a very high-energy flow that is capable of scraping mudstones along slope or proximal basin floor. Increased density difference within a turbulent flow, or a constant laminar flow may be responsible for rip-up clasts deposited at the bed top (Cartigny et al., 2013; Jackson et al., 2013).

The sand-rich turbidity flow can transport sediments as bedload and generate thick-bedded sandstones in distal basin floor setting (Mutti and Ricci Lucchi, 1972; Walker and Mutti, 1973). Thus, F2 can occur from slope channels where the flows are highly energetic and capable to transport coarse sediments to proximal or even distal (when channels are present) basin floor lobes. Migrating lobes associated with high density turbidity flows can sweep over abandoned, distal fringe areas (Lowe, 1982) as younger lobes prograde. The structureless, amalgamated bed patterns are generated by active switching of flow axis in lobe and stacking on top of previous deposits. Occasional scour-lag clasts found along amalgamation surfaces (Fig. 12a) indicate the high degree of basal plucking on lobe floor by high density turbidity flows, and clast-fill in deep eroded scours. It is also possible that coarse clasts were transported within a traction carpet of turbidity current which hardly incorporates into the overlying turbulent flow. As a consequence of the separation, large clasts highly concentrate at base of thick sandstone beds with limited transport distance due to high concentration flows or possibly slumping (Johansson and Stow, 1995).

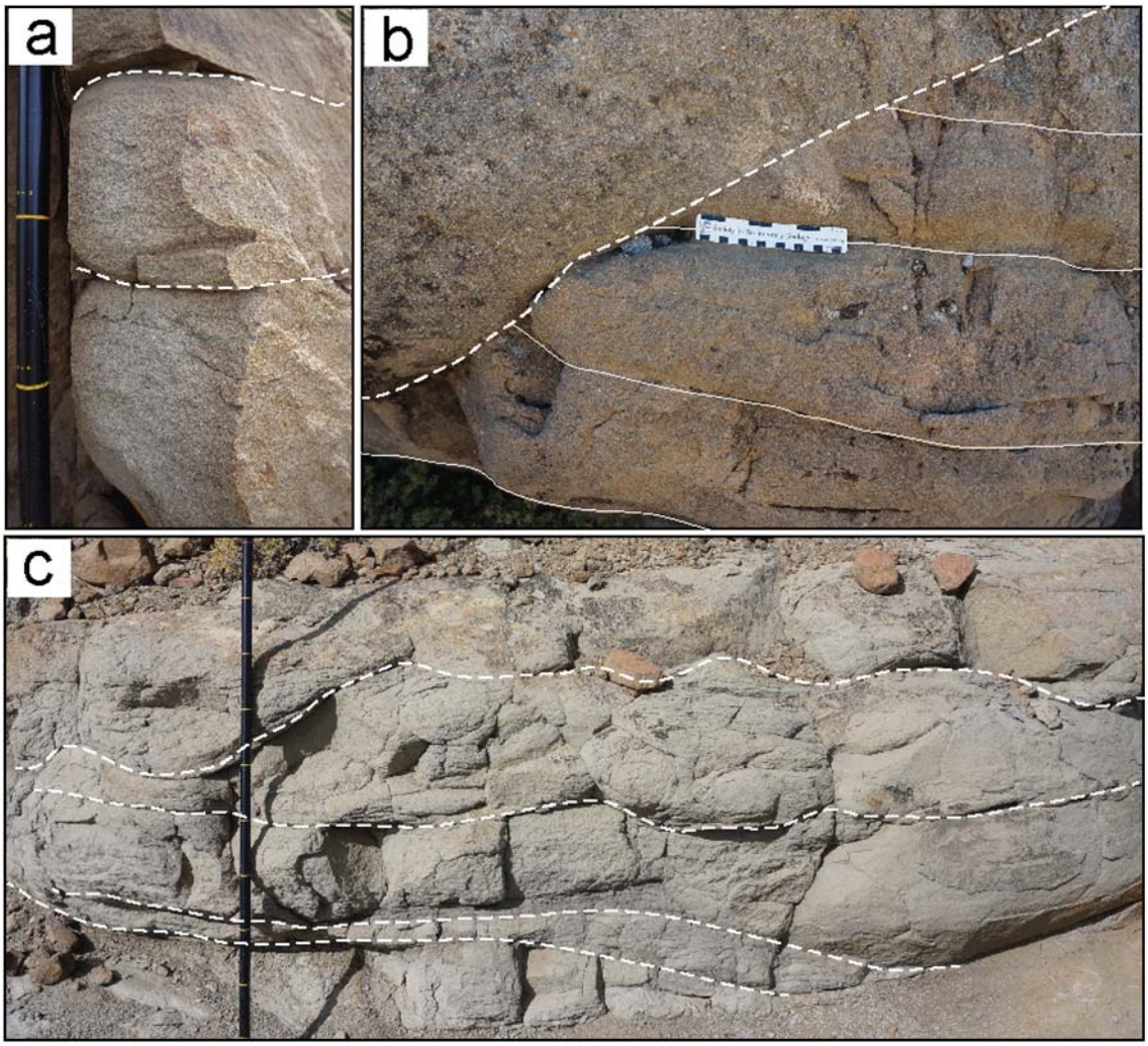

Figure 13: Facies 2 (F2): Amalgamated sandstone. (a) Three different sand-rich beds stacking together in an amalgamated form. Note structureless, massive, tabular structures of beds; Jacob's staff labeled 10cm increments. (b) Amalgamated beds cut by a tilted, blocky, very coarse sandstone. (c) Irregular contacts between bounding beds within an amalgamated sandstone; Jacob's staff labeled 10cm increments.

4.1.3 Facies 3 (F3): Normal-graded sandstone

Description: Laterally extensive (0.5-3 km, often over 4 km), normal-graded, and tabular sandstone is usually very coarse sand to medium gravel (<1.5 cm) at the lower part of the bed associated with sharp to erosive base, and gradually changes to medium and fine sandstone at the upper part of the bed (Fig, 14). A 0.2-1 m thick for a single bed while multiple beds (bedsets) stack up to 3 m thick. Underlying beds are occasionally scoured and filled. Some flute marks, fossil fragments or large clasts were found at the base of the beds. Very coarse to coarse grained, inverse-graded sandstones are occasionally found in conjunction with normal graded beds below. Normal graded beds commonly form amalgamated sandstones with undulating geometry at times. Rare flute casts indicated dominant NE paleoflow directions (Fig. 14b). The number of collected flow indicators is 3 in total.

Interpretation: As the high density turbidity flow decelerates in a downdip flow direction, coarse sediments as collapsed fall-out from the turbulent flow deposit first, and then fine sediments on top of the coarse beds after a period of suspension (Bouma, 1962; Lowe, 1982). These differences in settling velocities of different grain size fractions cause grading in the sand mainly due to the different time taken for grains of different sizes to settle through a flow, and continuous aggradation beneath a sustained high density turbidity flow (Lowe, 1982; Stow and Johansson, 2000). Simply, finer grains take longer time to settle down on a bed than that of coarser grains. In opposite, inverse grading reflects an increased energy in flow while aggrading the bed, possibly linked with local increase of velocities due to substrate irregularities (Kneller and Branney, 1995), or due to hyperpycnal flows from the river discharge (Mulder et al., 2003). However, the linkage between the river flow to deepwater basin is difficult (Lamb and Mohrig, 2009), especially on the basin floor. However, the inverse grading is secondary

and commonly associated with normal grading which suggest a more local variation of possible long-lived, high energy turbidity flow. The lack of other sedimentary structures such as parallel or cross laminations with normal graded beds may suggest rapid deposition. The deposition of such beds occurs typically in the proximal lobes, more likely near the flow axis where the flow transit from high to low energy and has a slower depositional rate than previously described facies (F1 and F2).

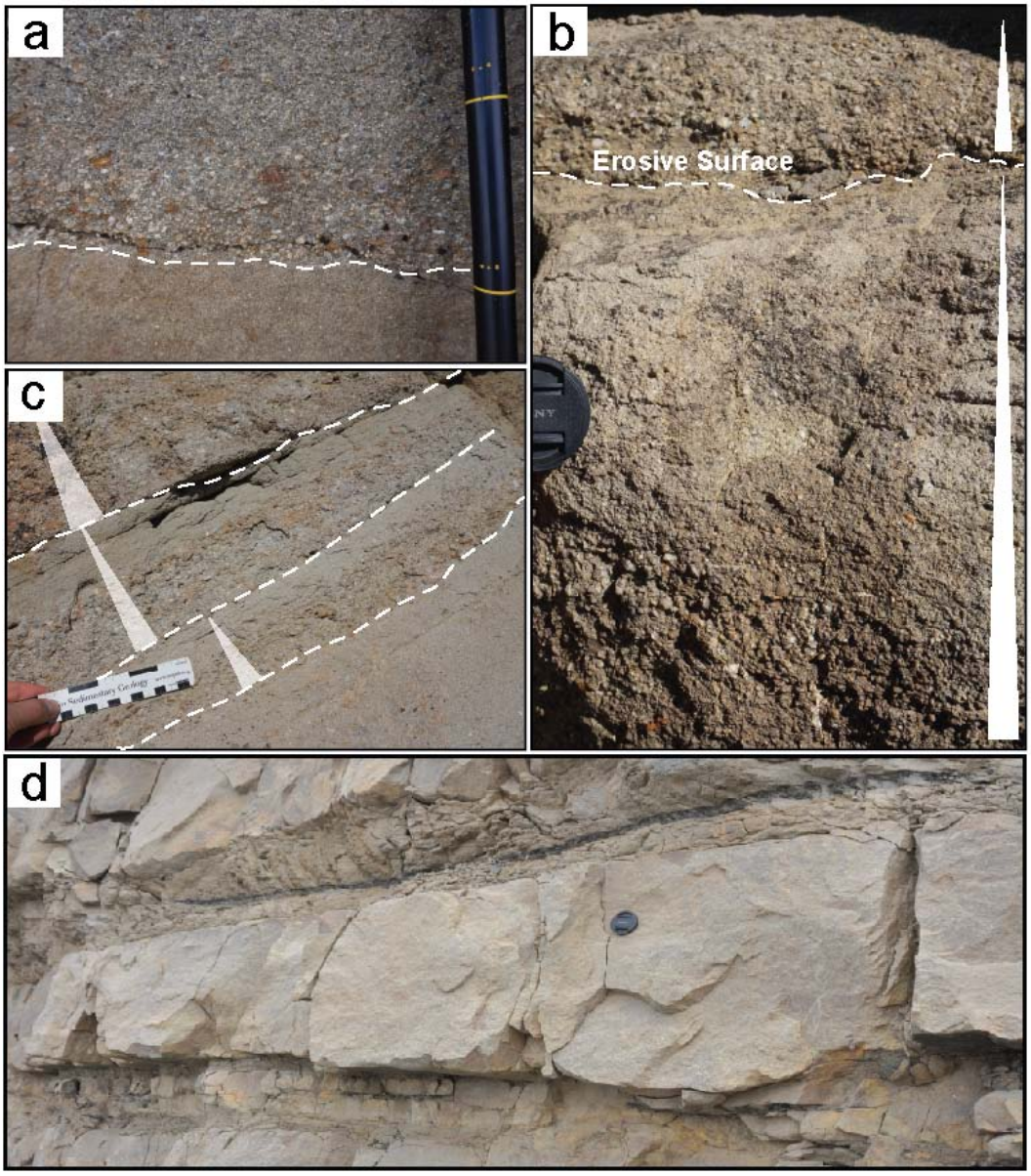

Figure 14: Facies 3 (F3): Normal-graded sandstone. (a) Very coarse, massive, thick-bedded (tens of centimeters to 1 m thick, bedsets up to 2-3 m), normal-graded, laterally extensive sandstones on top of another normal-graded bed. Note the presence of a sharp to erosional basal contact and a small-scale fracture at the base due to high porosity within coarse grains and high sediment loading; Jacob's staff labeled 10cm increments. (b) Normal grading in gravel to very coarse-grained sandstones. Notice erosive bed contacts; lens cap = 40 mm in diameter. (c) Three units of thin-bedded, fine gravels to medium grained sandstones. (d) Tabular, continuous, massive, normal graded sandstones alternating with laminated sandstones and heterolithics. Note the erosional base of the sandstone beds.

4.1.4 Facies 4 (F4): Parallel-laminated sandstone

Description: Conformably deposited on top of amalgamated beds, 5-70 cm thick, upper medium to very fine grained sandstones are planar- and/or low angle parallel-laminated (Fig. 15). The degree of lamination varies at different areas, but majority of the beds tend to be faint laminated. Laminations are frequently found capping graded and/or structureless sandstone beds while being laterally discontinuous.

Interpretation: The presence at the top of the beds, laterally discontinuous and locally faint characteristics imply a depletive flow (T_b) – waning of tractional flow within turbidity current that switches from sand-rich to sand-poor condition, which causes direct sediment fall-outs in association of both hindered settling and sediment reworking (Bouma, 1962; Lowe, 1988). Diluted, sand-poor turbidity current make relatively coarse laminated beds while sand-rich current causing massive and frictionless *en masse* flows below the parallel laminated beds (Talling et al., 2012).

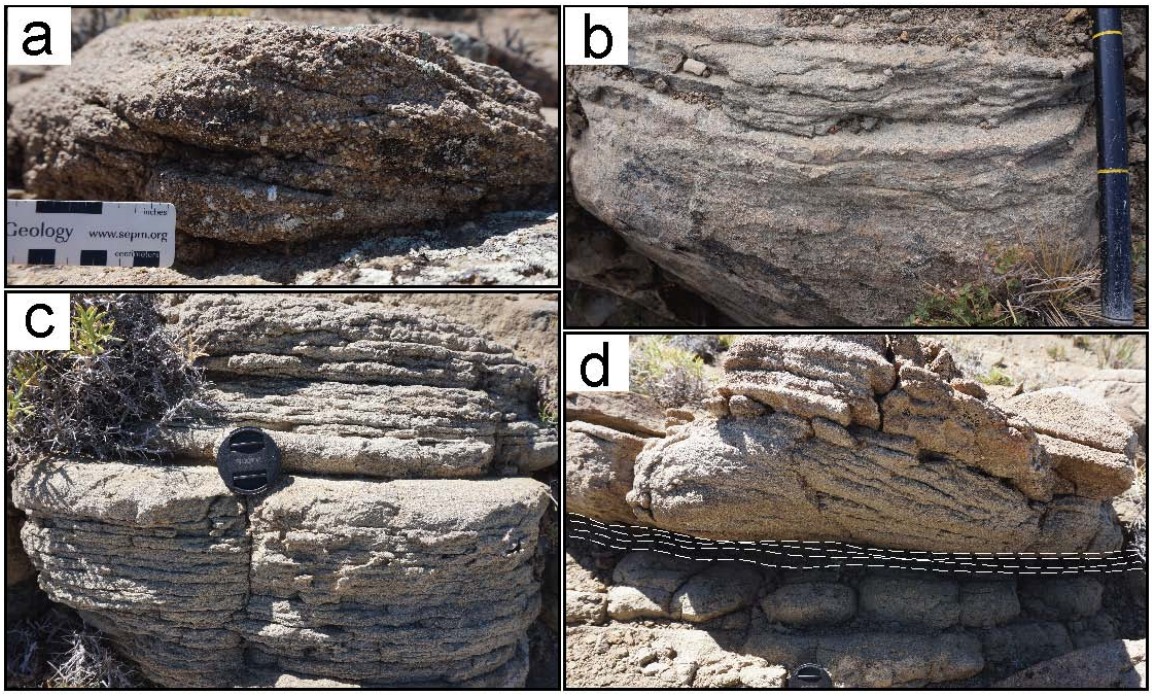

Figure 15: Facies 4 (F4): Planar- and parallel-laminated sandstone. (a) Inclined planar-lamination composed of small gravels and very coarse sands. (b) Facies change from structureless sandstone (F2) to parallel-laminated sandstone (F4); Jacob's staff labeled 10cm increments. (c) Faint lamination; lens cap = 40 mm in diameter. (d) Facies change from F3 to F7. Note that the dark, hidden layer is silty mudstone (F7); lens cap is 40 mm in diameter.

4.1.5 Facies 5 (F5): Ripple-laminated sandstone

Description: Medium to very fine grained, well-sorted, and ripple-laminated sandstones overlay F2-4 sandstones (Fig. 16). Faintly and thinly laminated, 3-dimensional ripples to cross strata in range of 5-30 cm thickness are exposed due to dipping angle of beds and erosion of overlying mud units. Normally sharp to transitional base contacts prevail in outcrop. NE to NNE paleoflows directions were measured by trough cross stratification of ripples. The number of collected flow indicators is 5 in total.

Interpretation: Strongly grain size dependent, ripples and cross-strata occur when particles begin tractional reworking upon encountering a hydraulic jump, an abrupt decrease in gradient and confinement within turbidity currents while subsequent reduction in flow velocity and thickness leads to suspended-load fallout (Bouma, 1962, Sumner et al., 2008, Jobe et al., 2012, Talling et al., 2012). Low density turbidity currents are mainly responsible for generating most of fine to very fine grained ripple-laminations when coarse to medium grained sands associated with suppressed bedload movements deposit in part of normal graded and/or amalgamated facies (Lowe, 1982).

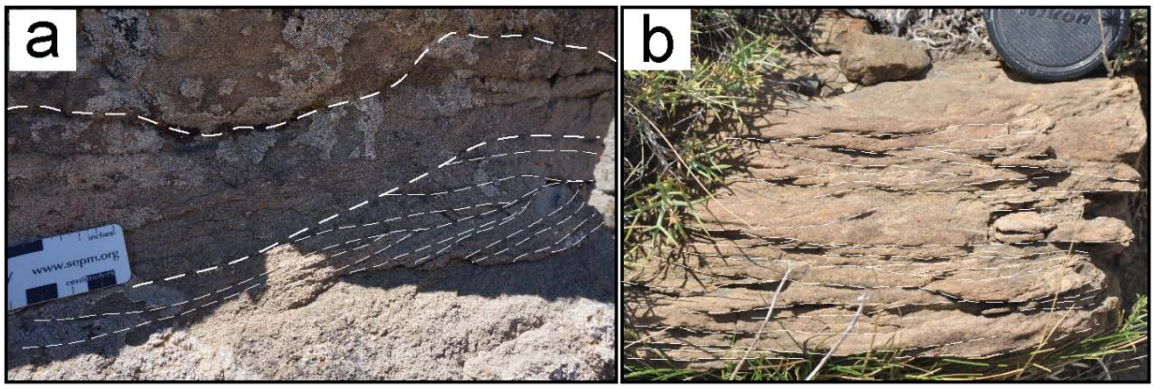

Figure 16: Facies 5 (F5): Ripple-laminated sandstone. (a) Ripple-lamination on top of normal-graded sandstone overlain by an erosive, medium-grained sandstone (b) A stack of ripple laminations; lens cap = 60 mm in diameter.

4.1.6 Facies 6 (F6): Interbedded sandstone-mudstone

Description: Beds of 5 to 30 cm thick, silty/very fine to medium, sharp-based, and transitional or sharp top sandstone form interbedded stacks up to 4-5 m with few millimeters to 15 cm thick, silty mudstone beds (Fig. 17a-b). While both sandy and muddy beds are thin and prone to soft sediment deformation (Fig. 17c), silty sandstone is lenticular and thicker than mudstone in general and often found oxidized to the orange and light brown color. In this facies some large soft sediment deformation (contorted beds) has been observed which was probably generated during *en mass* sediment transport (i.e. slumping).

Interpretation: The repetitive sand-mud deposits reflect alternating low- and high-energy density turbidity currents associated with the changes in grain sizes of suspension fallouts and rates during waning phases (Mutti and Ricci Lucchi, 1972; Lowe, 1982; Kneller and Branney, 1995, Talling et al., 2012). Sediments entrained turbulent flow in suspension spread out with the flow to long distances (tens of km) on the basin floor forming tabular and extensive beds (Mutti and Normark, 1987). The deposition of thin bedded sandstone and mudstone occurs at the base of slope and basin floor in distal and off-axis portion of depositional lobes. The repeated cycles of sheet-like sandstone and interbedded mudstone within basal lobes for kilometers form good reservoir geometries. The sandstone lobes maintain good lateral continuity, but thin bedded facies may depreciate vertical connectivity in reservoirs.

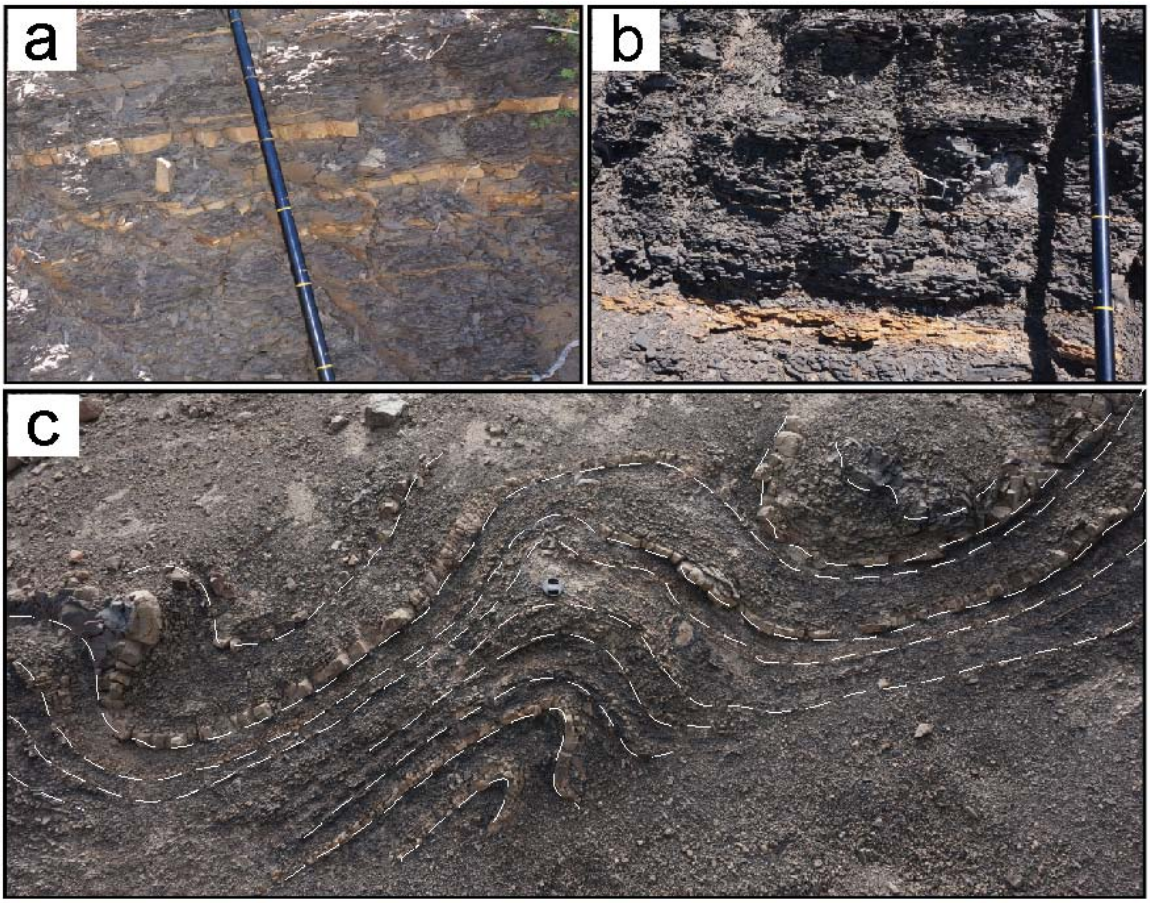

Figure 17: Facies 6 (F6): Interbedded mud-sandstone. (a) Interbedded very fine sandstone and silty mudstone. Note the oxidation on siltstone; Jacob's staff labeled 10cm increments. (b) Siltstone and silty mudstone with very low sand contents. (c) Soft sediment deformation occurring on interbedded sandstone and mudstone; lens cap = 40 mm in diameter.

4.1.7 Facies 7 (F7): Silty mudstone

Description: Dark grey, thinly parallel-laminated, silty to muddy deposits dominate at the base of the Los Molles Formation. Intervals of 1 to 20 cm thick beds, faintly laminated, silt-prone, with very fine sandstone beds commonly found in between. Laminations tend to cease upwards before overlain by coarse sandstones. The few millimeters to 10 cm thick, thinly bedded mudstone (Fig. 18a) beds stack up to ~15 m; however, its total thickness decreases upward stratigraphically. The mudstone facies are usually the most of covered layers (with scree and vegetation) in the measured sections. Microfaunas (~2-3 cm scale) including planktonic (radiolarian) specimens, fragmented bivalves (pelecypods), and ammonites have been discovered (Fig. 18d; Kochann et al., 2011). Also, petrified wood fragments (10-50 cm; Fig. 18c) are observed.

Interpretation: Muddy deposits in the study area relate to sediment settlement of low energy turbidity currents (T_{de} or T_e), combined with suboxic and hemipelagic deposits during a sea-level highstand, since terrigenous-clastic particles overwhelm the biogenic content in composition (Natland and Keunen, 1951; Natland, 1976). The silty mudstone is structureless and extensive at the base of the succession with some faint laminations because the progradation ceases and deep water deposition become temporarily abandoned at certain areas.

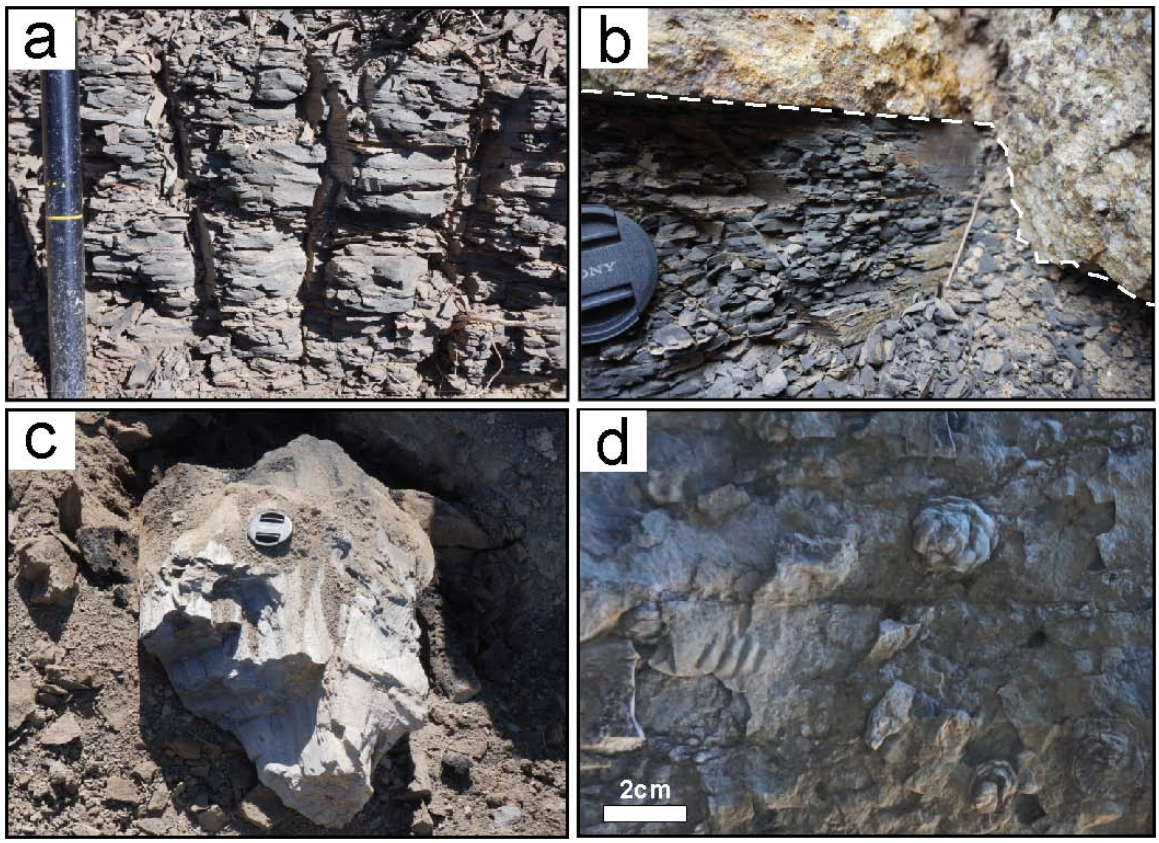

Figure 18: Facies 7 (F7): Silty mudstone. Silty mudstone facies. (a) Flat laminated, decimeter- to centimeter-thick, silt beds alternating with clay and fine silt; Jacob's staff labeled 10cm increments. (b) Flat laminated and homogenous muds overlain by an erosive conglomerate bed; lens cap is 40 mm in diameter. (c) Petrified wood fragments (10-50 cm) found at the base of a silty mudstone unit. (d) Ammonites and pelecypods < 2-3 cm in size.

Facies	Description	Interpretation	Depositional Environment	M12
(F1a) Clast-supported (ortho)conglomerate	Pebble to cobble conglomerate, normal graded, poorly sorted, extraformational clast-supported, 0.1-2 m thick, <15% matrix of medium to fine sand or finer sediments, clast size up to 70mm	Debris flow, high density turbidity current, possible evidence of bypass	High energy basin floor lobes, lower slope channel lag, slope channel axis	
(F1b) Matrix-supported (para)conglomerate	Granule to pebble conglomerate, very coarse to fine sand matrix, up to 3m thick, sandy matrix supported >15%, clast size up to 20mm	Debris flow (en masse freezing or part of traction carpet)	Moderate to low energy basin floor lobes, slope	
(F2) Amalgamated sandstone	Very coarse to fine sand, structureless, well to poorly sorted, a single bed up to 1 m thick, amalgamated up to 3 m thick, sharp base and top, few flute casts and tool marks, organic matters	Multiple high density turbidity flows stacking together, compensational stacking regionally	Basin floor lobes, slope channels	
(F3) Normal-graded sandstone	Pebble to fine sand, 0.2 - 3 m thick, sharp base, variable thickness	Rapid deposition of coarse grains within decelerating turbidity current followed by suspension of fine sediments	Proximal basin floor lobe axis, slope channel	
(F4) Parallel-laminated sandstone	Very coarse to fine sand, faintly laminted in general, wedge shaped, discontinuous, 5-50cm thick, mostly overlying amalgamated or normal-graded sandstone	Dilute, waning, low concentration turbidity current, space in between laminations indicating proximity to source	Proximal basin floor lobe axis, slope channel	
(F5) Ripple-laminted sandstone	Very coarse to fine sand, lenticular, 5-20cm thick, sharp base and top, faint lamination, bounded by muds	Dilute, turbulent suspension, low suspension fallout rates	Distal and off-axis basin floor lobes	

Table 1: Total of 7 facies identified and described for the lobe deposits of the Los Molles Formation in terms of grain size, thickness, depositional process, depositional environment, and probable location at lobe. Note that the representative measured log on the right column is matched with facies types.

(F6) Interbedded mud-sandstone	Alternating mud-silt and sandstone, mud-silt interbedded 1-10cm scale, coarse to fine sandstone up to 50cm thick, stack up to 30m, lenticular bodies, sharp base and top, slumps	Alternating suspension falls, weak and diluted low turbidity current	Distal and off-axis basin floor lobes	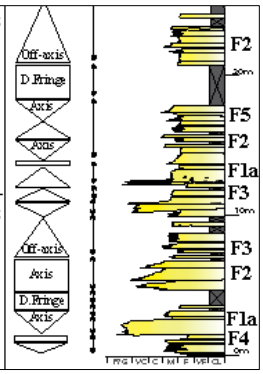
(F7) Silty mudstone	Dark gray, organic rich, faint lamination, bounded by sands, few mm to 10 cm thick, stack up to ~15 m, soft sediment deformation, slumps	Suspension fall, background sedimentation during avulsion, hemipelagic mud	Distal and off-axis basin floor lobes, slope	

Table 1: Table continued

4.2 FACIES ASSOCIATIONS

All facies types comprise sheet-like architecture elements with localized lenticular geometries and erosional contacts; however the facies can be grouped in different associations that represent changes in facies type, ratio of sandstone and mudstone facies, and distinct depositional sub-environment.

4.2.1 Facies Association 1 (FA1): Thick-bedded sandstone (Lobe axis/ Small channel)

FA1 comprises of thick-bedded (> 50 cm), very coarse to medium grained, massive, graded, and highly amalgamated sandstones (F2-3), and thin-bedded (< 50 cm), coarse to fine sandstones associated with ripple- or/and parallel laminations on top (F3-6) (Figs. 19, 20a-b). Thin-bedded (< 20 cm) silty mudstone beds are occasionally intercalated with thin laminated sandstones. The sheet-like, tabular, thick-bedded sandstones stack directly onto other beds and often build a thickness up to 6 m, whereas an amalgamated bedset within FA1 can be in range of 1-3 m (Fig. 12a-b). Mostly sharp-

based, thick-bedded sandstones show bed contacts by abrupt changes in grain sizes (from clay or very fine sand to very coarse sand) and sorting (to moderate or poor sorting). The transition from amalgamated or graded sandstones (F2-3) to laminated sandstones (F4-5) is often gradational. At times, within a bedset, it is difficult to observe amalgamated surfaces for bed contacts or degree of amalgamation because of the structureless nature of the facies. While slightly upward-thinning and fining, no sign of strong channelization or slump was identified, but small-scale (< 0.5m) local erosion in a few places.

Interpretation: Thick bedded, amalgamated facies association FA1 is interpreted to be deposited on a basin floor close to the axis of a basin floor lobe through high aggradation rate of high density turbidity currents (Lowe, 1982). Slight upward-thinning and fining (Fig. 20a) may be a result of decreasing aggradation and sediment dispersion before transitioning into a low-energy setting. Also, according to Prelat and Hodgson (2013), upward-thinning trend in bed thickness can be related to lateral shifting of lobes with landward stacking. High suspended-fallout rates can provide surging flows and rapid suspension-deposition that form beds of FA1 and also transport relative coarse sediments further down to unconfined locations (Lowe, 1982). The aggradation associated with waning and non-uniform turbidity currents cause local high sediment depositional rates and produce thick, tabular, structureless sandstones (Kneller and Branney, 1995).

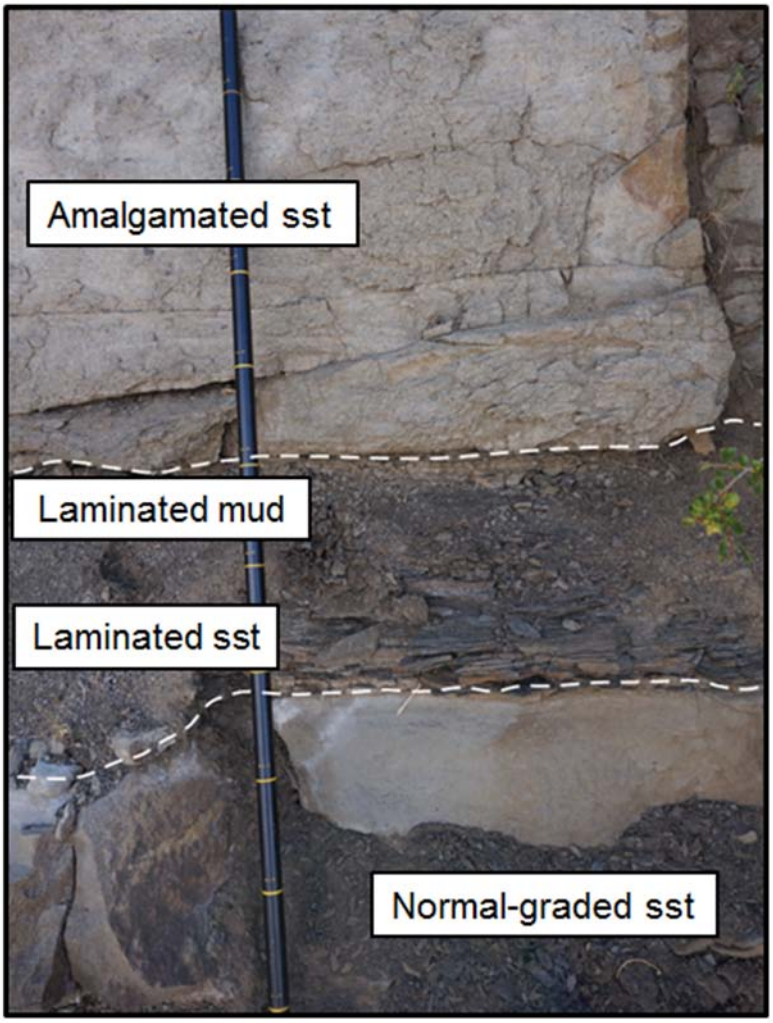

Figure 19: Facies association 1. A succession of 20 cm thick laminated mudstones and parallel-laminated sandstones bounded by a 30 cm thick normal graded sandstone and an amalgamated sandstone thicker than 50 cm.

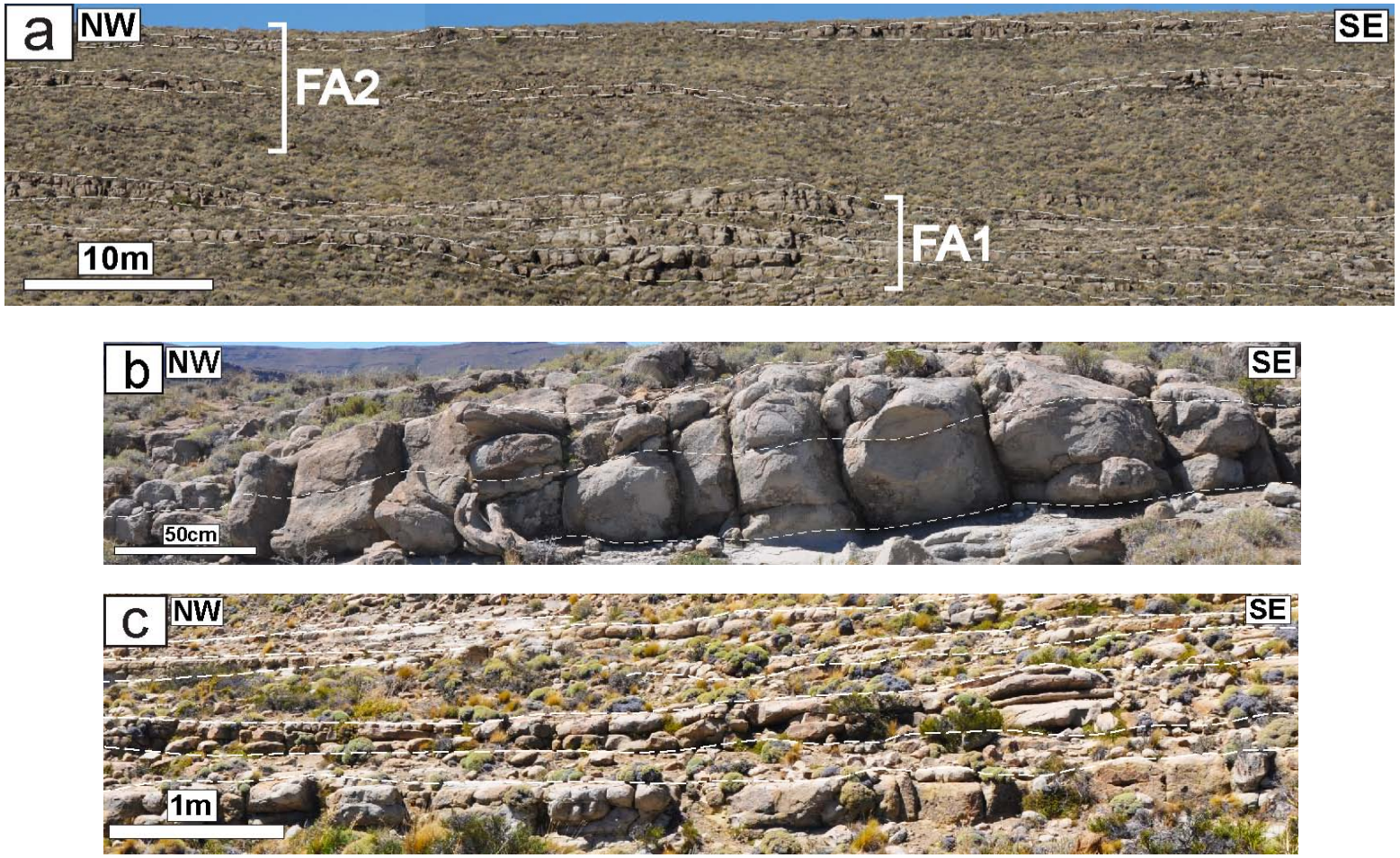

Figure 20: Facies associations 1 and 2 shown in outcrop. (a) FA 1 indicating an amalgamation of thick-bedded sandstones up to 7-8 m, of which thins out laterally. Note that rather discontinuous and thin-bedded (< 1 m) FA 2 is associated with 3-4 m thick vegetated covers (silty mudstones). (b) FA1 showing at least three amalgamated surfaces in a 0.75 m thick bed. (c) Thinly bedded (tens of centimeters thick, < 1m) sandstones and heterolithics dominating in FA2.

4.2.2 Facies Association 2 (FA2): Thin-bedded sandstone (Lobe axis to off-axis)

FA2 represents a bedset of thin-bedded (< 50 cm), coarse- to very fine-grained sandstones that occasionally include very fine grained, parallel- or ripple-laminations in upper half of the bed (F3-5; Fig. 20c), and very thinly bedded (1-30 cm), sheet-like, alternating, heterolithic fine sandstones and silty mudstones (F6, F7). Gradational base and sharp top contacts are frequently bounded by heterolithic, silt-prone mudstones. No trend in thickness or grain size is found.

Interpretation: Thinly bedded sandstone facies association (FA2) represent basin floor environments relative distal to the sediment source, dominated by weak, low- to medium-density turbidity currents. The interbedded thin beds in form of distal layered sheets reflect variations in time of the energy of the turbidity flows in this environment (Weimer et al., 2007). The distal turbidite currents (relative to the lobe apex) produce interbedded sand-rich and mud-rich beds in an area of the basin floor where the turbidity current decelerates and weakens to a point of which suspension settling overwhelms flow energy (Lowe, 1972; Mutti, 1992). Relatively thin-bedded sandstones (< 50-70 cm) placed in between large successions of silty mudstones (> 10 m) represent a sporadic large turbidity current during a dominantly quiescent time interval when only thin beds of weak low density turbidity currents deposit.

4.2.3 Facies Association 3 (FA3): Thin-bedded sand-bearing mudstone (Lobe Fringe)

FA3 comprises of interbedded silt-prone, fine to very fine sandstones and mudstones (F6; < 3 m), very coarse to medium grained, medium (< 1-2 m) to thin (< 1 m) -bedded, normal graded sandstones with rare amalgamation (F2, F3; 0.5-5 m), very thin parallel- and ripple-laminated sandstones (F4, F5; <30 cm), and silty mudstones (F7; <

2m) (The number next to facies types represents the average thickness of particular facies within FA3). The heterolithic, laminated, interbedded sand-mud unit prevails with high lateral continuity (> 4.5 km; larger than the outcrop extent). A total succession of FA3 is found as thick as 7-8 m. A few meters thick FA3 units show mostly gradational bases with underlying thick-bedded silty mudstones and relative sharp tops with onlapping mudstones or sandstones. The FA3 deposits in alternation with FA2 and reflect interlobe, which is usually < 2 m thick, mud-rich interval bounded by two different lobes.

Interpretation: The association of heterolithic muds and medium (< 1-2 m) to thin (< 1 m) sands indicate rapid settling of sediments within a turbulent flow of low density turbidity currents and waning energy of a turbidity flow based on existence of high laminations in both sandstone and mudstones and ripple-lamination (Bouma, 1962; Smith, 1971; Mutti, 1977). The differential settling of small and large grains, or low amplitude bed waves are responsible for generating parallel laminations while bedload reworking in turbulent flows highly affects the formation of ripples (Talling et al., 2012).

4.2.4 Facies Association 4 (FA4): Thick-bedded silty mudstone (Distal Lobe Fringe)

Dark grey, shaly, thinly bedded (tens of centimeters), laminated mudstones (F7; Fig. 21d) intercalated with heterolithic, very fine to silty sand and mudstones (F6; Fig. 21c) often form very thick intervals up to 15 m and begin a sequence of a fan system as located stratigraphically at base below other facies associations. Rarely, thin and fine to very fine sandstones (< 20-30 cm) are found at top (less than 5% of the total succession). Thick mudstone intervals are bounded by sharp top and gradational to sharp base. A single bed is few millimeters to 10 cm thick; an interval of FA4 can be as thick as ~ 10-15 m as observed in L12-L13 of Fan A, L19-L20 of Fan B, or directly above CU3 (Fig.

25). Very extensive, sheet-like geometry continues laterally a lot longer than the outcrop correlation (> 4.5 km) except when overlying sandstones or conglomerates erode and generate relief.

Interpretation: Thick stacks of mudstone beds up to ~15 m suggest low density turbidity currents and subsequent hemipelagic settling through slow suspension at distal fringes or lateral fringe of a lobe migrating laterally by turbidity currents (Mutti and Normark, 1987; Prelat at al., 2009). Reworked grains as bedload during fluid turbulence within a low density current continue to erode and accumulate over previously deposited lobe deposits (Talling et al., 2012). Very fine to silty grains or clay settle out by suspension after a series of low density currents, or by rapid deposition of flocs from mud-rich turbidity currents in a high-energy setting (Lowe, 1982; Pickering et al., 1986). The very low monotonous texture (Fig. 21d) without any ball/pillow or flame structures suggests muds were rather deposited by hemipelagic settling. Rare appearances of thin, fine sandstone beds may indicate residue of antecedent lobes.

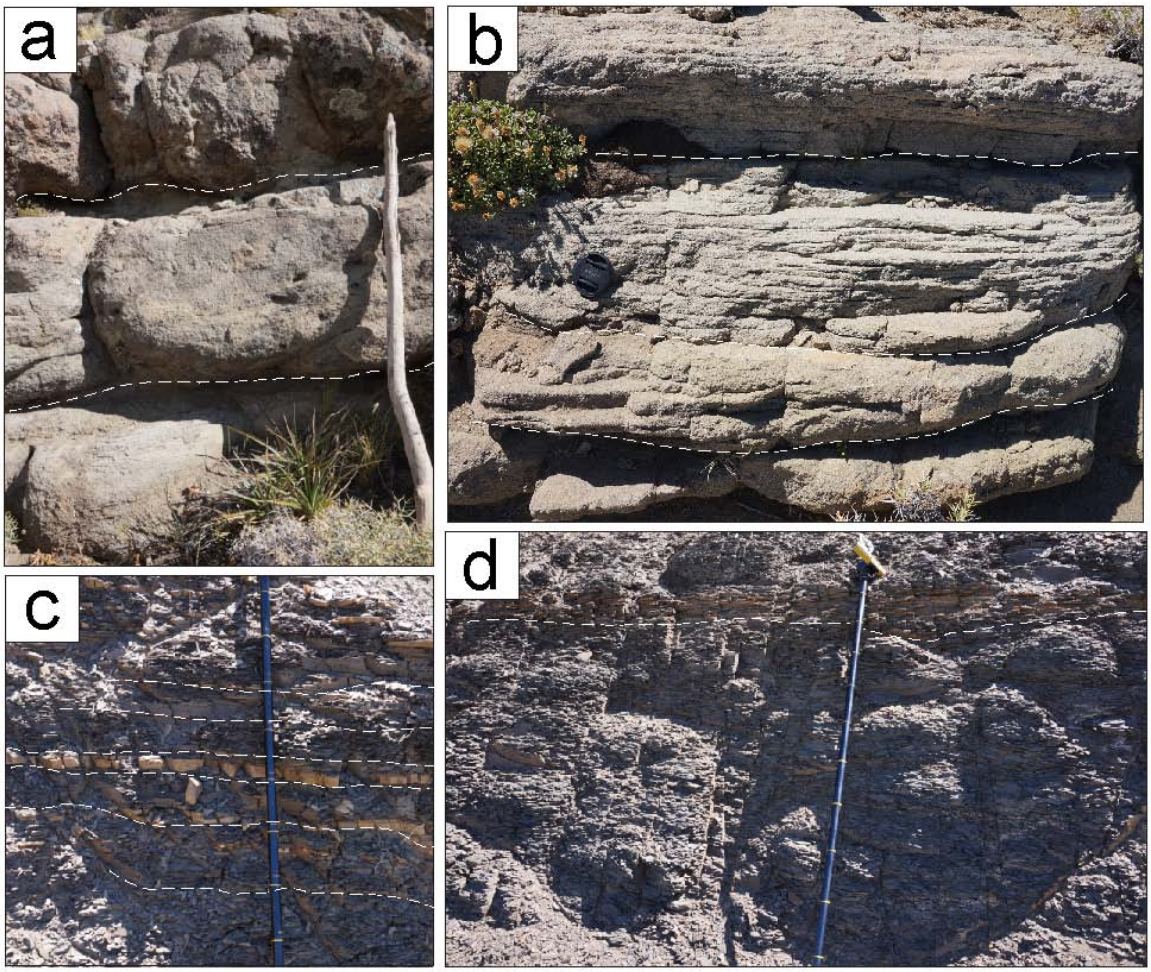

Figure 21: Close-up pictures of four different facies association (FA1-4). (a) Facies association 1 illustrating three 50-60 cm thick beds separated by very thin mudstone layers. (b) 10-30 cm thick parallel-laminated sandstones separated by very fine sandstones and siltstones. (c) Heterolithics comprised of centimeters-thick siltstones and laminated mudstones, capped by silt-bearing very fine sandstones. (d) Thick (> 2-3 m) to medium-bedded (< 1-2 m), laminated silty mudstones at base of the anticline (M6).

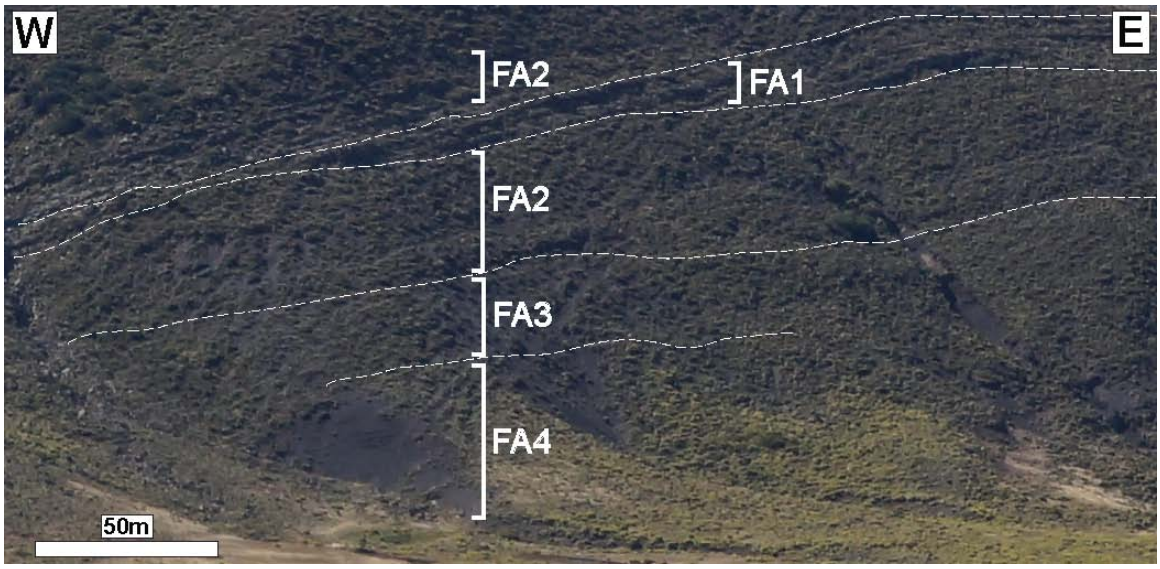

Figure 22: Overview of facies associations 1-4 located at the western flank of the outcrop correlation (between M1-M2). Note that FA1 in the figure includes a conglomerate unit (CU2).

4.2.5 Facies Association 5 (FA5): Erosional (bypassing) sandstone/ Channels

In FA5, there are recorded multiple high-energy flows (mostly debris flows) which truncate underlying beds and generate highly erosive bases and basal lags (Fig. 12b). Sediment bypass is suggested by discontinuous (lenticular) and undulating beds associated with conglomerate F1 with very coarse- to medium-grained sandstone beds. Normal-graded F3 dominate within a bed until capped by conglomerates, thick-bedded sandstones (FA1), or silty mudstones (FA4).

Interpretation: Facies association 5 is interpreted to represent channel deposits close to main sediment fairway on the basin floor (in proximity to lobe apex or lobe axis) based on the multiple erosional surfaces and alternating low- and high-density turbidity deposits (Lowe, 1982). The lateral discontinuity of bedding (few meters to tens of meters; Fig. 20a) that form lenticular beds is caused by localized deposition or post-depositional

erosion in an area of overall net-deposition (Myer and Ross, 2007), which fit with a channelized proximal basin floor, or slope environment.

4.2.6 Facies Association 6 (FA6): Conglomerates

FA5 comprises 3-4 m thick, poorly sorted, chaotic debris flow (F1a-1b) and high density deposits overlying thick-bedded sandstones (FA1) or silty mudstones (FA4). Intraclasts are consisted of extrabasinal quartz and feldspar cobbles or pebbles (few millimeters to 20 cm). Basal scours are abundant with erosive bed contacts. Thin-bedded sandstones or silty mudstones follow after erosive to gradational top.

Interpretation: Very high-energy, debris flows transport conglomerates and very coarse grains through hydroplaning on a wedge-shaped layer of water that provides a low-friction surface (Mohrig et al., 1998). Debris flows are able to travel long distances as much as hundreds of kilometers from the slope even at very low slope angles (<1°) (Gee et al., 1999; Schwab et al., 1996; Meyer and Ross, 2007). The high transport capacity of debris flows essentially explains the extensive deposition of conglomerates at distal lobes. However, there are also erosional based conglomerate beds and at times some crude internal sorting that indicate the possible high density turbidity flows for some of the beds.

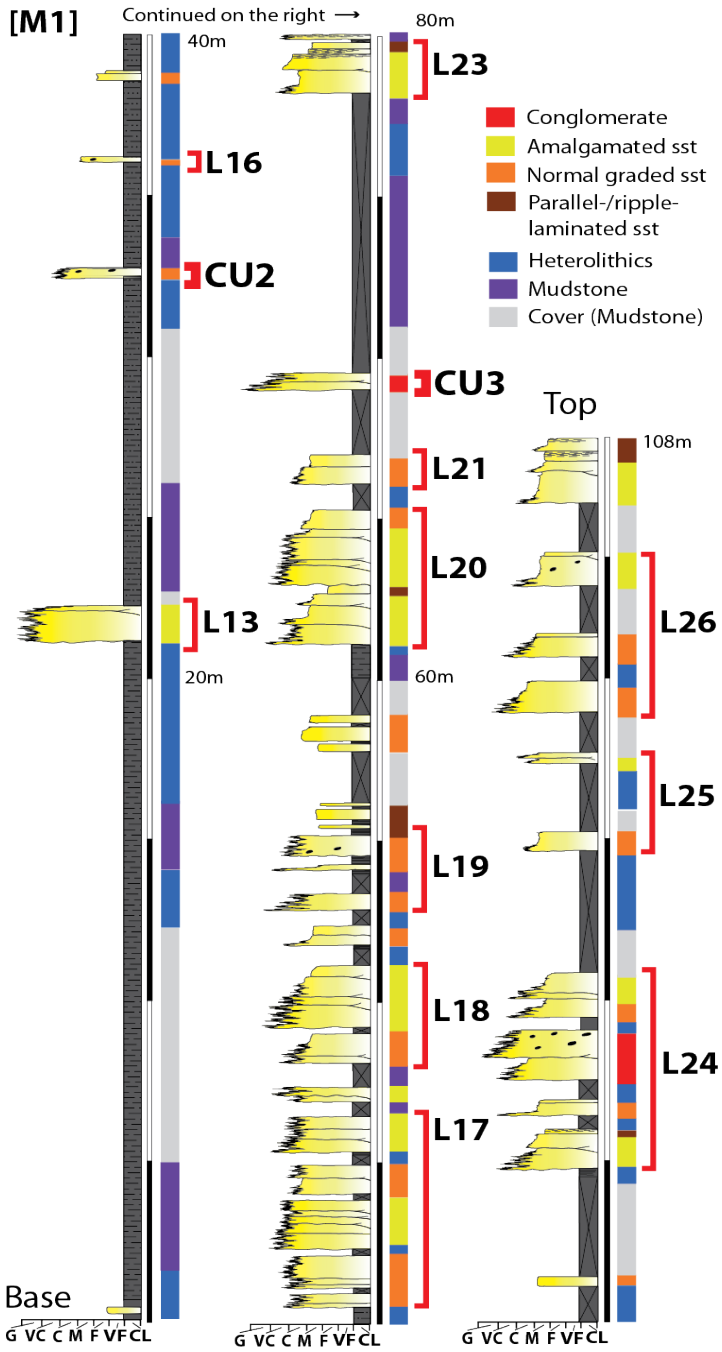

Figure 23: M1 – The westernmost measured section labeled with facies types. Thick, amalgamated, normal-graded, and very coarse to medium grained sandstone beds are dominant deposits within the sections. Note that two conglomerate beds (CU1-2) are overlain by thick successions of vegetated covers, which assumed as interbedded siltstone-mudstone or mudstone beds. See Fig.8 for the section location and Fig.24 for the legend.

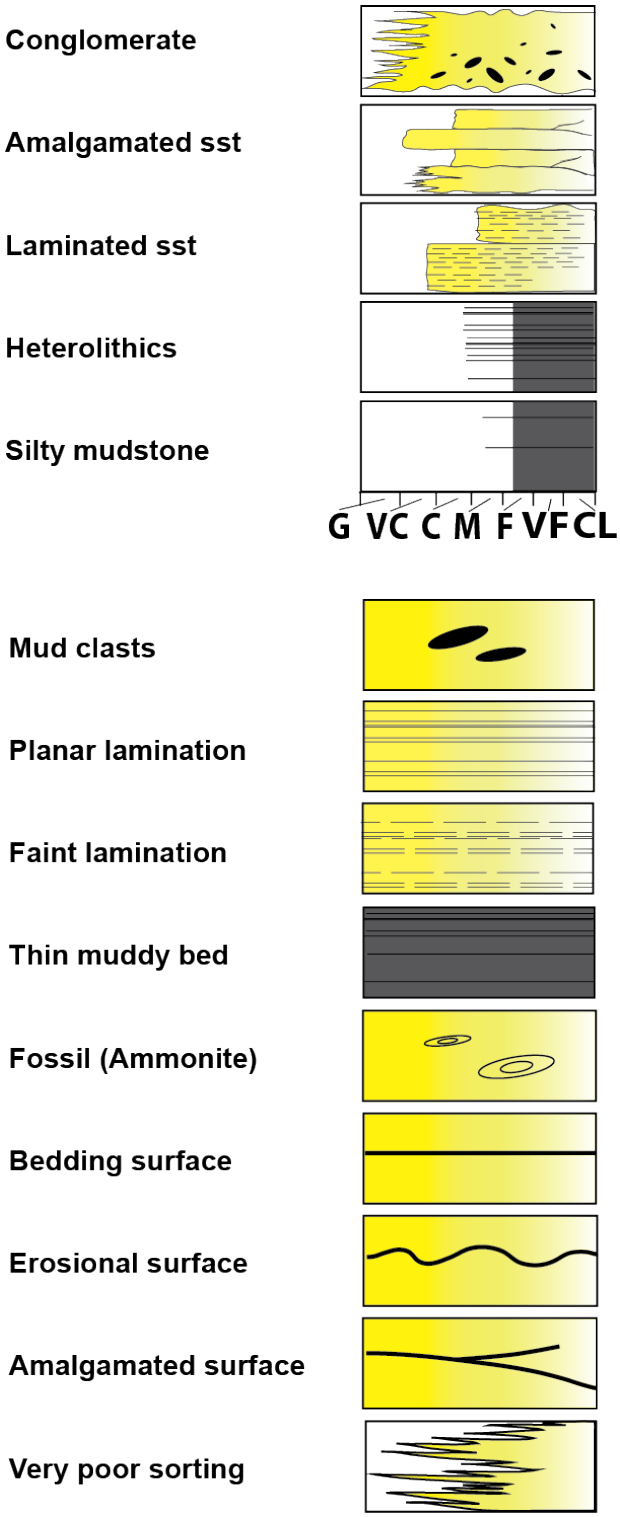

Figure 24: Legend for reading measured sections

4.3 THE LOS MOLLES FORMATION ARCHITECTURE

In outcrops of the source-to-sink system located in the La Jardinera region, the location of the coarse grained deposits are linked with architectural elements and sedimentary structures variability throughout the Los Molles system. Laterally extensive for kilometers in the study area, the stacked lobes in the lowermost fan of the Los Molles Formation display vertical changes in grain size pattern. To recognize each phase of large, high energy flow events that possibly relate to different depositional processes, the conglomeratic deposits are divided into units from oldest to youngest: CU1, CU2, and CU3. Each unit represents stacked lobes, so called 'lobe complex', according to the paleocurrents measured, prograded from the southwest to the north-northeast over younger deposits of silty mudstone. The outcrop is slightly oblique relative to the paleoflow direction, main direction of lobe progradation, and the progradation of the entire basin margin. CU1 consists of the coarsest, thickest, and most laterally extensive conglomerate unit (larger than the outcrop exposure). CU1 also has a high amalgamation ratio compared to CU2 or CU3 that become gradually thinning and discontinuous upwards.

4.3.1 Log Correlation

The 17 measured sections (M1-17) along the about 4 km long outcrop are examined at bed-by-bed scale and correlated with the help of photomosaics and 3D view of DEM image through Global Mapper. Two additional measured sections located at an opposite side of the outcrop transect across field (closer to the sediment source) are not applied into the correlation due to the large gap in between (~2 km). However, two logs are interpreted separately to identify constant trends in facies types and internal

structures. Each interval in the sub-regional correlation panel are separated into three different units and named after increasing numbers from bottom to top: CU (Conglomerate Unit) subdivided into three units (CU1-3), and L (Lobe unit) separated into a total of 26 units.

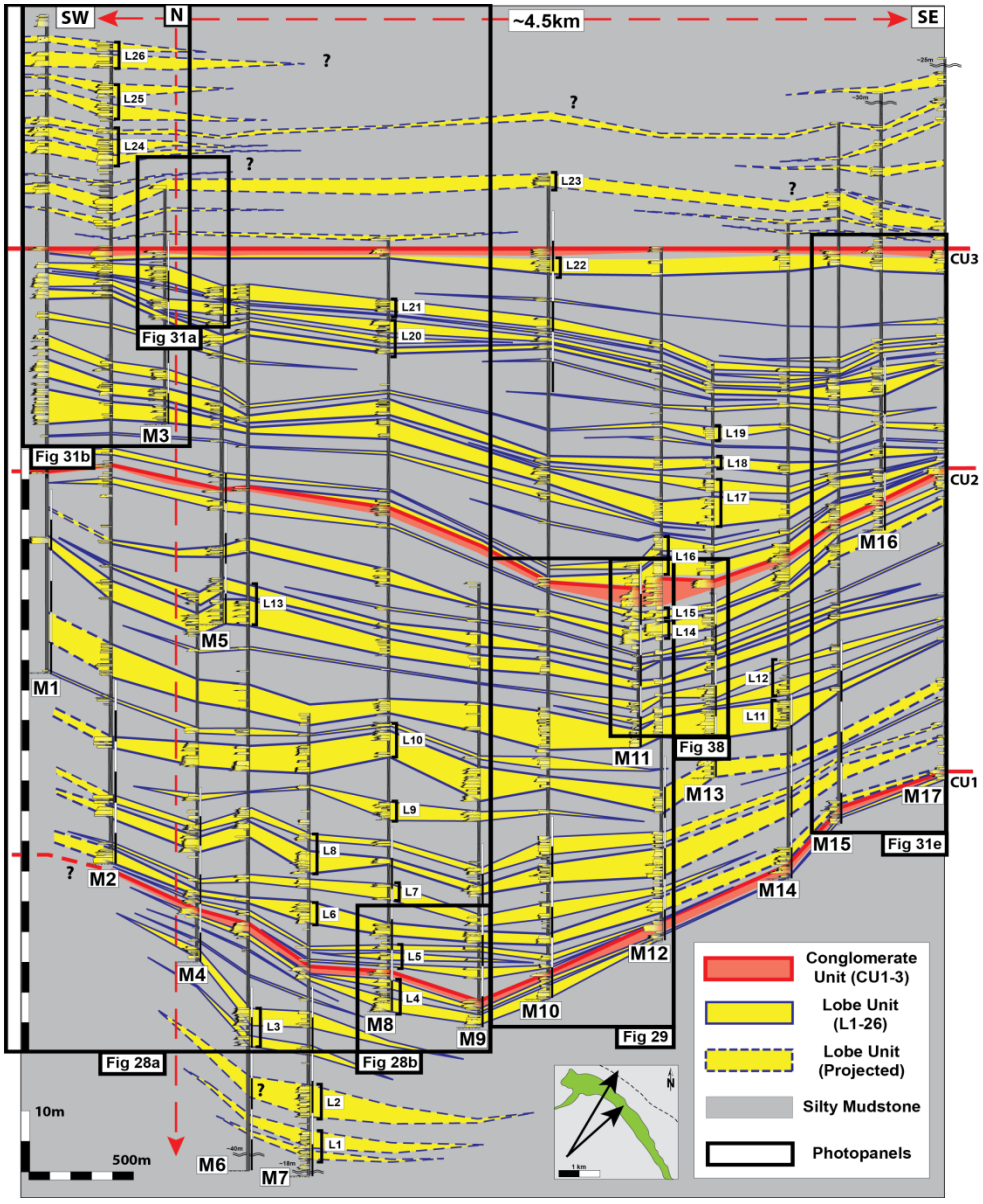

Figure 25: Correlation panel in oblique down-dip direction toward N-NE (into the panel). A SW-NE oriented, 0.9 km-long transect in west-end of the correlation representing 4 measured sections (M1-4) with an orientation change at ~0.7 km toward the northeast. Past M5, a NW-SE oriented, ~3.3 km-long, fairly straight transect including 13 measured sections (M5-17). Note that two extra measured sections (M18-19) out of the main outcrop, more proximal (South) to the source, are not correlated in the panel; however interpreted facies units appear to have a fair relationship to the correlation. The small lower right scheme shows the outcrop relative to the paleoflow direction (NNE). The correlation panel is also indicated on Fig. 18 with the base map. Full figure added in Appendix.

4.3.2 Conglomerate Architecture

The conglomerate deposits dominate the high energy facies in the study area. From bottom to top, three conglomerate units are described in order (CU1-3). CU1 represents the most extensive deposition while CU2 is the thickest yet discontinuous. CU3 is the thinnest unit with highly variable thickness and lenticular bodies. On the contrary to coarsening- and thickening-upward sandstone units, conglomerate units show fining- and thinning-upward sequence.

4.3.2.1 Conglomerate Unit 1 (CU1)

CU1 consists of extensive (> 4.5 km, larger than the outcrop extent) conglomerates on top of thin- to thick-bedded, sandstone deposits (all FA1-5). The lateral continuity of conglomerates is outstanding as few centimeters thick bed is present for ~4 km-long outcrop. Thick-bedded sandstones (FA1, ~0.5-2 m) and thin-bedded sandstones (FA2, ~10-50 cm), and very thin mudstones are deposited in order on top of a thick muddy interval (FA4; ~5m) before capped by the dominant conglomerate unit (CU1) (Fig. 12a, 12d-e). CU1 shows the maximum thickness of 2-2.5 m toward the eastern flank of the outcrop correlation and thinner beds at the western margin (tens of centimeters). In addition, CU1 shows clear variations in the grain size distribution westward as pebble-cobble sized clasts change to millimeter-scale granules and pebbles at the western flank. At the west, weak normal grading is found at the basal part, however still highly disorganized and poorly sorted. The occurrence of conglomerates is very limited so that no more than one bed was found below CU2. The hydroplaning is thought to occurs beneath a laminar flow and transport pebble-conglomerates through debris flows or co-genetic flows in distal region of a fan (Mohrig et al., 1998; Haughton et al., 2009), and

some of the conglomerate debris flow deposits were emplaced through this mechanism. However, it is questionable to generalize the same depositional processes from one conglomeratic bed to the next because all different elements (basin morphology, slope/basin floor gradient, autogenic processes) can be applied downdip, despite having the similar lithology.

4.3.2.2 Conglomerate Unit 2 (CU2)

CU2 exhibits a highly variable thickness and lateral continuity, with multiple abrupt changes in bed thickness (pinching-out geometry). However, the bed remains continuous at the same level over ~2.5 km distance. CU2 is bounded by structureless sandstone and silty mudstone below (Fig. 26c) and onlapping thin-bedded sandstone beds above. Within a distance of 500 m, CU2 decreases from 3 m to less than 50 cm in thickness when transitioning westward from M12. Also, the bed thickness is reduced to less than a quarter eastward from M12 within a 700 m extent. The unit displays the thickest bed (up to 2.5-3 m) in the eastern half (Fig. 26c), whereas thin beds (less than 20 cm) are observed at both sides toward the east and west. The blocky bed in the center and thin beds in the side suggest that it is the axis of the flow (channel conduit) with a paleocurrent oriented in SW to NE (Fig. 26). The thick-bedded conglomerates show the axis of flow while thinning sideways to the main paleoflow.

4.3.2.3 Conglomerate Unit 3 (CU3)

The uppermost CU3 comprises the thinnest and the most discontinuous conglomerates in the fan with slightly reduced clast sizes (mostly < 2-3cm, but still up to 7 cm; Fig. 26d). The thickness is mostly less than 50-70 cm while its lateral extent shows

continuity less than a distance of 0.5-1 km with 0.1-0.2 km long pinchouts. Overall, the unit still remains connected. CU3 sits on top of thick- and thin-bedded sandstones (FA1 and FA2; Fig. 26a) and gets overlain by a thick interval (~10 m) of silty mudstone beds.

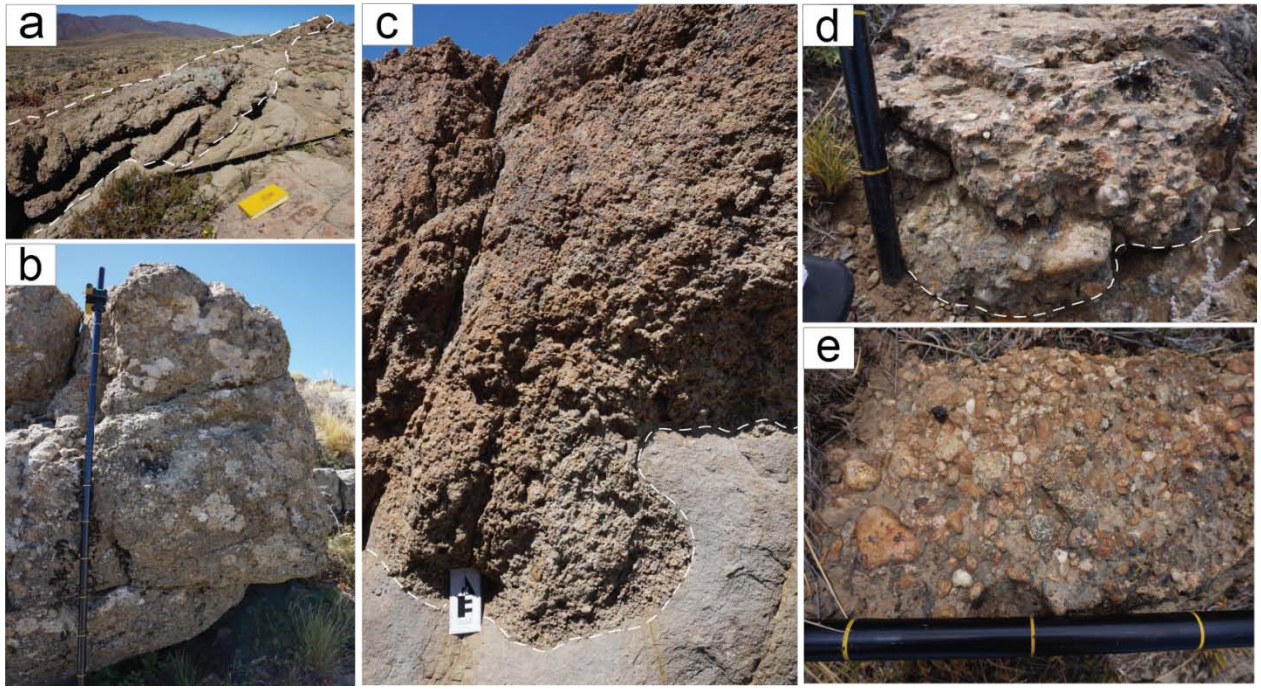

Figure 26: Overview of conglomerate units 1-4 (CU1-4) placed laterally from the western (Fig. 26a-b) to eastern (Fig. 26c-e) flank of the outcrop correlation. (a) Located upper left of the correlation panel (SW-NE oriented). A 0.6-0.8 m thick CU3 showing the continuous and lenticular conglomeratic bed while truncating amalgamated sandstones with erosive bases. (b) Located lower left of the correlation panel (SW-NE oriented). A 1 m thick CU1 showing a drastic grain size transition from pebble-cobble sized clasts to millimeter-scale granules and pebbles toward the west. A weak normal grading at the base, however still highly disorganized and poorly sorted. Only difference in general grain size. (c) CU2 located at slightly east to the center of correlation (NW-SE oriented). One of the thickest conglomeratic bed in the study area up to 2.1 m in thickness. Note the weak normal grading at base, large clasts (~ 6-7 cm), and erosive base truncating a structureless sandstone bed. (d) Toward the upper right panel, bed thickness of CU3 significantly varying and decreasing as thin as less than 20 cm while grain size being fairly constant (up to ~ 7cm). (e) Toward the lower right of the correlation, bed thickness and geometry of CU1 displaying similar characteristics with Fig. 26c. Figure from a top view.

4.3.3 Lobe Architecture

Based on observations of internal architectures and stratigraphic relationships exposed on outcrops (Fig. 19-22) and correlated measured sections (Fig. 25), three conglomerate units are established as bases (Fig. 26) to define lobe stacking patterns and depositional relationships of lobe, lobe complex, and fan. Deposits between CU1 and CU2 are interpreted as a fan system (Fan A) that is wider than the outcrop transect (> 4.5 km) and up to 80 m thick (Fig. 27). Between CU2- CU3, lobes form another fan (Fan B) that is also larger than the extent of correlation (> 4.5 km) and up to 60 m in thickness (Fig. 30). The turbidity-driven sandstones in each lobe represent sheet-like and tabular geometry with common sharp and erosional bases, but also include small-scale lobes that have lenticular sandbodies (0.5-1.5 km wide; Figs. 28-29), weakly erosional bases (Fig. 28), and localized scours at flow axis. All thickening-, thinning-, coarsening-, and fining-upward successions (Figs. 27, 30) exist in joint with another trend in the fan, however thickening-coarsening-upward trend prevails. Divisions of lobe complexes and lobes within each fan architecture are described in detail below. Although not every measured sections cover all three conglomerate associations, upper Fan A and lower Fan B successions, below and above Conglomerate Unit 2 (CU2), are interpreted thoroughly with its stratigraphic position between CU1 and CU3 units. Occasionally covered areas or ceased correlations below Fan A and above Fan B toward either the east or west are interpreted based on tracking sandstone beds scale within the photomosaics and general stratigraphic trend of lobe succession.

4.3.3.1 CU1-CU2 Fan Architecture (Fan A)

Within a hierarchical succession between CU1 and CU2, distinctive trends in bed thickness and grain size show alternating cycles of thickening-coarsening-upward and thinning-fining-upward beds. The entire succession can be divided into two lobe complexes (lobe complex A1: 25-50 m thick, lobe complex A2: 20-35 m thick) mainly separated by thick hemipelagic mudstones (>2 m; FA4), and a total of 11 lobes (L5-L15) in Fan A intercalated with a few centimeters to 2 m thick, silt-prone mud 'interlobes' (<2 m of thin-bedded siltstone-prone mud unit between lobes, sensu Prelat et al. (2009); FA3).

Lobe Complex A1

At the base, the extensive and continuous CU1 deposited over a 4.5 km long outcrop transect above a set of thin-bedded and thick-bedded sandstones (SU3). Thick sets of mud-rich beds (>2 m thick; FA4), interpreted as hemipelagic mudstones, appear to separate lobe complexes A1 and A2, between L11 and L12 in lobe scale. Intervening thin-bedded sandstones (<2 m for each bedset; FA2), and thin-bedded silt-prone mudstones regarded as interlobes (<2 m; FA3) build a lobe with thick deposits of thick-bedded sandstones (FA1). Conglomerate unit (CU1) shows laterally extensive (> 4.5 km), but slightly lenticular beds away from the center of outcrop (Fig. 27). However, the western flank was more difficult to correlate laterally because the SW-oriented, gentle dipping limb of the anticline disappears into the ground. Thus, two measured sections at the western flank (M1-M2) have bases above the conglomerates because the corresponding unit would be underground. Above the first conglomerate unit (CU1), alternating thin-bedded sandstone beds (20-50 cm thick beds, up to 1.5 m in total

thickness) and silty mudstones form a small, lenticular lobe (L5) with 1-2.5 km long lateral extent. Then, 1-5 m thick, tabular thick-bedded and thin-bedded sandstones are found above 5 m thick mudstones. L7 and L9 lobes are lenticular with abrupt thickness changes and have lateral extents of 3 km and 2.2 km, respectively. Alternating with 1-7 m thick sand/silt-prone mudstones, L6, L8, L10, and L11 lobes show high continuity covering the entire correlation panel (> 4.5 km) and tabular geometry with thickening-coarsening-upward trends consisted of both thick- and thin-bedded sandstones (Figs. 27,28) intercalated with interbedded silt-prone sandstones and mudstones (FA3). A stack of 7 lobes (L5-L11) build lobe complex A1 with a clear thickening-coarsening-upward trend (Figs. 27, 29). Lobes in the lower half (L5-L8) exhibit increasing thickness toward the east; each unit approximately doubles its thickness. Toward the southeast (M14-M17), the lateral continuity weakens significantly and thickness decreases to less than 1 m for all four L5-L8 units (Fig. 27). The absence of beds in M14 and M15 sections would be a result of thinning or disappearing beds, or poor exposure in the field due to heavy vegetation.

In contrast, above L9, thick lobes (L10, L11, L13) in the middle of the CU1-CU2 architecture show thickening-coarsening-upward trends to the west compared to those east-thickening lobes in the lower half (Fig. 27). The change in bed thickness and grain size illustrates the axis of lobes switching laterally from east to west (possible compensational stacking) while prograding and building forward-stacking patterns within a lobe complex. Minor changes in axis location also occurs at least three times for lobe complex A1 as three lobes at base (L5-L7) more likely stay the same paleoflow, two lobes in the middle (L8, L9) migrate toward the east, and next two lobes at top (L10, L11) migrate toward the west .

Lobe Complex A2

The general thickness of lobes drops abruptly above lobe complex A1. Not only decreasing the vertical thickness, lobe complex A2 also decreases in thickness toward the southeast. Starting from M10 to the east, thickness of sand-rich units becomes gradually thin (~1 m), almost half of the bed thickness found at the western flank. The thickening-coarsening-upward trend is dominant in the low-relief section of correlation (M10-14); however it diminishes toward the west where associations of silty mudstones (FA7) are abundant with thinning-upward lobes. The thicker mudstones in the upper half of lobe complex A2 has thickness up to 9 m in the western flank while they also shrink down to tens of centimeters toward the southeast. Overall, alternating sand-rich and mud-rich intervals build a ~80 m thick, mixed sand-mud lobe successions until they are capped by the second conglomerate unit (CU2). The lobes consist mainly of massive, tabular, and amalgamated bedding facies but the overall thickness varies vertically and laterally (Fig. 27). The net-to-gross (ratio of sand/mud) seems to increase toward the top of Lobe complex A1 then decrease into A2 (Fig. 27). The amalgamation of sandstones decreases toward the top as more thinly bedded units predominate in Fan B (Figs. 27, 29). Thin-bedded sandstones are highly discontinuous possibly by being cut by another erosive and bypassing turbidity flow. The thick mudstones intercalated with very fine-grained siltstones and mudstones alternate vertically with bounding sand-rich lobes as mudstones or interlobes thicken toward the top and thin toward the east.

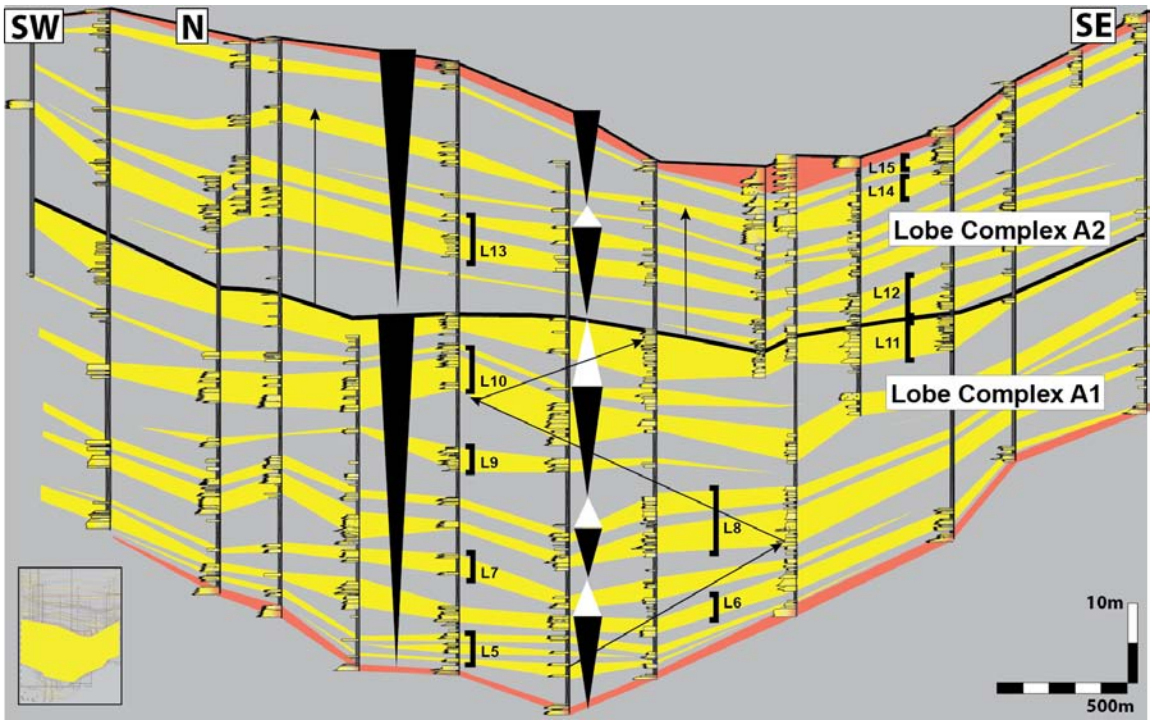

Figure 27: The 60-80 m thick Fan A in the study area indicating two lobe complexes separated by a black line above L11; 7 lobes for Lobe complex A1 and 4 lobes for Lobe complex A2. Note the highly amalgamated lobes for A1 and more mud-dominating nature of A2; both lobe complexes show thickening-coarsening-upward trends. For location, see Fig. 8.

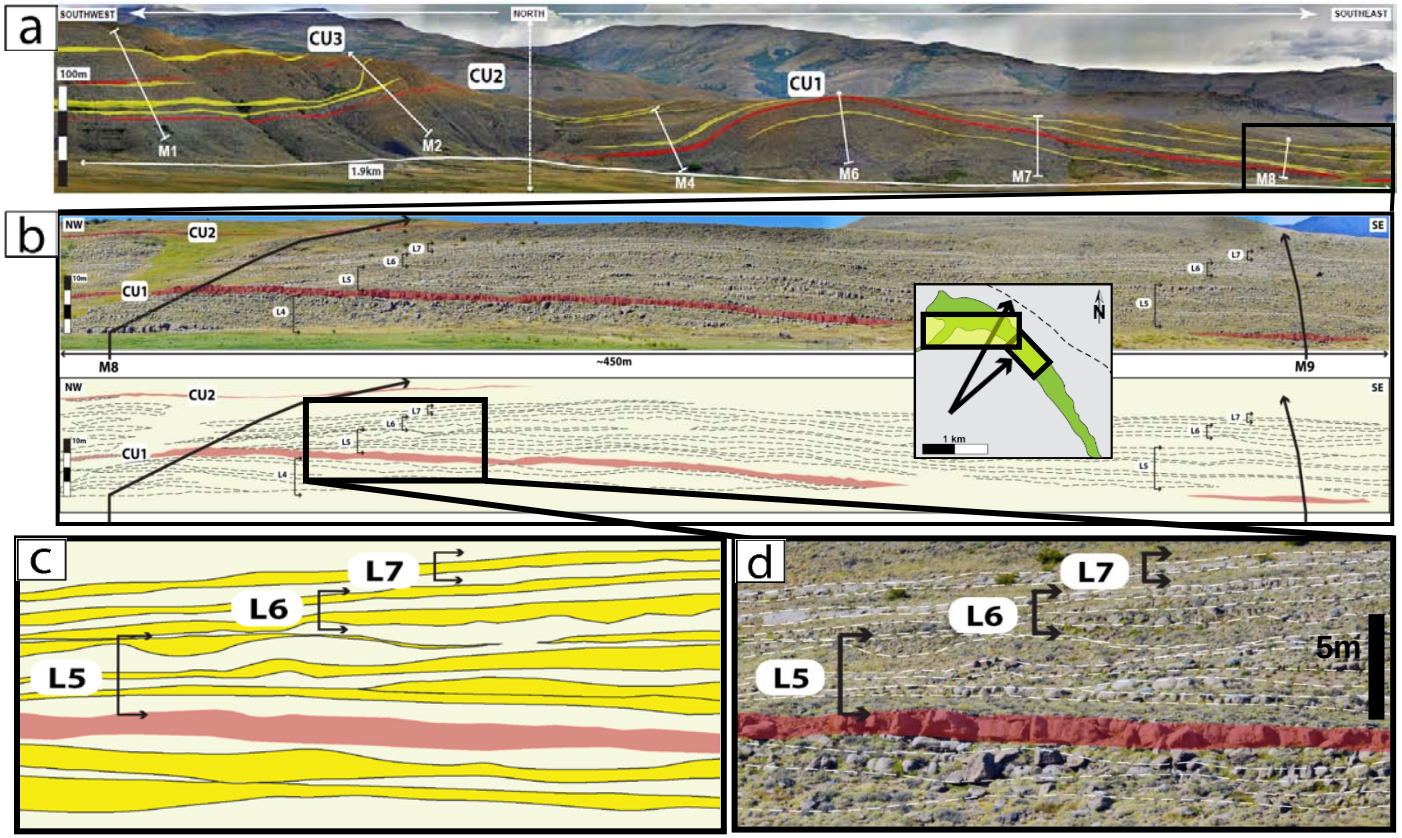

Figure 28: Western side outcrop exposures for Fan A. (a) The bottommost, thick mudstones overlain by the first conglomeratic unit (CU1), then followed by a succession of classical turbidites associated two more conglomerate layers (CU2-3). Looking into the north where the orientation breaks into SW-NE at the western flank and NW-SE at the eastern flank. Note the anticline in the center exposing thick basin floor mud deposits. (b) At the center of correlation panel, a 450 m long photomosaic of NW-SE oriented depositional strike showing very continuous yet lenticular lobes, and laterally extensive conglomerates (CU1) (c) A close-up scheme that represents three lobes deposited above CU1; erosive bases of L5 contains three sandy beds intercalated with thin-bedded heterolithics and mudstones. (d) An outcrop close-up showing the same location of figure 24c.

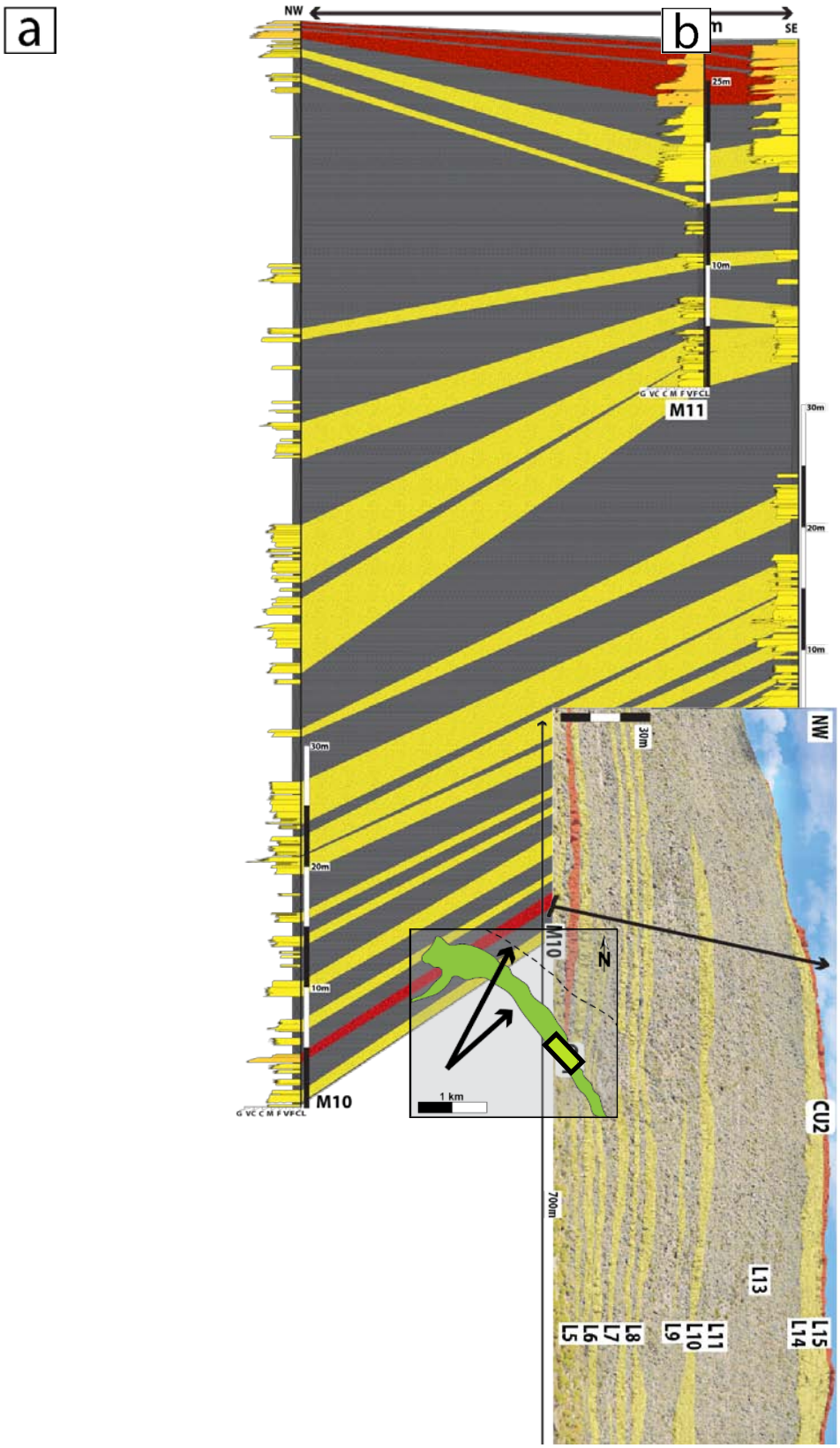
a
b
NW
SE
25m
10m
M11
30m
20m
10m
M10
N
1 km
CU2
700m
L13
L5
L6
L7
L8
L9
L10
L11
L14
L15

Figure 29: Center part of the NW-SE depositional strike that shows well-exposed laterally extensive sandy lobe deposits associated with heterolithic, interbedded silt-prone mudstones and conglomerates at the base and top (CU1, CU2). Total of 11 lobes deposited in Fan A; first 6 lobes (L5-10) colored in yellow. (a) the correlated measured sections of M10, M11, and M12 representing consistent bed thickness and grain size trends for lower units (L5-10) while the upper units (L11-15) shows varying lateral thickness and lower sand/mud ratio. (b) A photomosaic illustrating almost parallel and extensive lobe deposits intercalated with muddy units (vegetated cover).

4.3.3.2 CU2-CU3 Fan Architecture (Fan B)

Between CU2 and CU3, alternating cycles of thickening-coarsening-upward and thinning-fining-upward beds exist while thickening-coarsening-upward trend dominates. The entire succession can be divided into three lobe complexes (lobe complex B1: 8-27 m, lobe complex B2: 10-20 m, lobe complex B3: up to 18 m; varied laterally) separated by 1-15 m thick mudstones, and 7 lobes (L16-L22) (Fig. 30). The total thickness of all sand- and mud-rich units between CU2 and CU3 is about 45 m in average, thinner than the CU1-CU2 architecture (Fan A). The total thickness varies by locations, up to 55 m at M13 and decrease to about 35 m toward either flanks (M1 and M17).

Lobe Complex B1

Lobe complex B1 shows a thickness of 13 m associated with 4 lobes (L16-19). The location of first stratigraphic deposit (in M10-13) in base holds one of the thickest conglomerates (~3 m; CU2) and is located toward the east (0.9 km eastward) from Fan A axis (Fig. 29a-b). The eastward switching of stratigraphic low and the coarsest deposits matches with the paleoflow measurements toward the northeast and east. Above CU2, a decimeters thick, thin-bedded mudstone onlaps and a 5-7 m thick lobe (L16) formed. A high net-to-gross ratio with abundant thick-bedded and thin-bedded sandstones (FA1, FA2) is observed toward the east (Fig. 29). Toward the west, gradual increase in bed thickness in L17-19 indicates an aggradational stacking pattern of which generally prevails in lobe complex B1.

Lobe Complex B2

Upper part of Fan B (Lobe complex B2) has more discontinuous and thin lobes and thicker mudstone intervals (FA3, FA4) compared with Lobe complex B1. Especially, hemipelagites (FA4) between L19 and L20, or L21 and L22 display very thick mud-rich units (up to 15 m) with lateral thickness variations that become as thin as tens of centimeters toward the western flank (Fig. 29a). The lobes of Lobe complex B2 have more thin-bedded sandstones that often include significant amount of mudstone in between. Thus, higher mud content within a lobe covered by vegetation made the correlation challenging in terms of bed-by-bed scale. However, thickening-coarsening-upward trend within each lobe complex was very clear. Two lobes (L20-21) in Fan B shows a thickness range of 2-6 m. General lobe patterns demonstrate strong aggradational stacking before a thick (up to 15 m) mud interval of Lobe complex B3, which is consisted of thick-bedded mudstones at bottom and one lobe (L22) at top with an average thickness of 10 m.

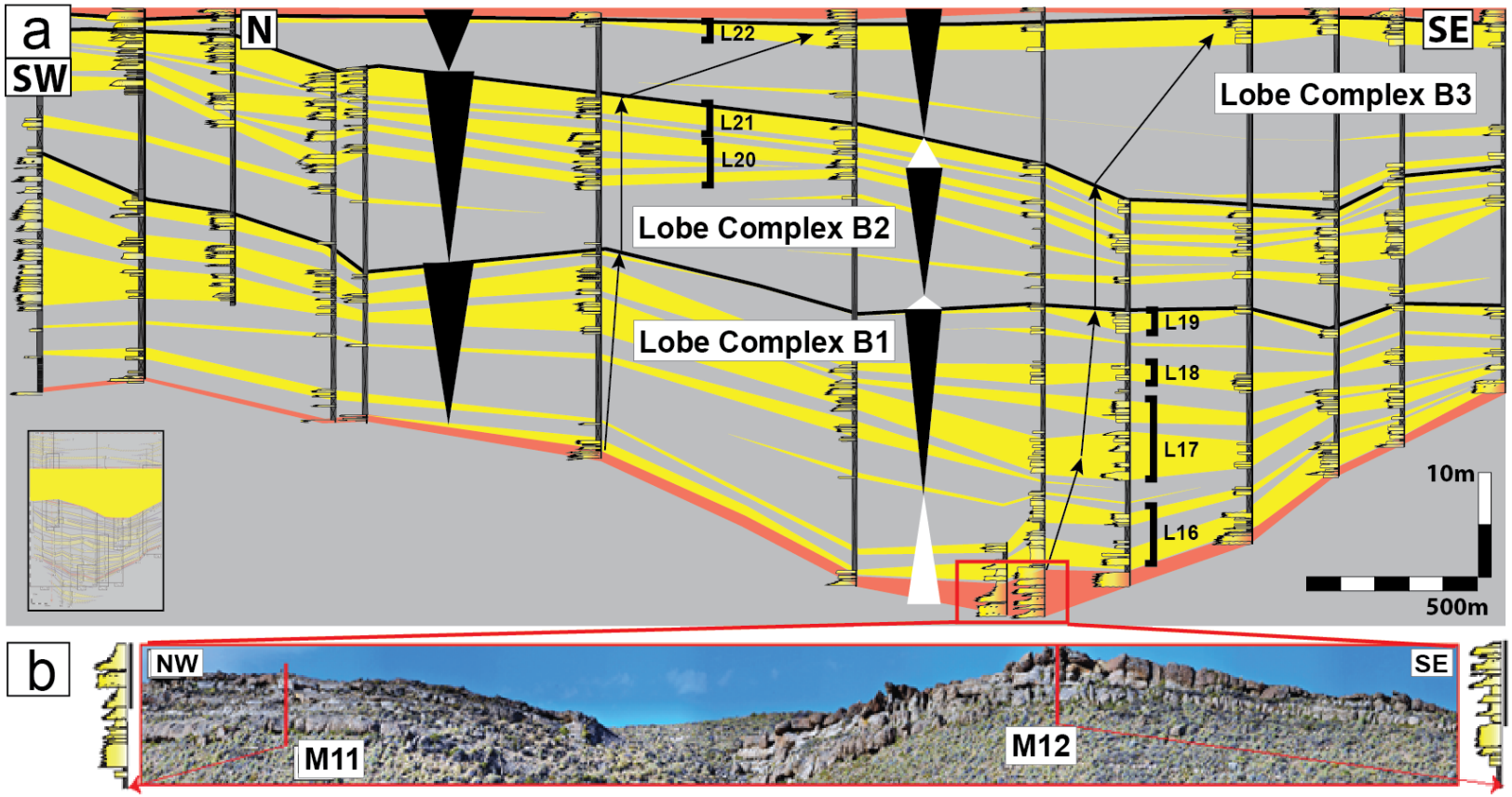

Figure 30: (a) The 40-60 m thick Fan B separated into three lobe complexes by black lines above L19 and L21; 4 lobes for Lobe complex B1 and 2 lobes for Lobe complex B2. Note the highly amalgamated lobes at the base producing a thinning-fining-upward trend before switching to thickening-coarsening-upward trend. B2 and B3 showing thicker mud units with clear thickening-coarsening-upward patterns. (b) A close-up of 2-3m thick conglomerates (CU2) overlying L14-15 lobes.

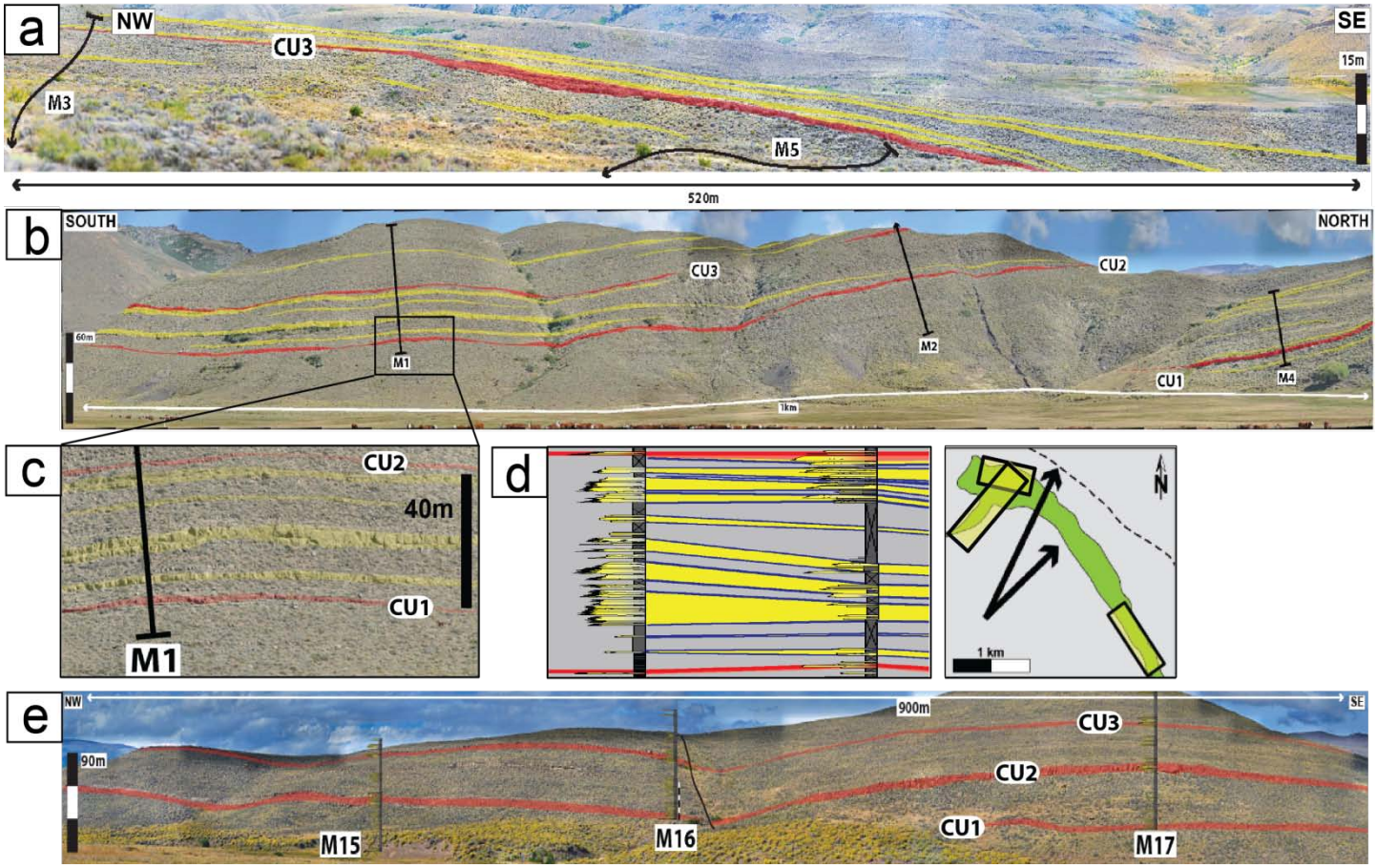
a
NW
SE
CU3
M3
M5
15m
520m
b
SOUTH
NORTH
CU3
CU2
M1
M2
M4
CU1
60m
1km
c
CU2
40m
CU1
M1
d
N
1 km
e
NW
SE
900m
90m
CU3
CU2
CU1
M15
M16
M17

Figure 31: Western side of Fan B outcrop exposure. (a) A 520 m-long, NW-SE trending outcrop that displays relatively thinner and continuous conglomerate unit (CU3) located above the cliff shown Fig 27b. (b) A 1 km-long, very continuous and sheet-like lobes (L17-26) and conglomerates (CU2-3) in SSW-NNE-oriented depositional (oblique) dip. (c) A part of correlation panel showing tabular and highly continuous bedding structure of lobes between M1 and M2. (d) A corresponding outcrop exposure shown for Fig 27c. (e) A 900 m-long, NW-SE outcrop associated with three continuous conglomerate units (CU1-3).

4.3.3.3 Lowermost Fan Architecture (Below CU1-CU2)

Below CU1, alternating cycles of thickening-coarsening-upward and thinning-fining-upward beds exist while thickening-coarsening-upward trend overwhelms. The entire succession can be divided into two lobe complexes (L1-L3: < 25 m, L4: 7-15 m; varied laterally) mainly separated by 5-12 m thick mudstones.

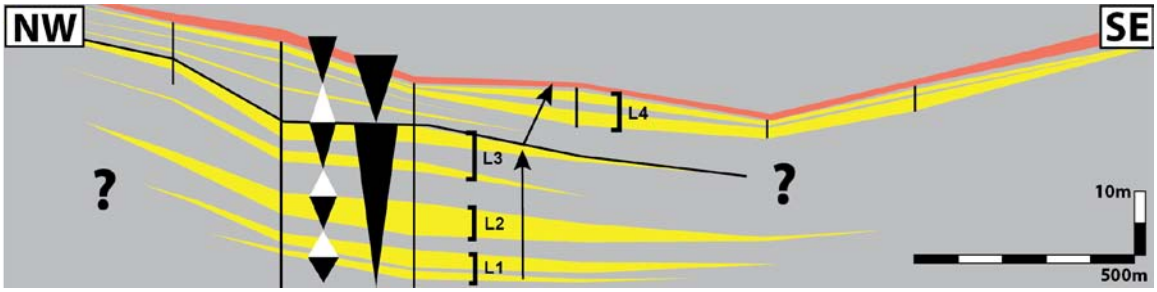

Figure 32: The lowermost fan below Fan A showing possibly two lobe complexes and four lobes (L1-4) associated with thickening-coarsening-upward stacking patterns. Only limited number of measured sections available due to the anticline structure.

4.3.3.3 Uppermost Fan Architecture (Above CU2-CU3)

Above CU3, both thickening-coarsening-upward and thinning-fining-upward beds are also observed with more abundant thickening-coarsening-upward architecture elements (Fig. 33). This topmost succession includes 4 constituting lobes (L23-L26) intercalated with 1-5 m thick interlobes forming two lobe complexes (L23-L24: < 35 m; L25-L26: < 25 m; varied laterally). Above CU3, both thickening-coarsening-upward and thinning-fining-upward beds are also observed with more abundant thickening-coarsening-upward architecture elements.

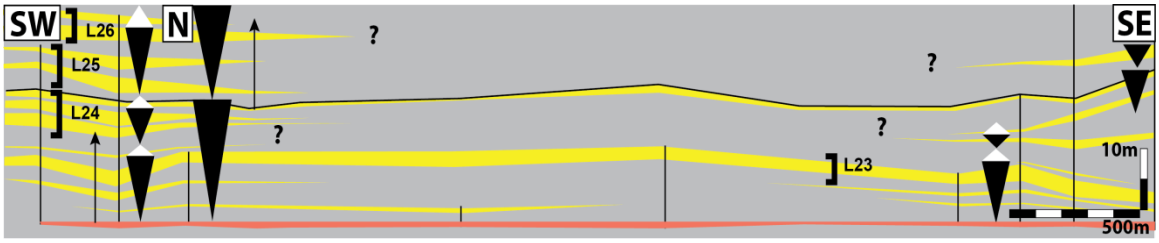

Figure 33: The uppermost fan above Fan B comprised of possibly more than two lobe complexes and four lobes (L23-26). Note the distinctive thickening-coarsening-upward stacking patterns.

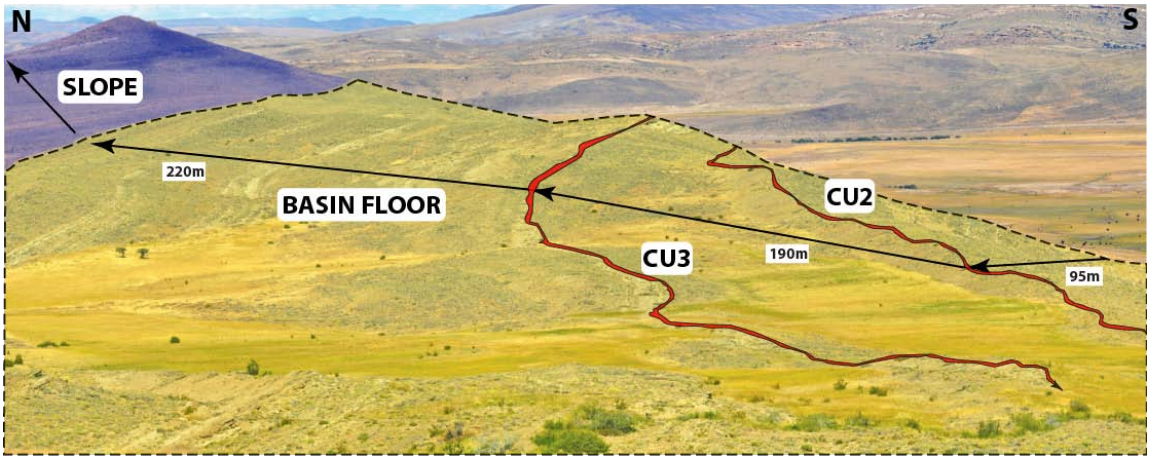

Figure 34: View from west to east above a high-relief hill showing the upper succession of lobes and conglomerates above CU2 before capped by slope deposits. The approximate distance measured in terms of map-view outcrop surface, not stratigraphic thickness.

4.4 LOBE STACKING PATTERNS

Analyzing vertical measured sections and correlated panels, multiple transitions can be identified as lobe stacking patterns vary laterally and vertically. Below CU1, alternating cycles of thickening-coarsening-upward and thinning-fining-upward beds exist while thickening-coarsening-upward trend overwhelms. The base and top of each conglomerate unit are bounded by silt-prone mudstones (F6-7) while underlying muddy

beds have varied thickness over different locations. Mudstones beneath CU1 and CU3 appear to be the thickest (up to 30 cm) at the center of correlation; however the thickness significantly decreases to a range of a few centimeter scale toward flank of the correlation. At the western flank of CU3, conglomerates almost lie directly on an underlying sandstone unit without mudstone in between. The direct emplacement of conglomerates on sandstones represents the proximity of axis of debris flow and the brief gap of retreat. Below CU2, the thickness of underlying mudstone varies between 0.2 m and 2 m, showing a lateral-thinning toward the eastern flank. This lateral change in mudstone thickness suggest the second pulse of high-energy conglomeratic flow (CU2) prograded toward the northeast, which is supported by the paleocurrent measurements from the field. The mudstone thickness variability may also indicate the temporal relationship of conglomerate deposition of which most likely initiates from active tectonic movements at the high-relief source area in the south. Compared to the thin mudstone beneath CU1 and CU3, the thicker interval of mudstone below CU2 suggests longer periods of post-retreat maintaining a quiescent environment before a subsequent debris flow.

Above L9, thick lobes (L10, L11, L13) in the middle of the CU1-CU2 architecture show thickening-coarsening-upward trends to the west compared to those east-thickening lobes in the lower half. This change in bed thickness and grain size illustrates the axis of lobes switching laterally from east to west while prograding and building forward-stacking patterns within a lobe complex. Minor changes in axis location also occurs at least three times for lobe complex A1 as three lobes at base (L5-L7) more likely stay the same paleoflow, two lobes in the middle (L8, L9) migrate toward the east, and next two lobes at top (L10, L11) migrate toward the west.

The lateral thickness variation of thick mudstones or interlobes may be resulted from a lateral switch of main axis of a high-energy flow such as high density turbidity current. High-energy gravity flows are able to avulse and build a new conduit for flow toward a low-relief area, generating a thin mudstone unit in between L14 and L15. Also, during the retrogradation (backward-stacking), the change in flow energy decreasing from high-density to non-cohesive, low-density turbidity current accelerates mud deposition with thin, depleted sands and eventually produces thinning-fining-upward trends. The degree of turbulence within low-density or surging turbidity flow is able to control the deposition of thin-bedded sandstones (FA2) (Mulder and Alexander, 2001).

Overall, the general stacking patterns of lobes indicate dominant progradation (forward-stacking) and minor retrogradation (backward-stacking). The inferred size of the relatively large fan system in La Jardinera (~30 km long, ~10 km wide; Wynn et al., 2002; Tudor, 2014) represents composite lobe complexes, suggesting the size of a lobe unit to a quarter or smaller (< ~7.5 km long, < ~2.5 km wide). A series of schemes for progradational lobe model (Fig. 35) represents a succession of the first conglomerate unit (CU1), and a lobe (L5) consisted of three thin-bedded sandstone units. For the conglomerates, initial debris flow sweeps over basin floor muds in NNE-oriented paleocurrent direction. And, subsequent three high density turbidity flows build prograding lobes onto the basin as lobes move forward. The uppermost bed in L5 is very coarse and more laterally extensive, building a thickening-coarsening-upward trend (Fig. 33).

The retrogradational lobe model (Fig. 37) shows sequential backward-stacking of beds within L16 above the second conglomerate unit (CU2). Located in the eastern margin of the outcrop, the succession of gradually thinning- and fining-upward beds explains the retrogradational stacking pattern of a lobe (Fig. 38). The lowermost bed

within L16 has the largest lateral extent with thicker beds and coarser sediments. The relatively discontinuous uppermost bed is fine grained and less than 50 cm in thickness.

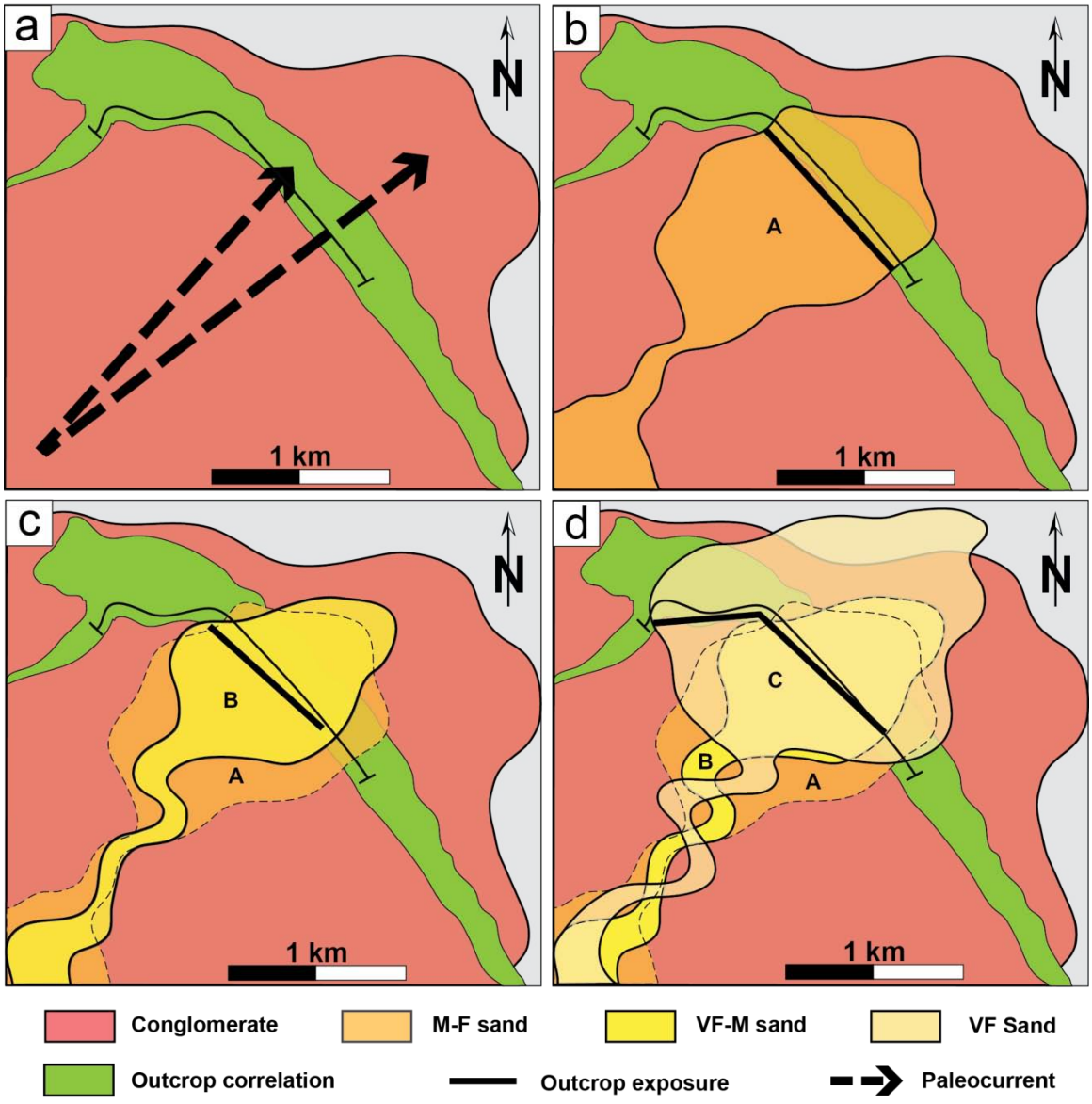

Figure 35: A series of depositional model representing prograding (forward-stacking) lobes. (a) Initial debris flow sweeping over basin floor muds in NNE-oriented paleocurrent direction. (b) A subsequent high density turbidity flow generating the initial lobe. (c) The second lobe prograding out further into the basin. Note the progradation of lobe apex (mouth). (d) The third lobe prograding with larger extent, and thicker and coarser-grained beds

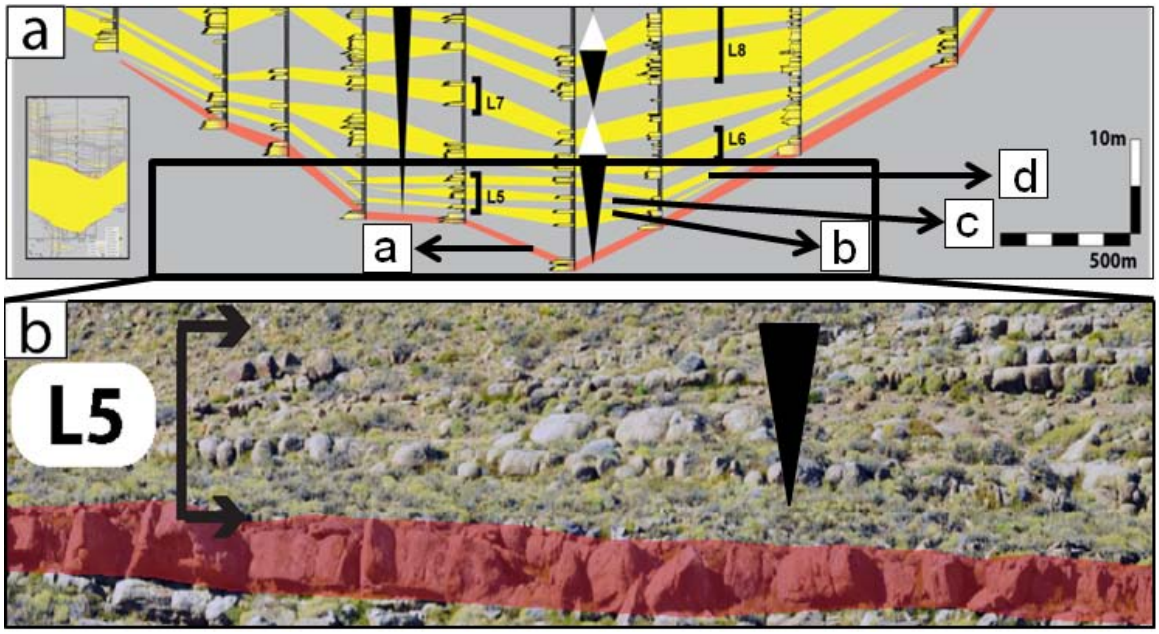

Figure 36: An outcrop analogue relative to prograding lobes shown in Fig. 35. (a) The correlation panel indicating three beds in L5 that corresponds to each prograding lobate flow. Note the thickening-coarsening-upward pattern. (b) The direct comparison of prograding beds in outcrop exposure.

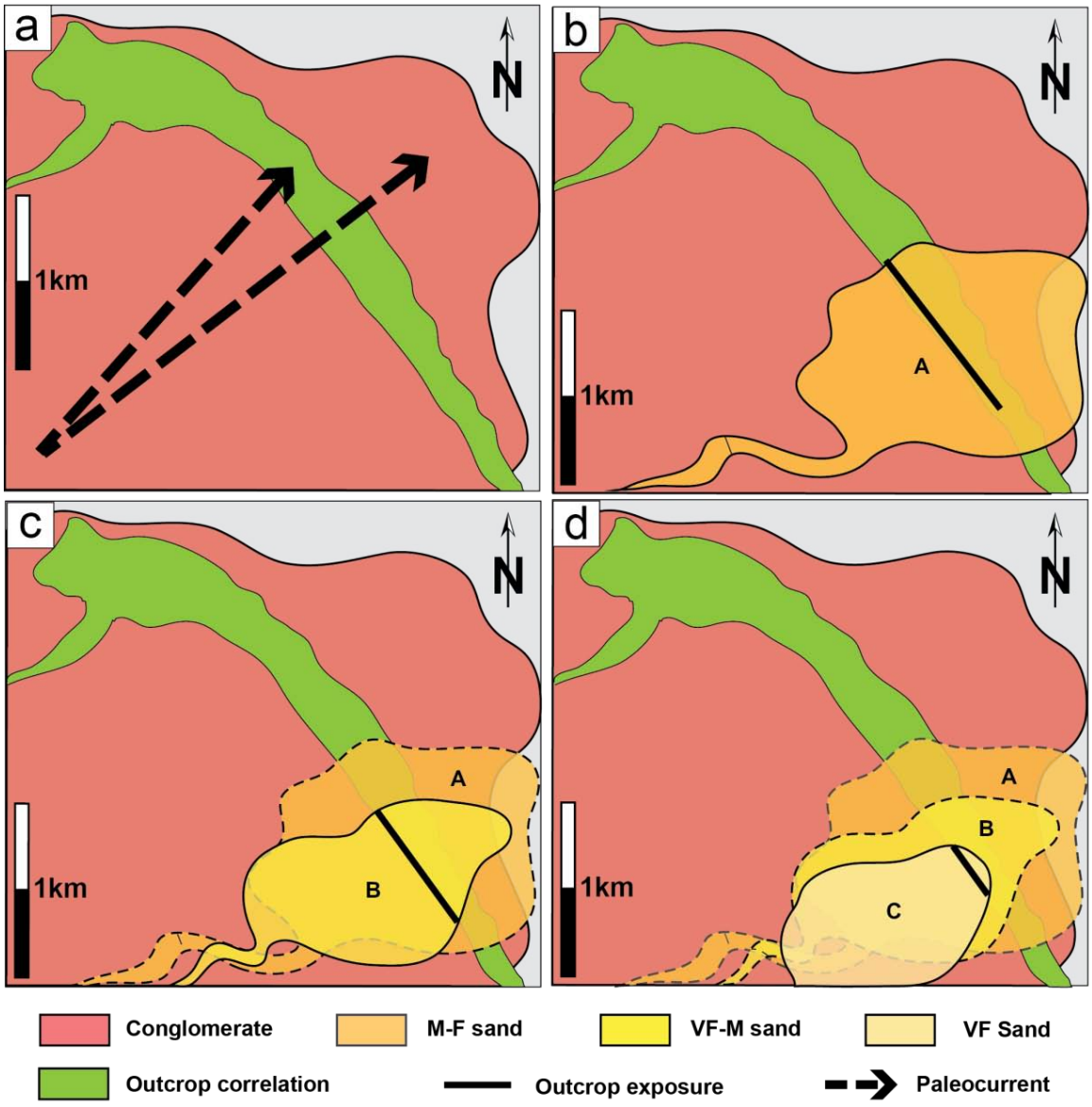

Figure 37: A series of depositional model representing retrograding (backward-stacking) lobes. (a) Initial debris flow over basin floor muds in NNE direction. (b) A following high density turbidity flow producing the initial lobe. (c) The second lobe retrograding with less marginal extent. Note backward-stacking of lobe apex (mouth). (d) The third lobe, primarily comprised of low density flows, retrograding with smaller extent, and thinner and finer-grained beds

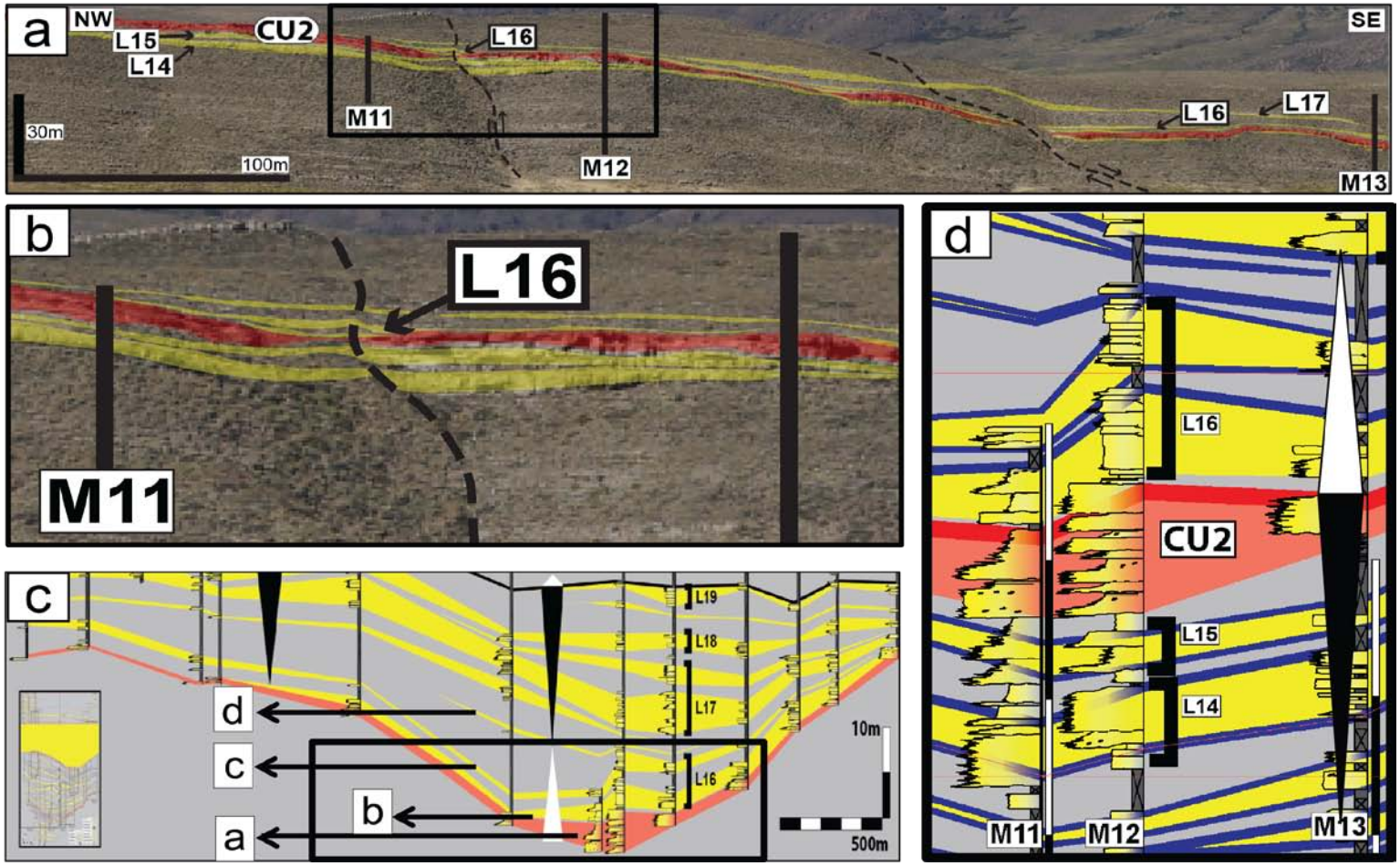

Figure 38: An outcrop analogue relative to retrograding lobes shown in Fig. 37. (a) A distant overview of continuous lobes (L14-17) and a conglomeratic unit (CU2) (b) A close-up of the direct comparison of retrograding beds in outcrop exposure. (c) The correlation panel indicating three beds in L16 that corresponds to each retrograding lobate flow. (d) Thinning-fining-upward pattern dominating above CU2 while vice versa below.

4.4 LATERAL FACIES VARIABILITY WITHIN PHOTOMOSAICS

Section 1 (SW-NE) – Five measured sections (M1-M5; Fig. 39) display the western margin of outcrop oriented SW-NE before the abrupt change in orientation at M6, possibly due to post-depositional events of local fault and folding. The significant folding between M2 and M6 stretches the outcrop aerially looking from the top; however facies units appear to be continuous in the correlation panel.

More than 140 m of basin floor deposits include two conglomerate units (CU2 and CU3) and multiple sheet-like sandstone and mudstone units over a 1.1 km-long transect. The western margin is located paleo-geographically closer to the source area (S-SW). Figure 27b illustrates a whole succession of CU2 and CU3 in red and bounding sandstone and mudstones units in yellow, overlying a very thick (~20 m) muddy unit at the bottom. About 2-3 m thick, CU2 and CU3 has erosional bases, but relatively sharp tops while both units show a good continuity (75-170 m in length) with sporadic zones of abrupt discontinuity (10-35 m in length). At CU3, the discontinuity increases and thickness varies much as the average thickness decreases to less than one meter. In contrast with conglomerates, very flat, continuous, and sharp-based sandstone units onlap mudstones located below. When comparing sandy turbiditic units and conglomerate units, high density turbidites demonstrate higher thickness, continuity, and amalgamation ratio. This relates to extensive and long run-out of highly concentrated pebble-cobble conglomerates in response to high inertial forces of flow head when transported from a high gradient slope, and their tendency to segregate at topographic lows in basin floor. Thus, the rugosity and gradient of slope and basin floor topography possibly impact the depositional pattern of turbidites in the study area.

The general bedding trend in mudstone units (interlobes) mostly resembles bounding sandstones except interlobes associated with small-scale, lenticular lobe

deposits internally. Less than few meters thick and very discontinuous, thinly bedded lobes can be encased within a thick mudstone interval, suggesting a weak low-density turbidity current within a small-scale lobe or above abandonment surfaces.

Section 2 (NW-SE) – 12 measured sections (M6-M17; Fig. 39) represent a NW-SE oriented outcrop correlation over a distance of 3.2 km. All three conglomerate units (CU1-CU3) and 27 lobe units are exposed as basin floor deposits up to 190 m in thickness. Two measured sections (M18 and M19), not shown in the correlation panel, describe units preserved at a slightly higher relief of 3.7 km-long, W-E trending depositional strike across the main outcrop toward the south. As expected, each facies unit shows a convincing correlation compared to units found in the main outcrop transect.

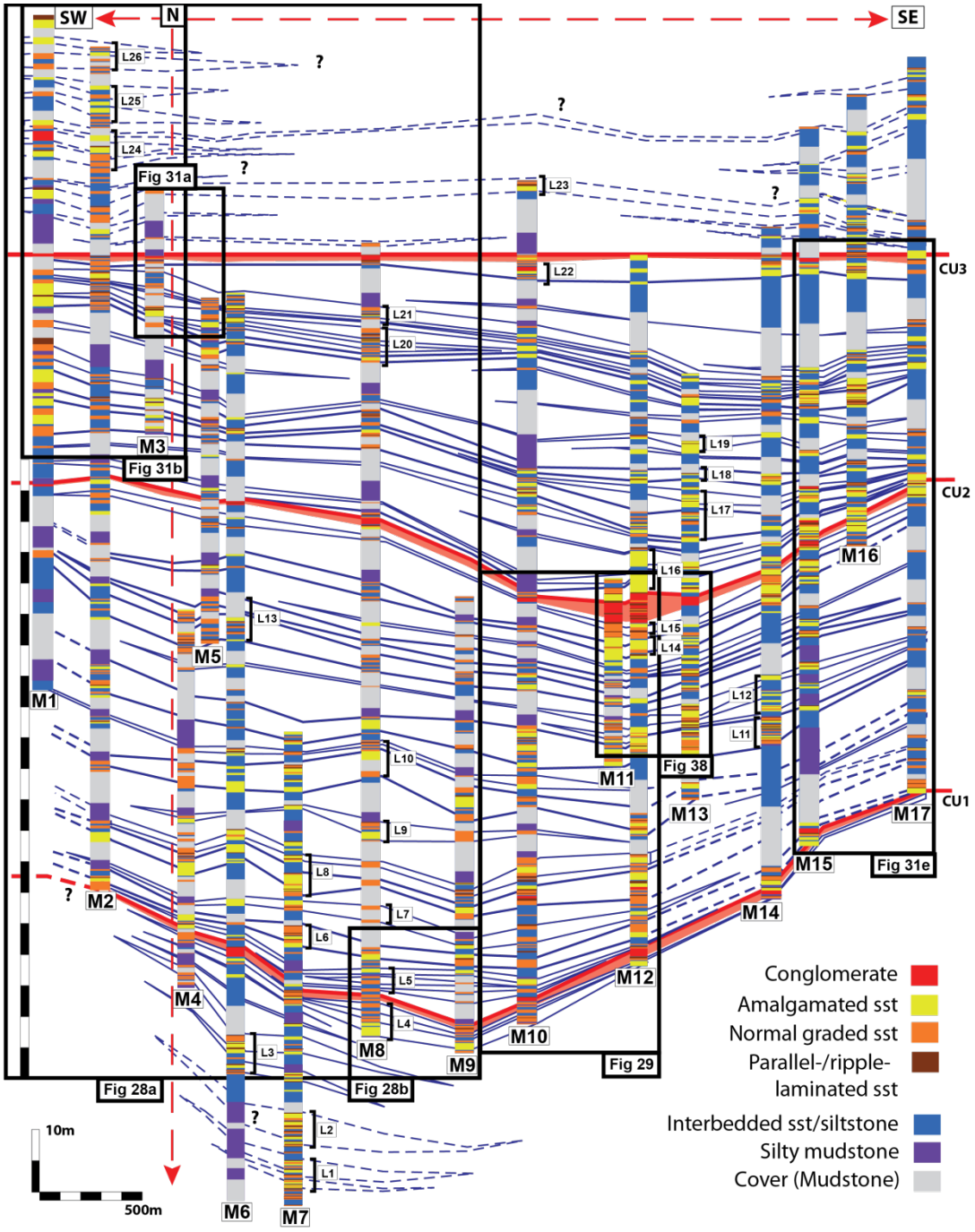

Figure 39: Facies correlation that highlights dominant mud intervals throughout the study area and specific areas concentrated with either sands or conglomerates. Note laterally changing sandy units in Fan A implying compensational stacking of lobes, while more likely aggradational patterns dominating in Fan B.

5. DISCUSSION

5.1 DEPOSITIONAL ENVIRONMENTS

5.1.1 Deepwater System

The succession of distal lobes is composed of: (1) high-energy, laterally continuous, mud clast-rich, massive conglomerates, and structureless or normal graded sandstones at lobe axis to lobe off-axis, (2) moderate-energy, very coarse to fine, amalgamated sandstone capped by interbedded sand-mud heterolithics at lobe off-axis, (3) low-energy, thin-bedded silty mudstone at lobe distal fringe. From proximal to distal basin-floor lobes, thick-bedded, amalgamated sandstones dominate in form of sheet-like complexes.

5.1.1.1 Facies

At distal basin floor, very few channelization observed with scarce incisions or weak erosive bases explains low-relief, compensational stacking of massive F2 or F3-type facies in high to moderate energy setting. Highly amalgamated sandbodies reflect the shifting axis of distal lobes stacking onto another as they keep migrating toward topographic lows (Fig. 39). Further away from the sediment source, structureless and amalgamated facies (F2) are found much less while normal graded (F3) and planar- or ripple-laminated (F4 or F5) facies increase. In a regional perspective, the long period of subsidence and regional inversion initiated by the late Triassic-early Jurassic Andean magmatic produced a steep margin, and led to the widespread and laterally continuous succession of conglomerate and subsequent turbidity-driven sandstone units at relatively high sedimentation rates. Hubbard et al. (2010) explains the strong tectonic influence contributes to the development of a high-relief margin, elongate basin, and higher rate of

sediment input than the rate of mobile substrata development on the slope, which leads to the efficient transfer of sediment to basin due to smooth slope profile. Simple, sheet-like stacking margins, less deep incisions, very few basal lags, and thick-bedded F2-F3 facies indicate a medial basin floor (> 10 km from toe of slope) where more net deposition occurs after bypassing the proximal area. Thicker beds may correspond to overlapped main axis of lobe deposition that stacks directly onto each other (Nilsen et al., 1994). In most cases, axis and off-axis of lobes switch while the lateral extent keeps constant for longer than 3 km. Small intervals of thin-bedded sandstones (F2-F5) intercalated with silty mudstones (F6-F7) exhibit loss of confinement which generates small-scale lobes (<1m thick) or entirely mud-dominated, distal fringe setting after a series of erosion.

No direct evidence of significant erosion or channelization suggests the lobe deposition occurred farther away from the slope or proximal fan setting. Also, thick intervals of laminated mudstone beds show a contrast with mudstones in slope as those are thinner and less abundant. The considerable increase in the occurrence and thickness of mudstones in Fan B compared with Fan A reflects reduced tectonic activities generated from the initial uplifts and opening of the basin in Late Triassic. Stabilized slope and flattening of margin gradient are possibly able to reduce erosion along slope and basin floor, and ultimately develop thick mudstones in relatively low energy settings when less external controls are received.

5.1.1.1 Depositional Processes

The very coarse grain size, cobble to very coarse sand, primarily found at the basin floor and the shelf margin reflects several evidences of a short, direct source-to-sink system in the La Jardinera region: (1) gravelly and sandy turbidites at both basin floor

and shelf hierarchically displaying sequences of similar architectural elements with partial or almost complete Bouma sequences, (2) high density turbidites in slope to basin floor, from confined to unconfined lobe deposits, representing abundant slope channelization and scours, and thicker bounding mud units downdip closer to basin floor, (3) prevalent mud rip-ups and small pieces of woods and trunks deposited randomly within beds, (4) cobble-pebble size intraclasts (single clasts within conglomerate unit, mudclasts, leaves, and woods/trunks) within conglomerates implying a direct continental source. The major depositional mechanism of conglomerates can be explained by existence of large clasts mixed with muddy matrix, which reflects en masse deposits without much of distinctive internal sedimentation patterns (Talling et al., 2012). The frictional freezing partitions a flow into different density flows as the matrix essentially serves as a pore-filling lubricant (Lowe, 1982; Talling et al., 2012). Different levels of traction in separated flow help transport denser and coarser sediment packages, and settling process follows for the suspended sediment fallouts (Lowe, 1982). Compared to conglomerates found at the toe of slope, proximal basin floor fans (< 1m; Tudor, 2014), and younger basin floor fans in La Jardinera (Fan B and above; CU2, CU3), the conglomerate unit at base of the study area (CU1) exhibits higher thickness (up to 2 m) and relatively bigger clast sizes (pebble to cobble sized, a clast up to 20 cm). This downslope difference in bed thickness and grain size suggests that the initial debris flow responsible for forming CU1 may have been the strongest in the basin since the conglomeratic units (CU1-3) become generally thinner and finer, reflecting waning distal flows from the source. Depocenters controlled by regional tectonism and subsequent subsidence develop a deep basin with high accommodation and high basin margin relief, which leads to thicker conglomerate units with larger intraclasts. Dominant intervening strata of hemipelagic muds and existing marine faunas in the study area indicate a

deepwater basin setting, easily differentiated from alluvial derived conglomerates that include coals, roots, paleosols, and non-marine faunas associated with clast imbrication (Nemec and Steel, 1984). When the gravity flow decelerates at the base of slope, lobe deposits appear to increase variability in terms of sedimentary structures and facies due to high volume of density and gravity flow, which accumulates very coarse, poorly sorted grains at base, normal graded and amalgamated sandstone beds in axis, and heterolithic silty mudstones in distal lobe off-axis areas (Fig. 40). In some areas, the settling velocity may exceed the shear velocity and promote higher net deposition of clay in a sheet-like form. Thick intervals of mudstones (F7) in the study area suggest periods of quiescent deposition with less turbidity currents and erosions during abandonment processes, or fringe areas with weak turbidity currents (Fig. 40). Both high- and low-density turbidity flows may cause the mud deposition while suspension playing a critical role in distal or off-axis lobes (Talling et al., 2012).

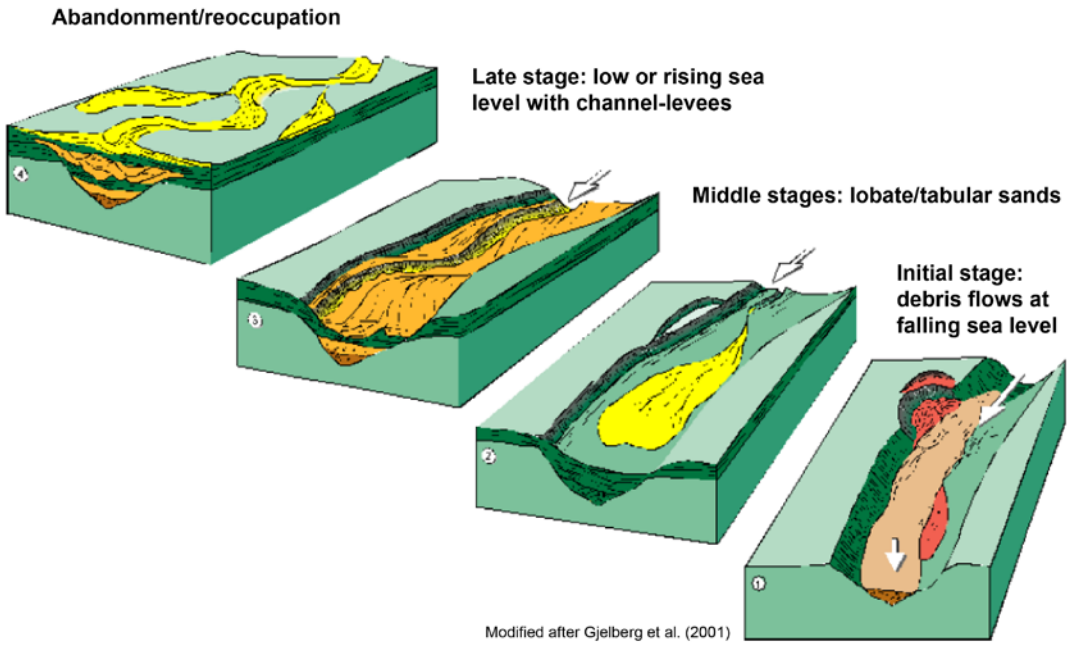

Figure 40: Generalized processes of active deepwater sedimentation during lowstands (Modified after Gjelberg et al., 2001).

5.1.2 Lobe Deposition

5.1.2.1 Proximal fan

Previous studies in La Jardinera area (Paim et al., 2008; Vann, 2013; Tudor, 2014) focused in the source-to-sink stratigraphy of the Los Molles Formation emphasizing turbidity deposits in the channel-lobe transition zone and proximal fan. Describing primarily on slope areas and associated confined to weakly confined lobe deposits, Vann (2013) and Tudor (2014) observed the initial fan deposit at base of the Los Molles Formation including meters thick conglomerate units over large distance. Turbidite channels with heterolithic siltstones, overbank deposits, and slumping are exclusive at lower slope as confined lobes develop downdip (Vann, 2013). One of the

most extensive and forming dominant cliffs, conglomerates are tens of meters thick at the upper shelf margin and transform to less coarse bypassing sandstones on slope, or channel infills (Vann, 2013), and eventually back to conglomeratic-coarse grained sandstones in the basin floor lobes with high degree of amalgamation and erosive bases (this study). The 4-5 km-long channel-to-lobe transition zone characterized by a series of erosional scours and slumping features infers a relatively large fan system (~30 km long, ~10 km wide) for the study area in La Jardinera (Wynn et al., 2002; Tudor, 2014). The inferred size of a fan represents composite lobe complexes, thus the size of a single lobe unit can decrease to one fourth or smaller (< ~7.5 km long, < ~2.5 km wide).

5.1.2.2 Distal Fan

Deposits described in this study are typical for the basin floor with outcrop dominated by thin-bedded and thick-bedded tabular turbidites, significant (kilometers) lateral continuity, planar geometry, rare channelization, and low sand/mud ratio in some interval of the deposits (Mutti, 1977; Mutti and Normark, 1987). The architecture elements within distal lobes significantly vary based on different location from the slope to basin floor with somewhat well-defined trends. The primary control on facies architecture of lobes and debris-flow deposits is the grain size of supplied systems sourced from superjacent delta and shore that reach the shelf-edge. The grain size distribution changes when slope angles vary in response to rate of deposition from the source. Types of source affect the formation of continental slope and basin floor morphology as point sources create fans and line sources form slope aprons (Galloway, 1998). Another element on facies variability is bed thickness which reflects characteristics of turbidite flows typically preserved with parallel and sheet-like geometry

at outcrop. Traditionally, varying bed thickness of turbidites has been incorporated into interpretation of lobes since the hierarchy of facies associations often shows very distinctive patterns such as thickening- and thinning-upward trend (Mutti and Normark, 1987). In the study area, the gravity flows consisted of gravels and coarse sands interbedded with mudstones accumulate at the basin floor in form of lobes (<10 m) and stack onto the other lobes forming lobe complexes (<50 m) within a fan. Consisted of two or more single event beds that deposited in few tens of cm to few m thick beds, a lobe is defined by laterally extensive bounding surfaces marked by abrupt changes in facies association (thickening- and thinning-upward), which is interpreted as avulsion of distributive channels at basin floor (Prelat and Hodgson, 2013). In vertical lobe sequences of the Los Molles Formation, lobes within each lobe complex display four types of trends associated with bed thickness and grain size variations: thickening-coarsening-upwards, thinning-fining-upwards, blocky, and disorganized. These stacking patterns reflect prograding, retrograding, aggrading, and lateral migrating of lobes in terms of stratigraphic records, respectively (Hodgson et al., 2006), yet both aggradation and progradation cause the formation of lobes with thickening-upward trend (Shanmugam and Moiola, 1988). The stratigraphic terminology for prograding and retrograding lobes are substituted to following synonyms such as forward-stacking and backward-stacking, because deepwater basin floor environments below the storm wave base can be unresponsive to relative sea level changes at times. The dominant sequences of basinward progradation (Figs. 35-36) imply a high sediment supply system in the region associated with forward-stacking of thickening-coarsening-upward lobes.

The unconfined lobes include highly amalgamated and continuous sandbodies in compensational packages intercalated by rather sharp-based mudstones. In terms of external lobe geometries, lobes have radial to elongate shape while quickly thickening at

proximal and slowly thinning at distal. Axial, off-axis, and lateral fringe areas of a single lobe exhibit specific facies at each different position are recognized by different facies types. Axis of a lobe displays thick-bedded and/or thin-bedded (FA1, FA2), normal-graded, and very coarse to fine sandstones associated with high amalgamation and thick bed sizes (Figs. 19, 20, 21a-b). Off-axis part of a lobe often includes thin-bedded sandstones (FA2) onlapped by planar- to ripple-laminations and interbedded sand- and mudstones (FA2, FA3) (Figs. 20, 21b-c). Fringe areas associated with silty mudstones and lenses of fine- to very fine-sandstones (FA3-5) represent laterally distal parts of a lobe (Figs. 20c-d). In scale of fan system (> 50 m), each fan A and B in the study area demonstrates the thickening-coarsening-upward trend of which is separated into a scale of lobe complex (8-40 m; Figs. 27, 30). The different stacking patterns of lobe-scale beds reflect different types of flow and deposition depending on the balance of autogenic compensation processes (channel migration or avulsion, topography, and other intrabasinal factors) to allogenic controls (eustasy, tectonic setting, and climates) (Prelat et al., 2009). Erosive flow of laterally migrating lobes can cut, amalgamate, and form a lenticular geometry with an apparent disorganized stacking pattern. The undulation and discontinuity of a single lobe may also indicate the erosional processes by multiple migrating lobes or avulsions (autogenic controls) while a thin-bedded lobe itself can make such characteristics through its depositional process. Thus, depending on external unit continuity and internal facies patterns, depositional position of lobe deposits can be classified and predicted. Fan A illustrates a clear transition in vertical depositional pattern, a drop in degree of amalgamation upwards from thick-bedded (lobe-axis) coarse grained sandstone units to thin-bedded units of medium to fine grained sandstones interfingering with interbedded silty mudstones (Fig. 39). This change in the vertical pattern suggests avulsion of flow and/or laterally shifting lobe axis to fringe zones where

often found with low- to non-channelization in a medial to distal fan system. At lobe off-axis or lobe fringes, abundant interbedded mudstones relates to the low energy environment because sandy turbidity currents rarely reach the distal location. In outcrop, thin-bedded and lenticular lobes (< 2-3m thick, < 3km wide; L5, L9) that thin toward edges (Fig. 27) indicate a complete 2D succession of relatively small-scale beds. These small lobes are bounded by laterally extensive and thick mudstone intervals, possibly suggesting an avulsed flow from a main feeder channel that usually produces thick and amalgamated composite lobes. In opposite, thick-bedded and very continuous lobes (< 6-7m thick, > 4.5km wide; L10, L11, L17) demonstrate lateral extent much larger than the outcrop exposure. The thickness of thick-bedded lobes varies over distance, however their grain size and continuity are held fairly constant (Figs. 20a-b). The general thickening trend of sandstones toward the western flank aligns with the paleoflow direction (Figs. 36b-d), because total sand content and lobe connectivity increase closer to the source area within a fan due to increased channel switching (Reading and Richards, 1994). High accommodation available at topographic lows (Mutti, 1992) leads to infilling the space as compensational bedding: thick, amalgamated packages of fine-grained sandstones and mudstones (Lobe complex B1; Fig. 30). In contrast, low accommodation to topographic highs may cause a high degree of lateral migration of lobes with high erosion (Lobe complex A1; Fig. 27).

5.2 CONGLOMERATES AT BASIN FLOOR

5.2.1 Transport Mechanism

The lack of any dominant conduit through the slope in the area demonstrates the unique setting of gravity-driven deposits. Rather than paving and creating a canyon structure, sediments bypass and generate incised channels in proximal fans in addition to frequent events of sliding and slumping that are able to transfer conglomerates for long run-out distances through *en masse* flow. The hydroplaning is thought to occur beneath a laminar flow and transport pebble-conglomerates through debris flows or co-genetic flows in distal region of a fan (Haughton, 2006), and some of the conglomerate debris flow deposits were emplaced through this mechanism. Detailed sediment flow system and its mechanism of the coarse sediment transfer from the source area to the deepwater basin not yet examined. However, both lower slope and basin floor areas in La Jardinera show the high continuity of sheet-like and turbidity-driven conglomerates and sandstones in the oblique, along-strike correlation panel. Along a rather steep slope (< 2-3°) (Vann, 2013), lobes within two fans migrate to N-NE in form of prograding clinoform with coarse sediments sourced directly from the shelf; its evidence for genetic link as source-to-sink is supported by existence of very similar clast-supported conglomerates found at the shelf. Stanley (1980) describes coarsening-upward successions of megasequences comprised of very coarse, lenticular, and disorganized conglomerates, and fine-grained sheet facies at a submarine slope and basin floor of the Var River system in the southern France, indicating fan lobes derived by debris flow and high-concentration turbidity currents. The proposed model of deepwater conglomerates in Var River System emphasizes strong tectonic overprints such as uplift and shift of the basin margin, and structurally induced diversion of fluvial systems (Stanley, 1980). Thus, occurring at a similar setting like a structurally active margin on edge of two different plates,

coarsening-upward sequences and dominant progradational stacking patterns in the Los Molles Formation indicate the interplay of tectonic-induced events and rapid sedimentation of coarse grains directly onto deepwater fan systems.

5.2.2 Triggering Mechanism

Interpretation of multiple architectural elements, facies types, downdip gradient, degree of erosion, degree of confinement, and regional tectonic history suggests medial to distal lobe complexes within a basin-floor submarine fan system for the main depositional setting of La Jardinera area. The shelf-slope-basin floor physiography is supported by a relationship of which both shelf and basin floor deposits contain very similar conglomeratic characteristics, possibly sourced from changing sea-level-induced shelf margin erosion, tectonic-induced submarine slumps or subaerial landslides, and uplifted continental systems prograding basinward. According to Talling et al (2007), highly erosive submarine turbidity flows can produce giant debrite or subsequent turbidite successions over several hundred kilometers from an initial landslide. Thus, extensive conglomerate units in the La Jardinera region beyond the lower slope may transport clasts via non-channelizing debris flow that runs out long across nearly flat basin floor. However, rare slumping or sliding features in slope in conjunction with abundant well-rounded extrabasinal conglomerates and very few centimeter-scale plant matters or fossils in all 7 facies indicate a direct feed from paleo-coastlines over a long run-out distance (> 30 km) when the sea level and uplift had substantial transitions. The abundance of widespread and thick mud-rich units, possibly deposited as the 4th order transgressive and highstand systems tracts, relates to an abandonment phase before any prominent change in sea level or tectonism (Paim et al., 2008). According to Burgess et

al. (2000), the location and style of turbidite deposition in the Los Molles Formation were controlled by basin floor topography related to extensional fault systems, because the major sediment transport was primarily fault parallel. In a bigger scale, the distribution of coarse grained lobes was strongly controlled by the location of major Jurassic fault trends (Fig. 3) that stabilized the position of the shelf-slope break in the Neuquén Basin (Dean, 1986). Initiated by the regional extensional faults, slope failures such as slump and slide seem to trigger rapid transport and deposition of conglomerate size clasts and sandy turbidity flows at basin floor with support of quasi-permanent sediment flux during coeval tectonism and steep slopes in the source area. Based on multiple facies associations and relationships, three conceptual models (Fig. 41) explain the origin of conglomerates and thick succession of turbiditic sandstones:

(1) The back-arc Neuquén Basin associated with active tectonic movements obtained extrabasinal clasts found in conglomerates from uplifted and faulted areas of the Northern Patagonian Massif and surrounding high-relief mountains in the south, a volcanic arc system toward the west, proto-Pacific Ocean, and lastly the Pampeano-Sierra Pintada Massif at the northeast (Paim et al., 2008; Ramos, 2008). The syn-rift sedimentation at the lowest Los Molles Formation is comprised of all sorts of continental deposits (alluvial, fluvial-deltaic, lacustrine, and pyroclastic) (Grimaldi and Dorobek, 2011). The volcanic arc formed in a linear shape parallel to the South American plate may have acted as a continental source of volcanic clasts in the basin, and the proto-Pacific Ocean began to supply open-marine deposits after the post-rift stage initiated at the Pliensbachian age (~191 Ma) (Vergani et al., 1995). The lasting of fault-related thermal subsidence and half grabens in the early to middle Jurassic maintained the low relief of the depocenters (Figs. 1, 2) and increased the gravity-driven sedimentation in the

Neuquén Basin, especially during the Toarcian-Aalenian periods (Franzese et al., 2003; Howell et al., 2005). Following the Early Jurassic development of a 200-km-long, east-west trending, right lateral shear zone called Huincul Arch toward the southeast of the study area (Grimaldi and Dorobek, 2011), frequent inversions may have led to multiple reactivations of previous faults and Triassic half-grabens, genetically linking with the deposition of three conglomerate units at the distal fan in terms of spatial and temporal relationship. Mattern (2005) states that construction of sand-rich submarine fans is mainly attributed to tectonic activities. Therefore, strong uplifts at the source area appear to be responsible for generating gravity-driven currents from shelf to basin floor.

(2) As the sea-level transitions into a lowstand, gravity-driven currents from the top shelf are able to transport all sediments downdip along a restricted and high relief margin. Many reconstructed models of global sea level fluctuations indicate an abrupt drop of relative sea level at the Triassic-Jurassic boundary severely devastating ecological niches, and slow recovery persisting throughout the Jurassic period (Vail et al., 1977; Hallam, 1983; Haq et al. 1987). Rapid, short-term, small-scale sea level rise in early to middle Jurassic periods could locally occur at the study area due to subducting of two colliding continental plates (South American plate and Nazca plate) that potentially displaced a massive amount of sea water. However, medial to distal fans in deepwater basin floor probably would have been insensitive to those small-scale variations in sea level. Regardless of sea level changes, coarse grained and massive sand-rich fans could form in relatively small, restricted, and tectonically active basins (Stow and Johansson, 2000). Decreased sea level can reduce accommodation space on coastal plains and shelves, and allow sediments to be more efficiently transported to basin floor by bypassing the shelf and slope (Reading and Richards, 1994). Thus, debris flows and turbidity flows are able to bypass channelized slope and proximal basin floor, and reach

distal, unconfined, outer fan systems where all high-energy gravity flows drop the coarse suspended load (including conglomerates) and begin to dilute basinward with fall-outs of finer grains. All inferred information associated sea level fluctuations suggests that the uplift and subsidence found in the southern rift zone of the Neuquén Basin could transport conglomerates and build coarse grained turbidite systems even during short highstands since the depositional setting (tectonism, basin size, water depth, distance from source, etc.) controls the major succession in distal fans.

(3) Large slope failures involved with regional-scale tectonism and local extensional faults may instantaneously transport large clasts to the lower slope or proximal fan areas and deposit in form of mass-transport-complex. In the study, conglomerate layers are onlapped by high amounts of mud, which reflects a sequence of rapid coarse-grain deposition followed by suspension of turbulence or hemipelagites. The near-absence of sandy units on top of conglomerates suggests an accelerated hydroplaning debris flow mixed with a basal lubricating layer and high sediment concentration (Mohrig et al., 1998). Rare intrabasinal clasts in conglomerates may indicate less erosion along the sediment pathway and reduced drag on beds, promoting high velocity of debris flows and long run-out distance of conglomerates.

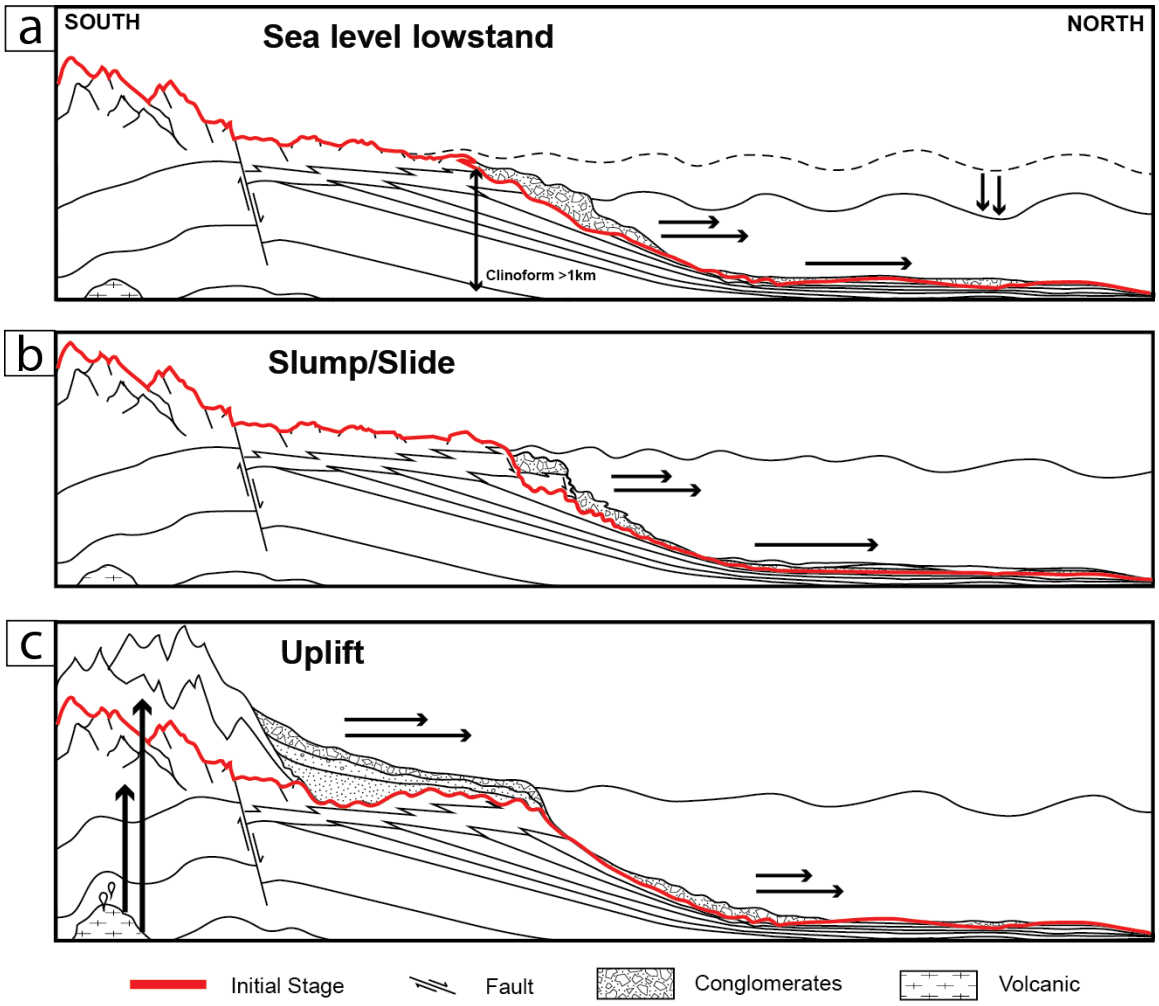

Figure 41: Three triggering mechanisms of conglomerate transport to distal fans. (a) Abrupt sea level fall at Triassic-Jurassic boundary and following sea level lowstands for the Early Jurassic periods. (b) Slump or slide occurring at upper slope associated with strong tectonic influences such as earthquakes and faults. (c) High relief, uplifting source areas impacted by two colliding continent plates at the coastal margin.

5.2.3 Modern Analogue

The equivalent study on pebbly conglomerates in a distal fan system has not been developed yet since the transport and deposition of such coarse grains onto basin floor rarely occur. In most cases, conglomerates in form of debris flow or mass transport complex accumulate on shelf, slope, or base of slope where gradient starts to become gentle. For example, Stanley (1980) focused on coarsening-upward successions of the Upper Eocene to Lower Oligocene Saint-Antonin conglomerates deposited at a submarine slope of the French Maritime Alps. Similar facies successions in the Alps such as disorganized conglomerates, coarse, lenticular, sheet-like sandstones, and microfossil-bearing silty shale-siltstones suggest submarine lobe progradation on a slope, or in a slope basin seaward of a fan delta system in an open deep marine environment close to tectonically-active margins (Stanley, 1980). While the author also argues a possibility of alluvial fan deposits for the study area, the evidence of migrating tongues of sand- and gravel-rich units on the upper slope affirms a strong tectonic overprint that initiated shifting of basin margins and switching of fan delta on shelf (Stanley, 1980). Steep slope gravel complex of the Quaternary Var River-Var Delta located at the west of Nice on the Mediterranean coast southeast of the Saint-Antonin conglomerates presents comparable attributes to the submarine conglomerates such as coarse debris deposits from the adjacent Maritime Alps and silty mud at the delta front and upper slope (Stanley and Unrug, 1972). These conglomerates are found to be transported downslope by gravity flows to basin floor when periodic displacements at shelf occur in response to tectonic movements (Bourcart, 1964; Gennesseaux, 1966). Therefore, with the structurally-induced narrow shelf and high relief steep margin of the Neuquén Basin, such coarse deposits could also evolve in response to multiple pulses of direct bypassing of coarse terrigenous grains from the shelf while tectonic processes heavily controlling the fan

growth. The reconstructed model of conglomerates and sandy lobes at the Los Molles Formation is developed relative to the depositional model by Stanley (1980) (Fig. 42). The dimensions of setting and regional environments are different in addition to location of conglomeratic deposits. At the La Jardinera area, conglomerate units spread over at basin floor and further out toward medial to distal fans. In contrast, Saint-Antonin conglomerates in the Var River system are found at lower slope to proximal fan areas. The short run-out distance of conglomerates from the source more likely relates to length and/or gradient of slope than that of shelf or source.

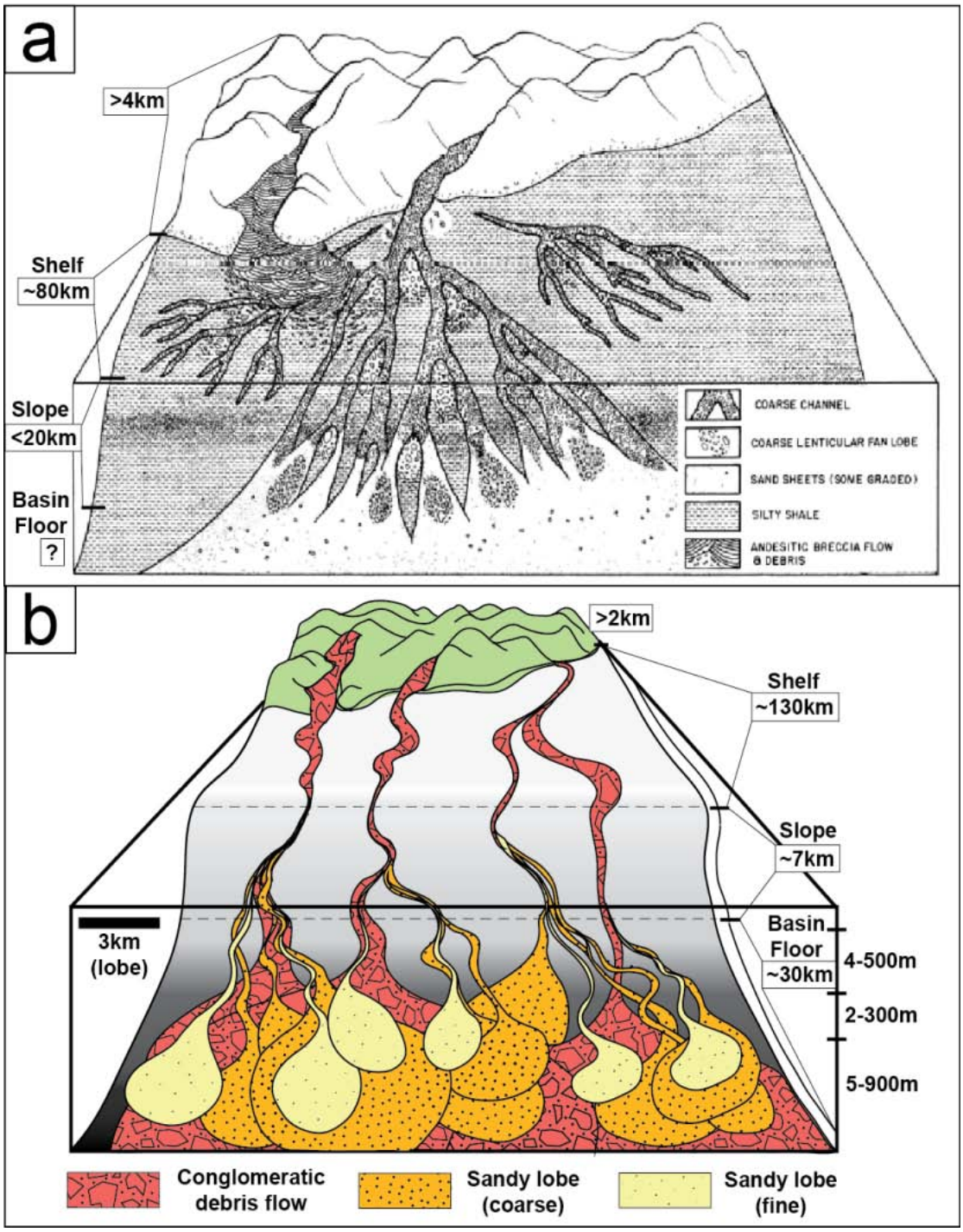

Figure 42: A direct comparison between (a) the depositional model by Stanley (1980) and (b) the Los Molles Formation model. Note that the dimensions of setting and regional environments are different, but conglomeratic deposits are found at basin floor (proximal deposition – a, distal deposition – b).

5.2.4 Hydrocarbon implications

The Los Molles Formation is traditionally considered one of the hydrocarbon sources in the Jurassic units (Martinez et al., 2008). Good reservoir-scale observation of lobe units in this study expands beyond up-to-date capability of exploration seismic data by revealing cm-scale sedimentary structures and correlating sub-units within lobes. Facies F1-F3 accommodate large, thick sets of sandbodies in highly amalgamated pattern as the deposition primarily occurs at axis or off-axis of a single lobe. Further away from the source and proximal areas, facies F3-F7 appear to form heterogeneous lobe sets and deposit at distal and lobe fringes while onlapping basin margins. These distal facies infer much poorer quality for hydrocarbon production due to extensive and continuous facies F6 and F7. Particularly, facies F7 work as a significant baffle or seal, hindering connectivity of bounding sandbodies since hemipelagites are expected to exhibit higher vertical permeability and lower horizontal permeability (Ochoa et al., 2013). Generally thicker lobes toward the SSW (location of source area) shown in the log correlation indicates higher lobe connectivity built by composite sandbodies of aggradational lobe axis. Since thick-bedded lobes build along the axis of distributary feeder channel, the accurate analysis of paleoflow for basin floor deposits can optimize estimation of net to gross ratio.

6. CONCLUSION

The early Jurassic back-arc basin developed by the Andean magmatic arc and intraplate extension led to the 1,000 m thick succession of the Los Molles Formation in Neuquén Basin, representing a wide range of grain sizes with different types of gravity flows. To characterize deepwater conglomerates and coarse grained sandstones, 7 facies types (F1-7) and 6 facies associations (FA1-6) are linked with a total of 19 measured sections (~2500 m in total thickness), photomosaics, paleocurrent measurements, and correlation-based models in primary focus of spatial variations in bed thickness, grain size, and geometry. The Los Molles Formation exhibits sheet-like and very coarse to fine grained lobe deposits in a distal fan setting and expands the range of possible submarine fan models by adding conglomerate units. Detailed description and interpretation of turbidites in the study area may help understanding of unconfined lobe networks for vertical and lateral spatial variability, which later can be applied to prediction of permeability and connectivity of sandbodies in reservoir scale.

Few meters thick conglomerate beds (2-3 m) were interpreted as debris flow or high density flow deposits. The three pebble- to cobble-rich conglomerate units (CU1-3) alternate with a few meters thick sandstone units interpreted as basin floor lobes (L1-26). A total of 27 lobes that form 5 lobe complexes and 2 fans have been mapped along a 4.5 km-long outcrop transect oriented SW-NE in west and NW-SE in east. The lower Los Molles lobes demonstrate an overall forward-stacking (prograding) pattern, with only a few lobe units that show back-stacking (retrograding) patterns. The entire 200 m interval in the study area indicates an overall coarsening upward (progradation-aggradation) pattern associated with compensational lobe stacking of which coarse grained lobes

preferentially fills topographic lows and shows lateral thickening toward axis and thinning toward fringes.

Coarse grained (conglomeratic) deposits formed through a combination of active tectonics and relative sea level changes (fall). Especially, long periods of subsidence and regional inversion generated depocenters in the basin filled by gravity-driven deposits along the steep slope margin (> 3-4°), high relief and narrow shelf, and high sediment flux. Thick (tens of meters) conglomerate beds found at the shelf edge within incised valleys show the source area for described fans at basin floor. More detailed studies can be followed to find if conglomerates are directly sourced from the river, or initially deposited at the shelf edge and later reworked into basin floor.

Appendices

Appendix 1 shows rose diagrams for paleoflow measurements. Appendix 2 includes 4 close-up figures of the measured sections used in the Fan A - Fan B correlation.

A supplementary CD contains additional materials.

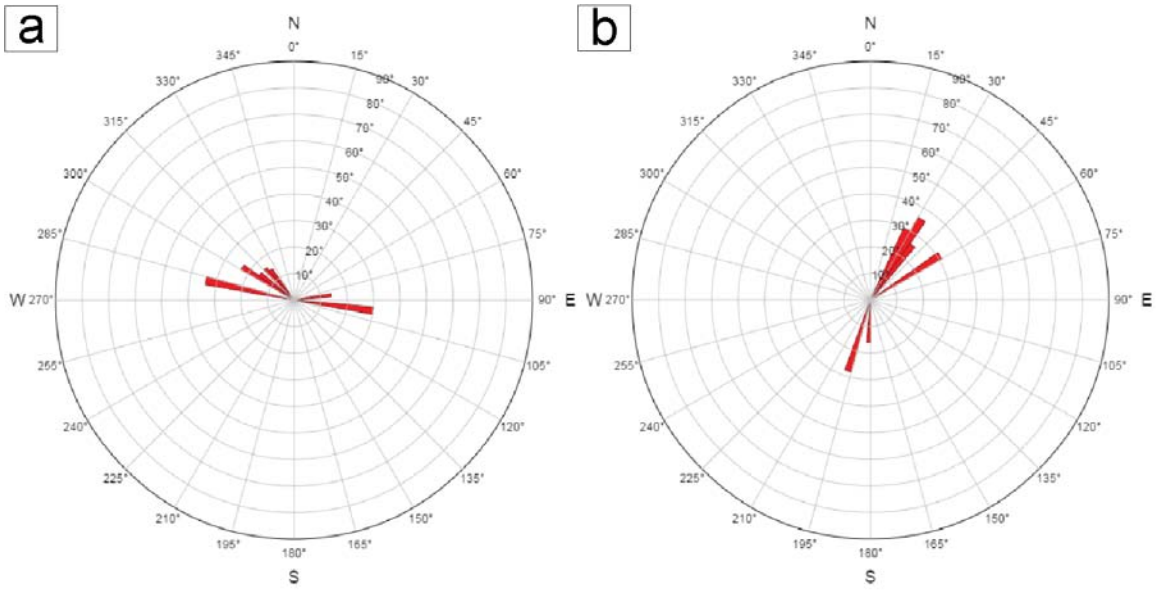

APPENDIX 1: ROSE DIAGRAMS FOR PALEOFLOW MEASUREMENTS. (A) W-E BIMODAL PALEOFLOW DIRECTIONS MEASURED BY TOOL MARKS FOUND AT THE BASAL BEDDING PLANE OF AMALGAMATED BEDS (N = 9). (B) NE TO NNE PALEOFLOWS MEASURED BY TROUGH CROSS STRATIFICATIONS (N = 5) AND A FEW FLUTE CASTS BENEATH PROTRUDING NORMAL-GRADED SANDSTONE BEDS (N = 3).

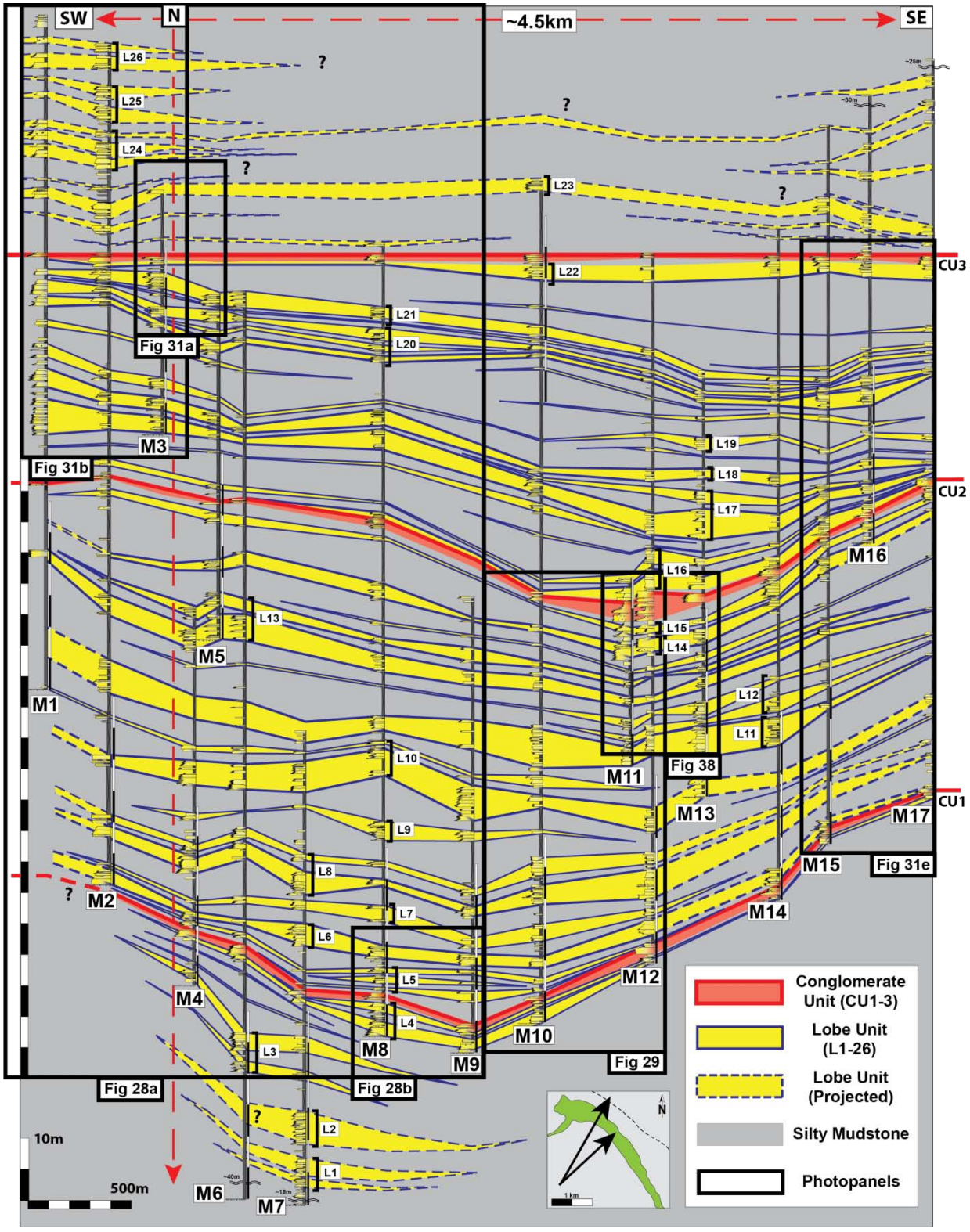

APPENDIX 2: MEASURED SECTIONS USED IN CORRELATION.

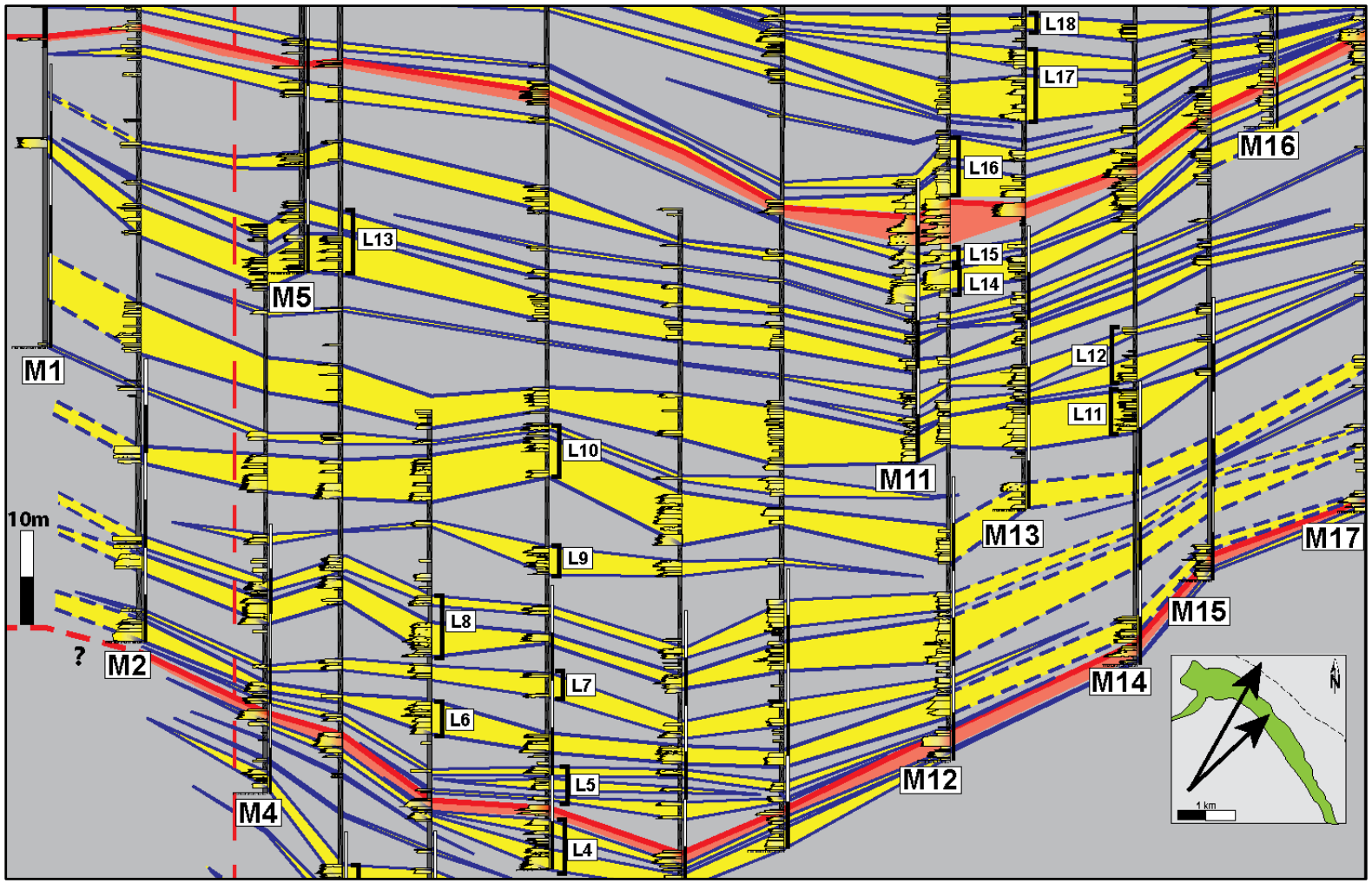
L18
L17
M16
L16
L13
L15
L14
M5
M1
L12
L11
L10
M11
M13
M17
10m
L9
L8
M15
?
M2
L7
M14
L6
L5
M12
M4
L4
N
1 km

FAN ‘A’

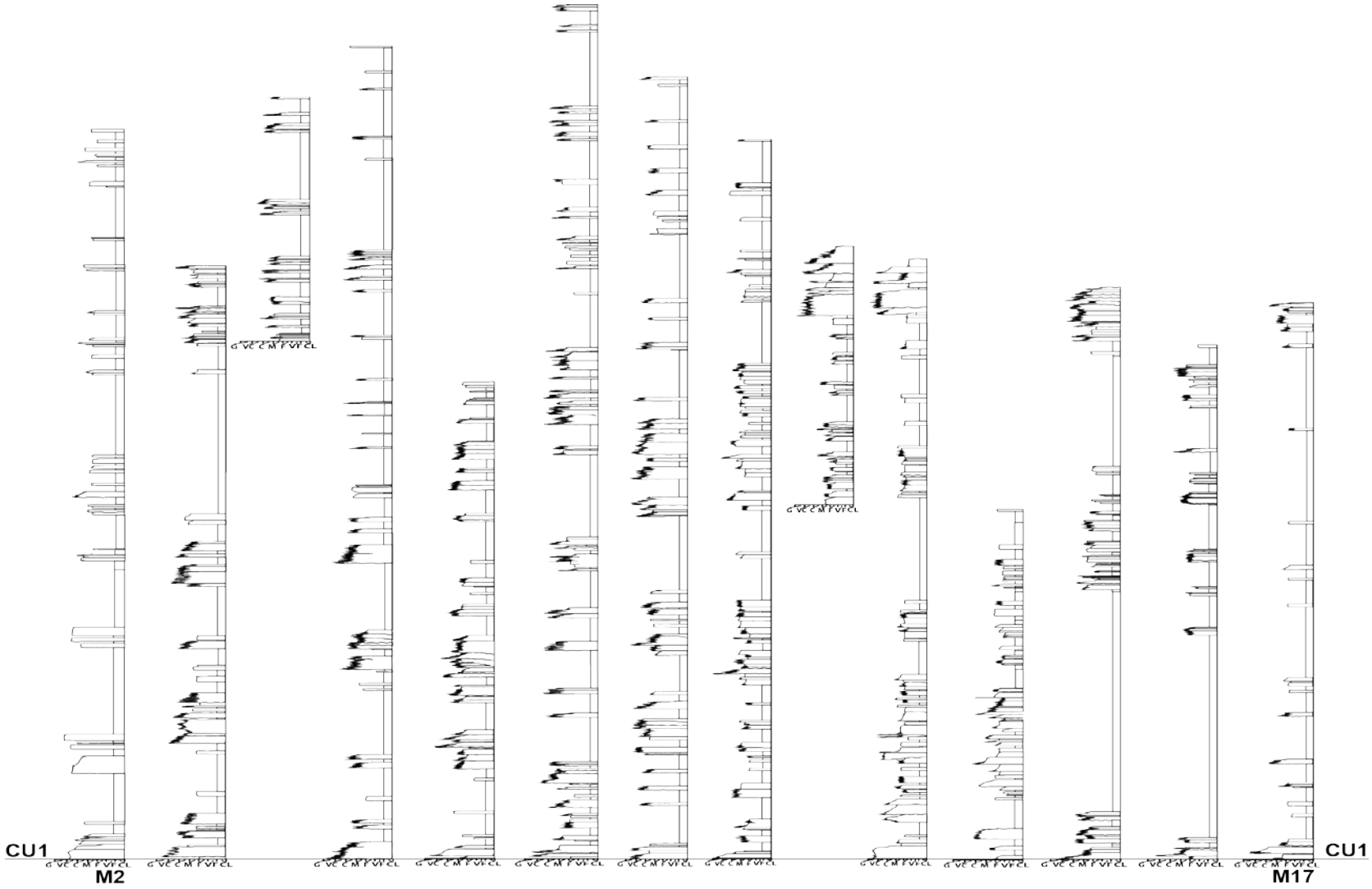

FAN ‘A’

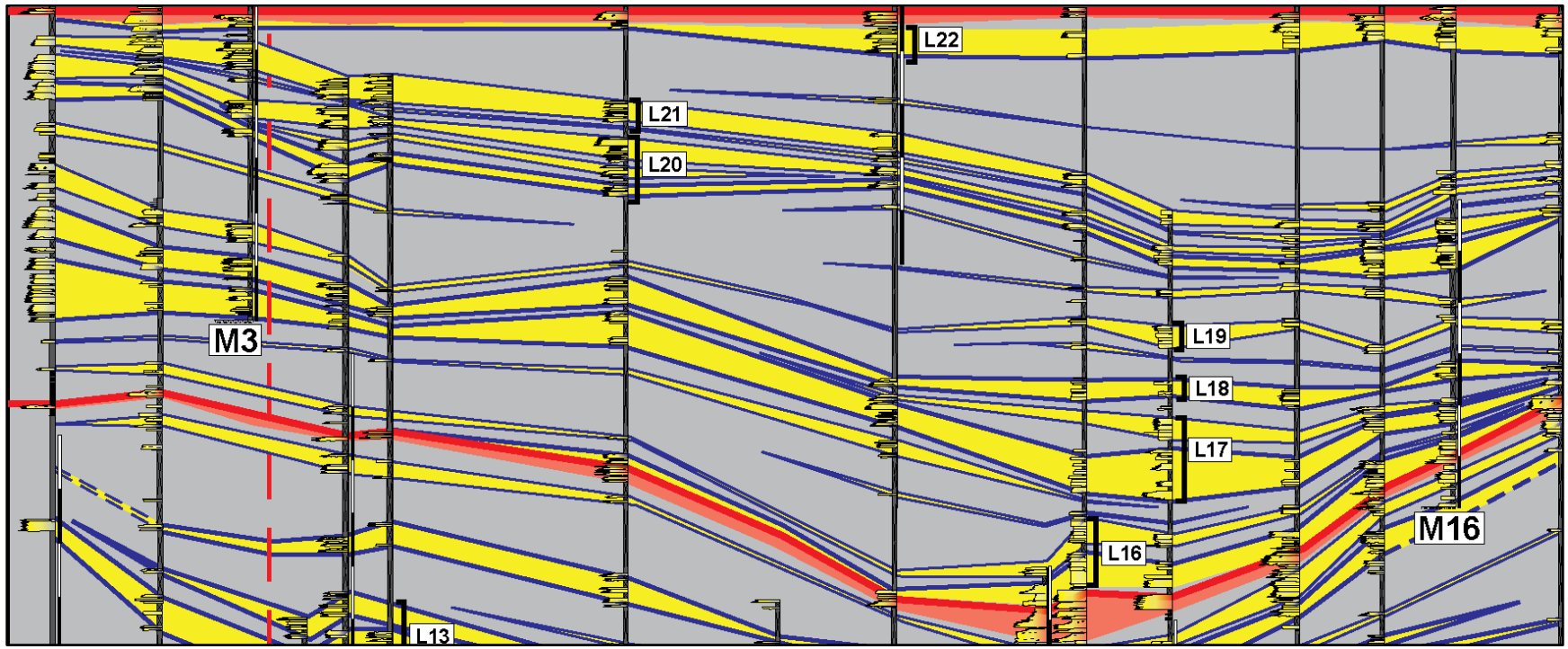

FAN ‘B’

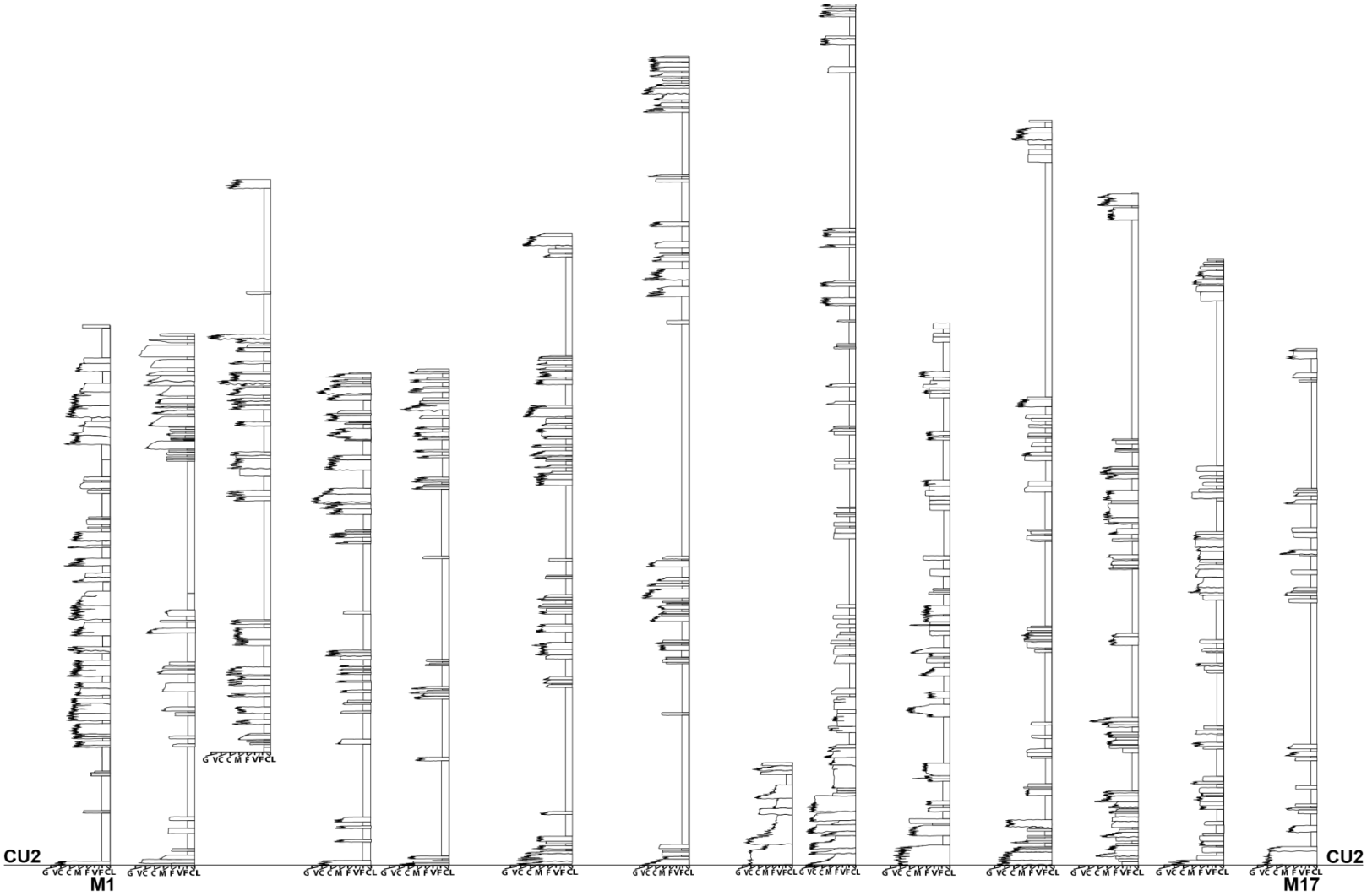

FAN ‘B’

Bibliography

Bouma, A. H. (1962). Sedimentology of Some Flysch Deposits. Elsevier, Amsterdam.

Bouma, A. H. (1968). Distribution of minor structures in Gulf of Mexico sediments. Gulf Coast Association of Geological Societies Transactions, 18, 26-33.

Bourcart, J. (1964). Les sables profonds de la Méditerranée occidentale. Developments in sedimentology, 3, 148-155.

Burgess, P. M., Flint, S., & Johnson, S. (2000). Sequence stratigraphic interpretation of turbiditic strata: An example from Jurassic strata of the Neuquen basin, Argentina. Geological Society of America Bulletin, 112(11), 1650-1666. doi: Doi 10.1130/0016-7606(2000)112<1650:Ssiots>2.0.Co;2

Butler, R. W. H., & Tavarnelli, E. (2006). The structure and kinematics of substrate entrainment into high-concentration sandy turbidites: a field example from the Gorgoglione 'flysch' of southern Italy. Sedimentology, 53(3), 655-670. doi: 10.1111/j.1365-3091.2006.00789.x

Cartigny, M. J. B., Eggenhuisen, J. T., Hansen, E. W. M., & Postma, G. (2013). Concentration-Dependent Flow Stratification In Experimental High-Density Turbidity Currents and Their Relevance To Turbidite Facies Models. Journal of Sedimentary Research, 83(12), 1046-1064. doi: 10.2110/jsr.2013.71

Clark, J. D., & Pickering, K. T. (1996). Architectural Elements and Growth Patterns of Submarine Channels: Application to Hydrocarbon Exploration16. AAPG Bulletin, 80(2), 194-221.

Dean, J. S. (1986). Sequence Architecture and Lithofacies Assemblages of Submarine Fan Deposits in Los Molles Formation (Jurassic), Neuquen Basin, Argentina

Franzese, J. R., & Spalletti, L. A. (2001). Late Triassic–early Jurassic continental extension in southwestern Gondwana: tectonic segmentation and pre-break-up rifting. Journal of South American Earth Sciences, 14(3), 257-270.

Franzese, J. R., Spalletti, L. A., Gomez-Perez, I., & Macdonald, D. (2003). Tectonic and paleoenvironmental evolution of Mesozoic sedimentary basins along the Andean foothills of Argentina (32-54 S). Journal of South American Earth Sciences(16), 81-90.

Franzese, J. R., Veiga, G. D., Schwarz, E., & Gomez-Perez, I. (2006). Tectonostratigraphic evolution of a Mesozoic graben border system: The Chachill depocentre, southern Neuquen Basin, Argentina Journal of the Geological Society, 163(2006), 707-721.

Galloway, W. (1998). Siliciclastic slope and base-of-slope depositional systems: component facies, stratigraphic architecture, and classification. AAPG Bulletin, 82, 569-595.

Gennesse. M. (1966). Prospection photographique des canyons sous-marins du Var et du Paillon (Alpes Maritimes) au moyen de la troïka. Revue de Geographie Physique et de Geologie Dynamique, 8(1), 3.

Gjelberg, J. G., Enoksen, T., Kj, P., Mangerud, G., Martinsen, O. J., Roe, E., & Vagnes, E. (2001). The Maastrichtian and Danian depositional setting, along the eastern margin of the Møre Basin (mid-Norwegian Shelf): implications for reservoir development of the Ormen Lange Field. Norwegian Petroleum Society Special Publications, 10, 421-440.

Grimaldi, G. O., & Dorobek, S. L. (2011). Fault framework and kinematic evolution of inversion structures: Natural examples from the Neuquén Basin, Argentina. AAPG Bulletin, 95(1), 27-60. doi: 10.1306/06301009165

Gulisano, C. A., and Pando, G. A. (1981). Estratigrafía y facies de los depósitos jurásicos entre Piedra del Aguila y Sañico, Departamento Collón Curá, Provincia del Neuquén: Octavo Congreso Geológico Argentino, San Luis, v. 3, p. 553–577.

Hallam, A. (1992). Phanerozoic Sea-Level Changes. NY: Columbia University Press

Haq, B. U., Hardenbol, J., & Vail, P. R. (1987). Chronology of fluctuating sea levels since the Triassic. Science, 235(4793), 1156-1167.

Haughton, P., Davis, C., McCaffrey, W., & Barker, S. (2009). Hybrid sediment gravity flow deposits – Classification, origin and significance. Marine and Petroleum Geology, 26(10), 1900-1918. doi: 10.1016/j.marpetgeo.2009.02.012

Haughton, P. D. W., Barker, S. P., & McCaffrey, W. D. (2003). 'Linked' debrites in sand-rich turbidite systems - origin and significance. Sedimentology, 50, 459-482.

Hickson, T. A., & Lowe, D. R. (2002). Facies architecture of a submarine fan channel–levee complex: the Juniper Ridge Conglomerate, Coalinga, California.Sedimentology, 49(2), 335-362.

Hinterwimmer, G. A. and J. M. Jauregui, (1984). Análisis de facies de los depósitos de turbiditas de la Formación Los Molles en el sondeo Barda Colorada Este, Provincia del Neuquén: Noveno Congreso Geológico Argentino, San Carlos de Bariloche, v. 5, p. 124–135.

Hodgson, D. M. (2009). Distribution and origin of hybrid beds in sand-rich submarine fans of the Tanqua depocentre, Karoo Basin, South Africa. Marine and Petroleum Geology, 26(10), 1940-1956. doi: 10.1016/j.marpetgeo.2009.02.011

Hodgson, D.M., Flint, S.S., Hodgetts, D., Drinkwater, N.J., Johannessen, E.P. and Luthi, S. (2006). Stratigraphic evolution of fine-grained submarine fan systems, Tanqua depocentre, Karoo Basin, South Africa. J. Sed. Res., 76, 20–40.

Howell, J. A., Schwarz, E., Spalletti, L. A., & Veiga, G. D. (2005). The Neuquén basin: an overview. Geological Society, London, Special Publications, 252(1), 1-14.

Hubbard, S. M., Fildani, A., Romans, B. W., Covault, J. A., & McHargue, T. R. (2010). High-relief slope clinoform development: insights from outcrop, Magallanes Basin, Chile. Journal of Sedimentary Research, 80(5), 357-375.

Jackson, C. A. L., Zakaria, A. A., Johnson, H. D., Tongkul, F., & Crevello, P. D. (2009). Sedimentology, stratigraphic occurrence and origin of linked debrites in the West Crocker Formation (Oligo-Miocene), Sabah, NW Borneo. Marine and Petroleum Geology, 26(10), 1957-1973. doi: 10.1016/j.marpetgeo.2009.02.019

Jobe, Z. R., Lowe, D. R., & Morris, W. R. (2012). Climbing-ripple successions in turbidite systems: depositional environments, sedimentation rates and accumulation times. Sedimentology, 59(3), 867-898.

Johansson, M., & Stow, D. A. (1995). A classification scheme for shale clasts in deep water sandstones. Geological Society, London, Special Publications,94(1), 221-241.

Johnson, B. A., & Walker, R. G. (1979). Paleocurrents and depositional environments of deep water conglomerates in the Cambro-Ordovician Cap Enrage Formation, Quebec Appalachians. Canadian Journal of Earth Sciences,16(7), 1375-1387.

Kane, I. A., Kneller, B. C., Dykstra, M., Kassem, A., & McCaffrey, W. D. (2007). Anatomy of a submarine channel–levee: an example from Upper Cretaceous slope sediments, Rosario Formation, Baja California, Mexico.Marine and Petroleum Geology, 24(6), 540-563.

Kane, I. A., Dykstra, M. L., Kneller, B. C., Tremblay, S., & McCAFFREY, W. D. (2009). Architecture of a coarse-grained channel–levée system: the Rosario Formation, Baja California, Mexico. Sedimentology, 56(7), 2207-2234.

Kane, I. A., & Ponten, A. S. M. (2012). Submarine transitional flow deposits in the Paleogene Gulf of Mexico. Geology, 40(12), 1119-1122. doi: 10.1130/g33410.1

Kneller, B. C., & Branney, M. J. (1995). Sustained high-density turbidity currents and the deposition of thick massive sands. Sedimentology, 42(4), 607-616.

Kochhann, K. G. D., Baecker-Fauth, S., Pujana, I., Santos da Silveira, A., & Fauth, G. (2011). Toarcian–Aalenian (Early–Middle Jurassic) radiolarian fauna from the Los Molles Formation, Neuquén Basin, Argentina: Taxonomy and paleobiogeographic affinities. Journal of South American Earth Sciences, 31(2-3), 253-261. doi: 10.1016/j.jsames.2011.01.001

Lamb, M. P., & Mohrig, D. (2009). Do hyperpycnal-flow deposits record river-flood dynamics?. Geology, 37(12), 1067-1070.

Legarreta, L., & Gulisano, C. A. (1989). Análisis estratigráfico secuencial de la cuenca neuquina (Triásico Superior-Terciario inferior), Argentina, in G. A. Chebli and L.

A. Spalleti, eds., Cuencas sedimentarias Argentinas: Serie Correlación Geológica 6, p. 221–243.

Legarreta, L., & Uliana, M.A. (1991). Jurassic–Cretaceous marine oscillations and geometry of backarc basin fill, central Argentine Andes, in McDonald, D.I.M., ed., Sedimentation, tectonics and eustasy: International Association of Sedimentologists Special Publication 12, p. 429–450.

Lowe, D. R. (1982). Sediment gravity flows: Depositional models with special reference to the deposits of high-density turbidity currents. Journal of Sedimentology and Petrology, 52, 280-297.

Lowe, D. R. (1988). Suspended-load fallout rate as an independent variable in the analysis of current structures. Sedimentology, 35(5), 765-776.

Martinez, M. A., Pramparo, M. B., Quattrocchio, M. E., & Zavala, C. (2008). Depositional environments and hydrocarbon potential of the Middle Jurassic Los Molles Formation, Neuquen Basin, Argentina: palynofacies and organic geochemical data. Revista Geologica de Chile, 2(35), 279-305.

Macdonald, D., I. Gómez Pérez, J. Franzese, L. Spalletti, L. Lawver, L. Gahagan, I. Dalziel, C. Thomas, N. Trewin, M. Hole and D. Paton, (2003). Mesozoic break-up of SW Gondwana: implications for regional hydrocarbon potential of the southern South Atlantic. Marine and Petroleum Geology 20:287-308.

Middleton, G. (1967). Experiments on density and turbidity currents III. Deposition of sediment. Canadian Journal of Earth Sciences, 4.

Middleton, G. V. & Hampton, M. A. (1973). Sediment gravity flows: mechanics of flow and deposition. In Turbidites and Deep Water Sedimentation G. V. Middleton and A. H. Bouma (eds.). Anaheim, California, SEPM. Short Course Notes, 38p

Morgans-Bell, H. S., & McIlroy, D. (2005). Palaeoclimatic implications of Middle Jurassic (Bajocian) coniferous wood from the Neuquen Basin, west-central Argentina. Geological Society, London, Special Publications, 252(1), 267-278. doi: 10.1144/gsl.sp.2005.252.01.13

Mohrig, D., K. X. Whipple, M. Hondzo, C. Ellis, and G. Parker, (1998). Hydroplaning of subaqueous debris flows, Geol. Soc. Am. Bull., 110, 387 – 394.

Mulder, T., & Alexander, J. (2001). The physical character of subaqueous sedimentary density flows and their deposits. Sedimentology, 48, 269-299.

Mulder, T., & Etienne, S. (2010). Lobes in deep-sea turbidite systems: State of the art. Sedimentary Geology, 229(3), 75-80. doi: 10.1016/j.sedgeo.2010.06.011

Mulder, T., Syvitski, J. P., Migeon, S., Faugeres, J. C., & Savoye, B. (2003). Marine hyperpycnal flows: initiation, behavior and related deposits. A review.Marine and Petroleum Geology, 20(6), 861-882.

Mutti, E. (1977). Distinctive thin-bedded turbidite facies and related depositional environments in the Eocene Hecho Group (South-central Pyrenees, Spain). Sedimentology, 24, 107-131.

Mutti, E. & Normark, W.R. (1987). Comparing examples of modern and ancient turbidite systems: Problems and Concepts. In: Legget, J.K. and Zuffa, G.G. (eds.), Marine Clastic Sedimentology: Concepts and Case Studies. Graham and Trotman, p. 1–38.

Mutti, E., & Normark, W. R. (1991). An integrated approach to the study of turbidite systems Seismic facies and sedimentary processes of submarine fans and turbidite systems (pp. 75-106): Springer.

Mutti, E., & Ricci Lucchi, F. (1972). Le torbiditi dell'Appennino settentrionale: introduzione all'analisi di facies. Mem. Soc. Geol. Ital, 11(2), 161-199.

Meyer, L., & Ross, G. M. (2007). Channelized lobe and sheet sandstones of the upper Kaza Group basin-floor turbidite system, Castle Creek South, Windermere Supergroup, British Columbia, Canada, in T. H. Nilsen, R. D. Shew, G. S. Steffens, and J. R. J. Studlick, eds., Atlas of deep-water outcrops: AAPG Studies in Geology 56, p. 85–88.

Natland, M. L., & Kuenen, P. H. (1951). Sedimentary history of Ventura Basin, California, and the action of turbidity currents: Turbidity currents and the transportation of coarse sediments to the deep water: SEPM Special Publication 2, p. 76–107.

Nemec, W., & Steel, R. J. (1984). Alluvial and coastal conglomerates: their significant features and some comments on gravelly mass-flow deposits.

Nilsen T. H., Imperato D. P., Moore D. W. (1994). Submarine Fans and Turbidite Systems, Reservoir geometry and architecture of productive upper Cretaceous mud-rich and sand-rich submarine-fan systems, Sacramento Basin, California, eds Weimer P., Bouma A. H., Perkins B. F. (GCSSEPM Foundation, Houston), pp269–280.

Normark, W. R. (1978). Fan valleys, channels, and depositional lobes on modern submarine fans: characters for recognition of sandy turbidite environments. AAPG Bulletin, 62(6), 912-931.

Ochoa, J., Wolak, J., & Gardner, M. H. (2013). Recognition criteria for distinguishing between hemipelagic and pelagic mudrocks in the characterization of deep-water reservoir heterogeneity. AAPG bulletin, 97(10), 1785-1803.

Olariu, M. I., Ferguson, J. F., & Aiken, C. L. V. (2008). Outcrop fracture characterization using terrestrial laser scanners: Deep-water Jackfork sandstone at Big Rock Quarry, Arkansas. [Article]. Geosphere, 4(1), 247-259. doi: 10.1130/ges00139.1

Paim, P. S. G., Silveira, A., Lavina, E., Faccini, U., Leanza, H., Teixeira de Oliveira, J. M. M., & D'avila, R. (2008). High resolution stratigraphy and gravity flow deposits in the Los Molles Formation (Cuyo Group - Jurassic) at La Jardinera Region, Neuquen Basin. Revista de la Asociacion Geologica Argentina, 63, 728-753.

Pickering, K. T., & Corregidor, J. (2005). Mass-transport complexes (MTCs) and tectonic control on basin-floor submarine fans, middle Eocene, south Spanish Pyrenees. Journal of Sedimentary Research, 75(5), 761-783.

Prelat, A., & Hodgson, D. M. (2013). The full range of turbidite bed thickness patterns in submarine lobes: controls and implications. Journal of the Geological Society, 170(1), 209-214. doi: 10.1144/jgs2012-056

Prelat, A., Hodgson, D. M., & Flint, S. S. (2009). Evolution, architecture and hierarchy of distributary deep-water deposits: a high-resolution outcrop investigation from the Permian Karoo Basin, South Africa. Sedimentology, 56(7), 2132-2154. doi: 10.1111/j.1365-3091.2009.01073.x

Ramos, V.A. (1988). The tectonics of the Central Andes; 30 to 33 S Latitude, in Clark, S.P.J., et al., eds., Processes in Continental Lithospheric Deformation: Geological Society America Special Paper 218, p. 31–54.

Ramos, V. A. (1999). Evolución tectónica de la Argentina. In: Caminos, R. (Ed.) Geología Argentina. Servicio Geológico Minero Argentino, Buenos Aires, Anales 29, pp. 715-784.

Ramos, V. A. (2008). Patagonia: A paleozoic continent adrift? Journal of Sedimentary Research(26), 235-251.

Reading, H.G. and Richards, M. (1994). Turbidite systems in deep-water basin margins classified by grain size and feeder system: AAPG Bulletin, v. 78, p. 792-822.

Riccardi, A. C., Leanza, H. A., Damborenea, S. E., Mancenido, M. O., Ballent, S. C., & Zeiss, A. (2000). Marine mesozoic biostratigraphy of the nenquen basio. Zeitschrift für angewandte Geologie, 103-108.

Shanmugam, G., & Moiola, R. J. (1988). Submarine fans: characteristics, models, classification, and reservoir potential: Earth-Science Reviews, v. 24, p. 383-428.

Shanmugan, G. (2006). Deep-water processes and facies models: implications for sandstone petroleum reservoirs. vol. 5. Elsevier.

Sinclair, H. D., & Cowie, P. A. (2003). Basin-Floor Topography and the Scaling of Turbidites. The Journal of Geology, 111, 277-299.

Smith, R., & Spalletti, L. (1995). Erosional, depositional and post-depositional features of a turbidite channel-fill: Jurassic of the Neuquén basin, Argentina. ln: Atlas of Deep Water Environments: Architectural Style in Turbidity Systems (K.

Pickering, R. Hiscott. N. Kenyon, F. Ricci Lucchi. y R. Smith, Eds.): Chapman and Hall, London.

Spalletti, L.A., J. Franzese, S.D. Matheos and E. Schwarz, (2000). Sequence stratigraphy in tidally-dominated carbonate-siliciclastic ramp, the Tithonian of the southern Neuquén Basin, Argentina. Journal of the Geological Society 157:433-446.

Spalletti, L. A., & Veiga, G. D. (2007). Variability of continental depositional systems during lowstand sedimentation: an example from the Kimmeridgian of the Neuquen Basin, Argentina. Latin American Journal of Sedimentology and Basin Analysis, v. 14 (2): 85-104.

Stanley, D. J. & Unrug, R. (1972). Submarine Channel Deposits Fluxoturbidites and Other Indicators of Slope and Base of Slope Environments in Modern and Ancient Marine Basins. In J. K. Rigby and W. K. Hamblin, editors, Recognition of Ancient Sedimentary Environments. Society of Economic Paleontologists and Mineralogists Special Publication, 16:287-340. Tulsa, Oklahoma.

Stanley, D. J. (1980). The Saint-Antonin conglomerate in the Maritime Alps: a model for coarse sedimentation on a submarine slope. Smithsonian Contributions to the Marine Sciences. 5.

Steel, R., & Olsen, T. (2002). Clinoforms, clinoform trajectories and deepwater sands. In: Sequence Stratigraphic Models for Exploration and Production: Evolving Methodology, Emerging Models and Applications Histories (Eds J.M. Armentrout and N.C. Rosen). Gulf Coast Section SEPM Proc. 22nd Annu. Res. Conf., 367-380.

Stow, D. A., & Johansson, M. (2000). Deep-water massive sands: nature, origin and hydrocarbon implications. Marine and Petroleum Geology, 17(2), 145-174.

Sumner, Esther J., Amy, Lawrence A. and Talling, Peter J. (2008). Deposit structure and processes of sand deposition from a decelerating sediment suspension. Journal of Sedimentary Research, 78, (8), 529-547.

Talling, P. J., Amy, L. A., Wynn, R. B., Peakall, J., & Robinson, M. (2004). Beds comprising debrite sandwiched within co-genetic turbidite: origin and widespread occurrence in distal depositional environments. Sedimentology,51(1), 163-194.

Talling, P. J., Amy, L. A., & Wynn, R. B. (2007). New insight into the evolution of large-volume turbidity currents: comparison of turbidite shape and previous modelling results. Sedimentology, 54(4), 737-769. doi: 10.1111/j.1365-3091.2007.00858.x

Talling, P.J., Masson, D.G., Sumner, E.J., Malgesini, G. (2012). Subaqueous sediment density flows: Depositional processes and deposit types, Sedimentology (2012) 59, 1937-2003.

Tudor, E. P. (2014). Facies variability in deep water channel-to-love transition zone: Jurassic Los Molles Formation, Neuquén Basin Argentina. Thesis for the Masters

Degree in Stratigraphy/Sedimentology, Department of Geological Science, The University of Texas at Austin, USA.

Vail, P. R., Mitchum Jr, R. M., & Thompson III, S. (1977). Seismic Stratigraphy and Global Changes of Sea Level: Part 4. Global Cycles of Relative Changes of Sea Level.: Section 2. Application of Seismic Reflection Configuration to Stratigraphic Interpretation.

Vann, N. K. (2013). Slope to basin floor evolution of channels to lobes, Jurassic Los Molles Formation, Neuquen Basin, Argentina. Thesis for the Masters Degree in Stratigraphy/Sedimentology, Department of Geological Science, The University of Texas at Austin, USA.

Vergani, G. D., Tankard, A. J., Belotti, H. J., & Welsink, H. J. (1995). Tectonic evolution and paleogeography of the Neuquen Basin, Argentina AAPG Memoir, 62, 383-402.

Walker, R. G., & Mutti, E. (1973). Turbidite facies and facies associations. In Middleton, G. V., and Bouma, A. H. (Eds.), Turbidites and Deep Water Sedimentation, SEPM Pacific Section Short Course, Anaheim (1973), pp. 119-158.

Walker, R. G. (1975). Generalized facies models for resedimented conglomerates of turbidite association. Geological Society of America Bulletin,86(6), 737-748.

Weimer, P., Slatt, R. M., & Bouroullec, R. (2007). Introduction to the petroleum geology of deepwater settings. AAPG/Datapages.

Westermann, G.E.G., and Riccardi, A.C. (1979). Middle Jurassic ammonoid fauna and biochronology of the Argentine-Chilean Andes. II. Bajocian Stephanocerataceae. Palaeontographica A 164: 85-118.

Wynn, R. B., Kenyon, N. H., Masson, D. G., Stow, D., A. V., & Weaver, P. P. E. (2002). Characterization and recognition of deep-water channel-lobe transition zones.

Zavala, C. (1996). Sequence stratigraphy in continental to marine transitions. An example from the Middle Jurassic Cuyo Group, South Neuquen Basin, Argentina. GeoResearch Forum, 1-2, 285-294.

Zumberge, J. E. (1993). Organic geochemistry of Estancia Vieja oils, Río Negro norte block, in M. H. Engel and S. A. Macko, eds., Organic geochemistry: New York, Plenum Press, p. 461–471.